



Kevin P. Riley
Nuclear Support Services Manager
Shearon Harris Nuclear Power Plant
5413 Shearon Harris Road
New Hill, NC 27562-9300

10 CFR 50.4

October 23, 2019
Serial: RA-19-0403

ATTN: Document Control Desk
U.S. Nuclear Regulatory Commission
Washington, DC 20555-0001

Shearon Harris Nuclear Power Plant, Unit 1
Docket No. 50-400/Renewed License No. NPF-63

Subject: Submittal of the Summary Technical Report for the Reactor Pressure Vessel
Surveillance Program Capsule Z

Ladies and Gentlemen:

In accordance with Title 10 of the Code of Federal Regulations (10 CFR) Part 50, Appendix H, "Reactor Vessel Material Surveillance Program Requirements," Part IV, Duke Energy Progress, LLC (Duke Energy), submits the attached summary technical report for the reactor pressure vessel surveillance program Capsule Z, withdrawn from the Shearon Harris Nuclear Power Plant, Unit 1 (HNP).

Duke Energy withdrew Capsule Z on April 19, 2018. The cited requirement would require submission of the summary technical report by April 19, 2019 (i.e., 1 year after capsule withdrawal). By letter dated September 17, 2018 (Agencywide Documents Access and Management System (ADAMS) Accession No. ML18260A025), Duke Energy requested extension of the submission of the summary technical report to November 19, 2019. By letter dated December 4, 2018 (ADAMS Accession No. ML18303A048), the Nuclear Regulatory Commission staff found the proposed extension of the submission deadline acceptable.

10 CFR 50, Appendix H, paragraph IV.C, also requires the expected date for the submittal of the revised Technical Specifications (TSs) be reported, if a change is required in the pressure-temperature limits contained within the TS. Duke Energy expects to submit a license amendment request by April 30, 2020, to revise the pressure-temperature limit curves for HNP. The operational curves, used by the main control room to operate the plant, are conservative with respect to the new pressure-temperature limits and remain valid.

There are no regulatory commitments contained within this report.

Please refer any questions regarding this submittal to Kevin Riley at (984) 229-2124.

Sincerely,

A handwritten signature in black ink, appearing to read 'K. P. Riley', with a stylized flourish at the end.

Kevin P. Riley

Enclosure: Framatome ANP-3798NP Revision 0, "Analysis of Capsule Z, Duke Energy Shearon Harris Nuclear Power Plant, Reactor Vessel Material Surveillance Program"

cc: J. Zeiler, NRC Senior Resident Inspector, HNP
M. Barillas, NRC Project Manager, HNP
NRC Regional Administrator, Region II

U.S. Nuclear Regulatory Commission
Serial: RA-19-0403, Enclosure

SERIAL: RA-19-0403

ENCLOSURE

**FRAMATOME ANP-3798NP REVISION 0,
ANALYSIS OF CAPSULE Z,
DUKE ENERGY SHEARON HARRIS NUCLEAR POWER PLANT,
REACTOR VESSEL MATERIAL SURVEILLANCE PROGRAM**

DOCKET NO. 50-400

RENEWED LICENSE NUMBER NPF-63



**Analysis of Capsule Z
Duke Energy Shearon Harris
Nuclear Power Plant**

ANP-3798NP
Revision 0

Reactor Vessel Material Surveillance
Program

September 2019

(c) 2019 Framatome Inc.

Copyright © 2019

**Framatome Inc.
All Rights Reserved**

Framatome Inc.

ANP-3798NP

Revision 0

Analysis of Capsule Z

Duke Energy Shearon Harris Nuclear Power Plant

Reactor Vessel Material Surveillance Program

Page i

Nature of Changes

| Item | Section(s) or Page(s) | Description and Justification |
|------|--------------------------|-------------------------------|
| 1 | All | Initial Issue |

Contents

| | <u>Page</u> |
|--|-------------|
| 1.0 INTRODUCTION | 1-1 |
| 2.0 BACKGROUND | 2-1 |
| 3.0 SURVEILLANCE PROGRAM DESCRIPTION | 3-1 |
| 4.0 TESTS OF UNIRRADIATED MATERIAL | 4-1 |
| 5.0 POST-IRRADIATION TESTING | 5-1 |
| 5.1 Capsule Disassembly and Inventory | 5-1 |
| 5.2 Thermal Monitors | 5-1 |
| 5.3 Tension Test Results | 5-3 |
| 5.4 Charpy V-Notch Impact Test Results | 5-13 |
| 5.5 Compact Fracture Toughness and Bend Bar Specimens | 5-32 |
| 6.0 NEUTRON FLUENCE | 6-1 |
| 7.0 DISCUSSION OF CAPSULE RESULTS | 7-1 |
| 7.1 Unirradiated Material Property Data | 7-1 |
| 7.2 Irradiated Property Data | 7-1 |
| 7.2.1 Tensile Properties | 7-1 |
| 7.2.2 Impact Properties | 7-3 |
| 8.0 SUMMARY OF RESULTS | 8-1 |
| 9.0 SURVEILLANCE CAPSULE REMOVAL SCHEDULE | 9-1 |
| 10.0 REFERENCES | 10-1 |
| APPENDIX A REACTOR VESSEL SURVEILLANCE PROGRAM BACKGROUND DATA AND INFORMATION | A-1 |
| APPENDIX B UNIRRADIATED AND IRRADIATED TENSILE DATA FOR THE HNP RVSP MATERIALS | B-1 |
| APPENDIX C UNIRRADIATED AND IRRADIATED CHARPY V-NOTCH IMPACT SURVEILLANCE DATA FOR THE HNP RVSP MATERIALS USING HYPERBOLIC TANGENT CURVE-FITTING METHOD | C-1 |
| APPENDIX D CHARPY V-NOTCH SHIFT COMPARISON: HAND- DRAWN CURVE FITTING VS. HYPERBOLIC TANGENT CURVE FITTING | D-1 |
| APPENDIX E FLUENCE ANALYSIS METHODOLOGY | E-1 |
| APPENDIX F CAPSULE SURVEILLANCE DATA CREDIBILITY ASSESSMENT | F-1 |

List of Tables

| | |
|--|------|
| Table 3-1. Test Specimens Contained in HNP Capsule Z..... | 3-2 |
| Table 3-2. Chemical Composition of HNP Capsule Z Surveillance Materials..... | 3-2 |
| Table 3-3. Chemical Analysis Results of Selected Charpy Specimens from HNP Capsule U for Copper and Nickel Contents..... | 3-3 |
| Table 3-4. Heat Treatment of the Surveillance Materials in Capsule Z | 3-3 |
| Table 5-1. Tensile Properties of HNP Capsule Z Reactor Vessel Surveillance Materials, Irradiated to 9.25×10^{19} n/cm ² (E>1.0 MeV)..... | 5-3 |
| Table 5-2. Charpy V-Notch Impact Results for HNP Capsule Z Base Metal Plate, Heat No. B4197-2, Irradiated to 9.45×10^{19} n/cm ² (E>1.0 MeV) Longitudinal (LT) Orientation | 5-14 |
| Table 5-3. Charpy V-Notch Impact Results for HNP Capsule Z Base Metal Plate, Heat No. B4197-2, Irradiated to 9.45×10^{19} n/cm ² (E>1.0 MeV) Transverse (TL) Orientation | 5-14 |
| Table 5-4. Charpy V-Notch Impact Results for HNP Capsule Z Weld Metal, Wire Heat No. 5P6771/Flux Lot 0342, Irradiated to 9.45×10^{19} n/cm ² (E>1.0 MeV) | 5-15 |
| Table 5-5. Charpy V-Notch Impact Results for HNP Capsule Z Base Metal Plate, Heat-Affected-Zone, Irradiated to 9.45×10^{19} n/cm ² (E>1.0 MeV) | 5-15 |
| Table 5-6. Hyperbolic Tangent Curve Fit Coefficients for the HNP Capsule Z Surveillance Materials | 5-16 |
| Table 7-1. Summary of HNP Reactor Vessel Surveillance Capsules Tensile Test Results | 7-2 |
| Table 7-2. Measured vs. Predicted 30 ft-lb Transition Temperature Changes for HNP Capsule Z Surveillance Materials – 9.45×10^{19} n/cm ² | 7-3 |
| Table 7-3. Measured vs. Predicted Upper-Shelf Energy Decreases for HNP Capsule Z Surveillance Materials – 9.45×10^{19} n/cm ² | 7-3 |
| Table 7-4. Summary of HNP Reactor Vessel Surveillance Capsules Charpy Impact Test Results..... | 7-4 |
| Table A-1. HNP Surveillance Capsule Identifications, Original Locations, and Design Lead Factors | A-1 |
| Table A-2. Description of the HNP Reactor Vessel Beltline Region Materials..... | A-2 |
| Table A-3. Heat Treatment of the HNP Reactor Vessel Beltline Region Materials..... | A-3 |
| Table B-1. Unirradiated Surveillance Tensile Properties of HNP Base Metal Plate, Heat No. B4197-2, Longitudinal Orientation | B-1 |

| | |
|--|-----|
| Table B-2. Unirradiated Surveillance Tensile Properties of HNP Base Metal Plate, Heat No. B4197-2, Transverse Orientation | B-1 |
| Table B-3. Unirradiated Surveillance Tensile Properties of HNP Weld Metal, Wire Heat 5P6771 / Flux Lot 034..... | B-1 |
| Table B-4. HNP Capsule U Surveillance Tensile Properties of Base Metal Plate, Heat No. B4197-2, Irradiated to 5.52×10^{18} n/cm ² (E>1.0 MeV) Longitudinal Orientation..... | B-2 |
| Table B-5. HNP Capsule U Surveillance Tensile Properties of Base Metal Plate, Heat No. B4197-2, Irradiated to 5.52×10^{18} n/cm ² (E>1.0 MeV) Transverse Orientation | B-2 |
| Table B-6. HNP Capsule U Surveillance Tensile Properties of Weld Metal, Wire Heat 5P6771 / Flux Lot 0342, Irradiated to 5.52×10^{18} n/cm ² (E>1.0 MeV)..... | B-2 |
| Table B-7. HNP Capsule V Surveillance Tensile Properties of Base Metal Plate, Heat No. B4197-2, Irradiated to 1.32×10^{19} n/cm ² (E>1.0 MeV) Longitudinal Orientation..... | B-3 |
| Table B-8. HNP Capsule V Surveillance Tensile Properties of Base Metal Plate, Heat No. B4197-2, Irradiated to 1.32×10^{19} n/cm ² (E>1.0 MeV) Transverse Orientation | B-3 |
| Table B-9. HNP Capsule V Surveillance Tensile Properties of Weld Metal, Wire Heat 5P6771 / Flux Lot 0342, Irradiated to 1.32×10^{19} n/cm ² (E>1.0 MeV)..... | B-3 |
| Table B-10. HNP Capsule X Surveillance Tensile Properties of Base Metal Plate, Heat No. B4197-2, Irradiated to 3.25×10^{19} n/cm ² (E>1.0 MeV) Longitudinal Orientation..... | B-4 |
| Table B-11. HNP Capsule X Surveillance Tensile Properties of Base Metal Plate, Heat No. B4197-2, Irradiated to 3.25×10^{19} n/cm ² (E>1.0 MeV) Transverse Orientation | B-4 |
| Table B-12. HNP Capsule X Surveillance Tensile Properties of Weld Metal, Wire Heat 5P6771 / Flux Lot 0342, Irradiated to 3.25×10^{19} n/cm ² (E>1.0 MeV)..... | B-4 |
| Table C-1. Unirradiated Surveillance Charpy V-Notch Impact Data for HNP Base Metal Plate, Heat No. B4197-2, Longitudinal (LT) Orientation..... | C-1 |
| Table C-2. HNP Capsule U Surveillance Charpy Impact Data for Base Metal Plate, Heat No. B4197-2, Irradiated to 5.52×10^{18} n/cm ² (E>1.0 MeV) Longitudinal (LT) Orientation | C-2 |

| | |
|---|------|
| Table C-3. HNP Capsule V Surveillance Charpy Impact Data for Base Metal Plate, Heat No. B4197-2, Irradiated to 1.32×10^{19} n/cm ² (E>1.0 MeV) Longitudinal (LT) Orientation | C-3 |
| Table C-4. HNP Capsule X Surveillance Charpy Impact Data for Base Metal Plate, Heat No. B4197-2, Irradiated to 3.25×10^{19} n/cm ² (E>1.0 MeV) Longitudinal (LT) Orientation | C-4 |
| Table C-5. Hyperbolic Tangent Curve Fit Coefficients for HNP Base Metal Plate, Heat No. B4197-2, Longitudinal (LT) Orientation..... | C-5 |
| Table C-6. Unirradiated Surveillance Charpy V-Notch Impact Data for HNP Base Metal Plate, Heat No. B4197-2, Transverse (TL) Orientation | C-6 |
| Table C-7. HNP Capsule U Surveillance Charpy Impact Data for Base Metal Plate, Heat No. B4197-2, Irradiated to 5.52×10^{18} n/cm ² (E>1.0 MeV) Transverse (TL) Orientation | C-7 |
| Table C-8. HNP Capsule V Surveillance Charpy Impact Data for Base Metal Plate, Heat No. B4197-2, Irradiated to 1.32×10^{19} n/cm ² (E>1.0 MeV) Transverse (TL) Orientation | C-8 |
| Table C-9. HNP Capsule X Surveillance Charpy Impact Data for Base Metal Plate, Heat No. B4197-2, Irradiated to 3.25×10^{19} n/cm ² (E>1.0 MeV) Transverse (TL) Orientation | C-9 |
| Table C-10. Hyperbolic Tangent Curve Fit Coefficients for HNP Base Metal Plate, Heat No. B4197-2, Transverse (TL) Orientation | C-10 |
| Table C-11. Unirradiated Surveillance Charpy V-Notch Impact Data for HNP Weld Metal, Wire Heat 5P6771/Flux Lot 0342 | C-11 |
| Table C-12. HNP Capsule U Surveillance Charpy Impact Data for Weld Metal, Wire Heat 5P6771/Flux Lot 0342, Irradiated to 5.52×10^{18} n/cm ² (E>1.0 MeV) Transverse (TL) Orientation | C-12 |
| Table C-13. HNP Capsule V Surveillance Charpy Impact Data for Weld Metal, Wire Heat 5P6771/Flux Lot 0342, Irradiated to 1.32×10^{19} n/cm ² (E>1.0 MeV) Transverse (TL) Orientation | C-13 |
| Table C-14. HNP Capsule X Surveillance Charpy Impact Data for Weld Metal, Wire Heat 5P6771/Flux Lot 0342, Irradiated to 3.25×10^{19} n/cm ² (E>1.0 MeV) Transverse (TL) Orientation | C-14 |
| Table C-15. Hyperbolic Tangent Curve Fit Coefficients for HNP Weld Metal, Wire Heat 5P6771/Flux Lot 0342 | C-15 |
| Table C-16. Unirradiated Surveillance Charpy V-Notch Impact Data for HNP Heat-Affected-Zone Material | C-16 |
| Table C-17. HNP Capsule U Surveillance Charpy Impact Data for Heat-Affected-Zone Material, Irradiated to 5.52×10^{18} n/cm ² (E>1.0 MeV) | C-17 |

| | |
|---|------|
| Table C-18.HNP Capsule V Surveillance Charpy Impact Data for Heat-Affected-Zone Material, Irradiated to 1.32×10^{19} n/cm ² (E>1.0 MeV)..... | C-18 |
| Table C-19.HNP Capsule X Surveillance Charpy Impact Data for Heat-Affected-Zone Material, Irradiated to 3.25×10^{19} n/cm ² (E>1.0 MeV)..... | C-19 |
| Table C-20.Hyperbolic Tangent Curve Fit Coefficients for HNP Heat-Affected-Zone Material..... | C-20 |
| Table D-1. Comparison of Curve Fit Transition Temperature Shifts for HNP Surveillance Material, Base Metal Plate, Heat No. B4197-2, Longitudinal (LT) Orientation | D-1 |
| Table D-2. Comparison of Curve Fit Transition Temperature Shifts for HNP Surveillance Material, Base Metal Plate, Heat No. B4197-2, Transverse (TL) Orientation | D-2 |
| Table D-3. Comparison of Curve Fit Transition Temperature Shifts for HNP Surveillance Material, Weld Metal, Wire Heat 5P6771/Flux Lot 0342..... | D-3 |
| Table D-4. Comparison of Curve Fit Transition Temperature Shifts for HNP Surveillance Material, Heat-Affected-Zone Material | D-4 |
| Table F-1. Credibility Assessment for HNP-1 Surveillance Materials..... | F-2 |
| Table F-2. Regulatory Guide 1.99, Revision 2/10 CFR 50.61, Table Chemistry Factor Conservatism Assessment for HNP-1 Base Metal B4197-2 & Weld Metal 5P6771 Surveillance Data..... | F-3 |
| Table F-3. Calculation of Base Metal Heat No. B4197-2 Chemistry Factor Using HNP-1 Surveillance Data..... | F-4 |
| Table F-4. Calculation of Weld Wire Heat 5P6771 Chemistry Factor Using HNP-1 Surveillance Data..... | F-5 |

List of Figures

| | |
|--|-----|
| Figure 3-1. Reactor Vessel Cross Section Showing Location of Capsule Z in Shearon Harris Unit 1 | 3-4 |
| Figure 3-2. Surveillance Capsule Assembly Showing Location of Specimens and Monitors for HNP Capsule Z..... | 3-5 |
| Figure 5-1. Photographs of Thermal Monitors Removed from the HNP RVSP Capsule Z | 5-2 |
| Figure 5-2. Tension Test Stress-Strain Curve for Base Metal Plate, Heat No. B4197-2, Longitudinal Orientation, Specimen No. QL18, Tested at 175°F | 5-4 |
| Figure 5-3. Tension Test Stress-Strain Curve for Base Metal Plate, Heat No. B4197-2, Longitudinal Orientation, Specimen No. QL17, Tested at 275°F | 5-4 |
| Figure 5-4. Tension Test Stress-Strain Curve for Base Metal Plate, Heat No. B4197-2, Longitudinal Orientation, Specimen No. QL16, Tested at 550°F | 5-5 |
| Figure 5-5. Tension Test Stress-Strain Curve for Base Metal Plate, Heat No. B4197-2, Transverse Orientation, Specimen No. QT17, Tested at 200°F | 5-5 |
| Figure 5-6. Tension Test Stress-Strain Curve for Base Metal Plate, Heat No. B4197-2, Transverse Orientation, Specimen No. QT16, Tested at 300°F | 5-6 |
| Figure 5-7. Tension Test Stress-Strain Curve for Base Metal Plate, Heat No. B4197-2, Transverse Orientation, Specimen No. QT18, Tested at 550°F | 5-6 |
| Figure 5-8. Tension Test Stress-Strain Curve for Weld Metal, Wire Heat 5P6771/Flux Lot 0342, Specimen No. QW18, Tested at 100°F | 5-7 |
| Figure 5-9. Tension Test Stress-Strain Curve for Weld Metal, Wire Heat 5P6771/Flux Lot 0342, Specimen No. QW16, Tested at 250°F | 5-7 |
| Figure 5-10. Tension Test Stress-Strain Curve for Weld Metal, Wire Heat 5P6771/Flux Lot 0342, Specimen No. QW17, Tested at 550°F | 5-8 |
| Figure 5-11. Photographs of Tested Tension Test Specimen QL-18 and Corresponding Fracture Surfaces – Base Metal Plate, Heat No. B4197-2, Longitudinal Orientation, 175°F | 5-8 |
| Figure 5-12. Photographs of Tested Tension Test Specimen QL-17 and Corresponding Fracture Surfaces – Base Metal Plate, Heat No. B4197-2, Longitudinal Orientation 275°F | 5-9 |

| | |
|---|------|
| Figure 5-13. Photographs of Tested Tension Test Specimen QL-16 and Corresponding Fracture Surfaces – Base Metal Plate, Heat No. B4197-2, Longitudinal Orientation 550°F | 5-9 |
| Figure 5-14. Photographs of Tested Tension Test Specimen QT-17 and Corresponding Fracture Surfaces – Base Metal Plate, Heat No. B4197-2, Transverse Orientation 200°F | 5-10 |
| Figure 5-15. Photographs of Tested Tension Test Specimen QT-16 and Corresponding Fracture Surfaces – Base Metal Plate, Heat No. B4197-2, Transverse Orientation 300°F | 5-10 |
| Figure 5-16. Photographs of Tested Tension Test Specimen QT-18 and Corresponding Fracture Surfaces – Base Metal Plate, Heat No. B4197-2, Transverse Orientation 550°F | 5-11 |
| Figure 5-17. Photographs of Tested Tension Test Specimen QW-18 and Corresponding Fracture Surfaces – Weld Metal, Wire Heat 5P6771/Flux Lot 0342, 100°F | 5-11 |
| Figure 5-18. Photographs of Tested Tension Test Specimen QW-16 and Corresponding Fracture Surfaces – Weld Metal, Wire Heat 5P6771/Flux Lot 0342, 250°F | 5-12 |
| Figure 5-19. Photographs of Tested Tension Test Specimen QW-17 and Corresponding Fracture Surfaces – Weld Metal, Wire Heat 5P6771/Flux Lot 0342, 550°F | 5-12 |
| Figure 5-20. Charpy Impact Data for Irradiated Base Metal Plate, Heat No. B4197-2, Longitudinal (LT) Orientation..... | 5-17 |
| Figure 5-21. Charpy Impact Data for Irradiated Base Metal Plate, Heat No. B4197-2, Transverse (TL) Orientation | 5-18 |
| Figure 5-22. Charpy Impact Data for Irradiated Weld Metal Wire Heat 5P6771/Flux Lot 0342 | 5-19 |
| Figure 5-23. Charpy Impact Data for Irradiated Base Metal Plate Heat-Affected- Zone | 5-20 |
| Figure 5-24. Photographs of Charpy Impact Specimen Fracture Surfaces, Base Metal Plate, Heat No. B4197-2, Longitudinal (LT) Orientation..... | 5-21 |
| Figure 5-25. Photographs of Charpy Impact Specimen Fracture Surfaces, Base Metal Plate, Heat No. B4197-2, Transverse (TL) Orientation | 5-24 |
| Figure 5-26. Photographs of Charpy Impact Specimen Fracture Surfaces, Weld Metal Wire Heat 5P6771/Flux Lot 0342..... | 5-27 |
| Figure 5-27. Photographs of Charpy Impact Specimen Fracture Surfaces, Base Metal Plate, Heat-Affected-Zone | 5-30 |

| | |
|---|------|
| Figure 7-1. Comparison of Unirradiated and Irradiated Charpy Impact Data Curves for Base Metal Plate, Heat No. B4197-2, Longitudinal (LT) Orientation | 7-5 |
| Figure 7-2. Comparison of Unirradiated and Irradiated Charpy Impact Data Curves for Base Metal Plate, Heat No. B4197-2, Transverse (TL) Orientation | 7-6 |
| Figure 7-3. Comparison of Unirradiated and Irradiated Charpy Impact Data Curves for Weld Metal (Wire Heat 5P6771/Flux Lot 0342) | 7-7 |
| Figure 7-4. Comparison of Unirradiated and Irradiated Charpy Impact Data Curves for Heat-Affected-Zone Material | 7-8 |
| Figure A-1. Locations and Identifications of Materials Used in the Fabrication of the HNP Reactor Pressure Vessel | A-4 |
| Figure A-2. Locations of Longitudinal Welds in HNP Reactor Pressure Vessel Upper and Lower Shell Courses | A-5 |
| Figure A-3. Locations of Surveillance Capsule Irradiation Sites in the HNP Reactor Pressure Vessel | A-6 |
| Figure C-1. Unirradiated Surveillance Charpy V-Notch Impact Data for HNP Base Metal Plate, Heat No. B4197-2, Longitudinal (LT) Orientation - Refitted Using Hyperbolic Tangent Curve-Fitting Method | C-21 |
| Figure C-2. HNP Capsule U Surveillance Charpy V-Notch Impact Data for Base Metal Plate, Heat No. B4197-2, Longitudinal (LT) Orientation - Refitted Using Hyperbolic Tangent Curve-Fitting Method | C-22 |
| Figure C-3. HNP Capsule V Surveillance Charpy V-Notch Impact Data for Base Metal Plate, Heat No. B4197-2, Longitudinal (LT) Orientation - Refitted Using Hyperbolic Tangent Curve-Fitting Method | C-23 |
| Figure C-4. HNP Capsule X Surveillance Charpy V-Notch Impact Data for Base Metal Plate, Heat No. B4197-2, Longitudinal (LT) Orientation - Refitted Using Hyperbolic Tangent Curve-Fitting Method | C-24 |
| Figure C-5. Unirradiated Surveillance Charpy V-Notch Impact Data for HNP Base Metal Plate, Heat No. B4197-2, Transverse (TL) Orientation - Refitted Using Hyperbolic Tangent Curve-Fitting Method | C-25 |
| Figure C-6. HNP Capsule U Surveillance Charpy V-Notch Impact Data for Base Metal Plate, Heat No. B4197-2, Transverse (TL) Orientation - Refitted Using Hyperbolic Tangent Curve-Fitting Method | C-26 |
| Figure C-7. HNP Capsule V Surveillance Charpy V-Notch Impact Data for Base Metal Plate, Heat No. B4197-2, Transverse (TL) Orientation - Refitted Using Hyperbolic Tangent Curve-Fitting Method | C-27 |

| | |
|--|------|
| Figure C-8. HNP Capsule X Surveillance Charpy V-Notch Impact Data for Base Metal Plate, Heat No. B4197-2, Transverse (TL) Orientation - Refitted Using Hyperbolic Tangent Curve-Fitting Method | C-28 |
| Figure C-9. Unirradiated Surveillance Charpy V-Notch Impact Data for HNP Weld Metal, Wire Heat 5P6771/Flux Lot 0342 - Refitted Using Hyperbolic Tangent Curve-Fitting Method | C-29 |
| Figure C-10. HNP Capsule U Surveillance Charpy V-Notch Impact Data for Weld Metal, Wire Heat 5P6771/Flux Lot 0342 - Refitted Using Hyperbolic Tangent Curve-Fitting Method | C-30 |
| Figure C-11. HNP Capsule V Surveillance Charpy V-Notch Impact Data for Weld Metal, Wire Heat 5P6771/Flux Lot 0342 - Refitted Using Hyperbolic Tangent Curve-Fitting Method | C-31 |
| Figure C-12. HNP Capsule X Surveillance Charpy V-Notch Impact Data for Weld Metal, Wire Heat 5P6771/Flux Lot 0342 - Refitted Using Hyperbolic Tangent Curve-Fitting Method | C-32 |
| Figure C-13. Unirradiated Surveillance Charpy V-Notch Impact Data for HNP Heat-Affected-Zone Material - Refitted Using Hyperbolic Tangent Curve-Fitting Method | C-33 |
| Figure C-14. HNP Capsule U Surveillance Charpy V-Notch Impact Data for Heat-Affected-Zone Material - Refitted Using Hyperbolic Tangent Curve-Fitting Method | C-34 |
| Figure C-15. HNP Capsule V Surveillance Charpy V-Notch Impact Data for Heat-Affected-Zone Material - Refitted Using Hyperbolic Tangent Curve-Fitting Method | C-35 |
| Figure C-16. HNP Capsule X Surveillance Charpy V-Notch Impact Data for Heat-Affected-Zone Material - Refitted Using Hyperbolic Tangent Curve-Fitting Method | C-36 |

EXECUTIVE SUMMARY

This report describes the results of the examination of the fifth capsule removed (Capsule Z) as part of the Carolina Power & Light Company (CP&L) Shearon Harris Nuclear Power Plant (HNP) Reactor Vessel Surveillance Program (RVSP). The objective of the RVSP is to monitor the effects of neutron irradiation on the mechanical properties of the reactor vessel materials by testing and evaluation of tension test and Charpy V-notch impact specimens. The program was designed in accordance with the requirements of Code of Federal Regulations, Title 10, Part 50, (10 CFR 50) Appendix H and ASTM Standard E 185-82.

Capsule Z was removed from the HNP reactor vessel at the end-of-cycle 21 (EOC-21) for testing and evaluation. The capsule received an average fast fluence of $9.45 \times 10^{19} \text{ n/cm}^2$ ($E > 1.0 \text{ MeV}$). Based on the calculated twenty-one-cycle-average full power flux, the projected end-of-life (55 EFPY) peak fast fluence at the base metal-clad interface of the HNP reactor vessel is $6.87 \times 10^{19} \text{ n/cm}^2$.

The results of the tension tests indicated that the HNP surveillance materials exhibited normal behavior relative to the neutron fluence exposure. The Charpy impact data results for the HNP surveillance materials exhibited the characteristic behavior of transition temperature shifting to a higher temperature as a result of neutron fluence damage and a decrease in upper-shelf energy.

1.0 INTRODUCTION

This report presents the examination results of the fifth reactor vessel surveillance capsule (Capsule Z) removed from the Duke Energy Progress's Shearon Harris Nuclear Power Plant (HNP) reactor vessel. Note Capsule W was removed at the end-of-cycle 16 (EOC-16) and placed in storage; therefore, Capsule Z is the fifth capsule removed, but the fourth capsule tested for HNP. The capsule was removed and the contents evaluated after being irradiated in the HNP reactor vessel as part of the reactor vessel surveillance program (RVSP) documented in WCAP-10502^[1]. Capsule Z was removed at the EOC-21, the first scheduled outage where the capsule estimated fluence reached the projected 80 calendar year peak reactor pressure vessel (RPV) fluence of 9.15×10^{19} n/cm², which is consistent with the recommendations of MRP-326^[2]. This report describes the testing and the post irradiation data obtained from the HNP Capsule Z after receiving an average fluence of 9.45×10^{19} n/cm² ($E > 1.0$ MeV). The data are compared to previous HNP RVSP results from Capsule U^[3], Capsule V^[4], and Capsule X^[5].

The objective of the program is to monitor the effects of neutron irradiation on the mechanical properties of reactor vessel materials under actual plant operating conditions. The program was planned to monitor the effects of neutron irradiation on the reactor vessel materials for the 40 year design life of the RPV. The HNP RVSP was designed and furnished by Westinghouse Electric Corporation and was based on American Society for Testing and Materials (ASTM) Standard E 185-82^[6] and is in compliance with the Code of Federal Regulations, Title 10, Part 50, (10 CFR 50) Appendix H^[7]. The current HNP RVSP requirement for the current licensing basis (60 calendar years) is 10 CFR 50 Appendix H, ASTM E185-82, and NUREG-1801, Revision 2, per Accession No. ML11293A076^[8], requires HNP to test a surveillance capsule at the approximate 80 calendar year fluence. Reactor vessel surveillance Capsule Z is tested to meet this commitment in the HNP CLB RVSP.

2.0 BACKGROUND

The ability of the reactor vessel to resist fracture is a primary factor in ensuring the safety of the primary system in light water-cooled reactors. The reactor vessel beltline region is the most critical region of the vessel because it is exposed to the highest level of neutron irradiation. The general effects of fast neutron irradiation on the mechanical properties of low-alloy ferritic steels used in the fabrication of reactor vessels are well characterized and documented. The low-alloy ferritic steels used in the beltline region of reactor vessels exhibit an increase in ultimate and yield strength properties with a corresponding decrease in ductility after irradiation. The most significant mechanical property change in reactor vessel steels is the increase in the ductile-to-brittle transition temperature accompanied by a reduction in the Charpy upper-shelf energy (CvUSE) value.

10 CFR 50 Appendix G, *"Fracture Toughness Requirements,"*^[9] specifies minimum fracture toughness requirements for the ferritic materials of the pressure-retaining components of the reactor coolant pressure boundary (RCPB) of light water-cooled power reactors and provides specific guidelines for determining the pressure-temperature limitations for operation of the RCPB. The fracture toughness and operational requirements are specified to provide adequate safety margins during any condition of normal operation, including anticipated operational occurrences and system hydrostatic tests, to which the pressure boundary may be subjected over its service lifetime. Although the requirements of 10 CFR 50, Appendix G, became effective on August 16, 1973, the requirements are applicable to all boiling and pressurized water-cooled nuclear power reactors, including those under construction or in operation on the effective date.

10 CFR 50, Appendix H, *"Reactor Vessel Materials Surveillance Program Requirements,"* defines the material surveillance program required to monitor changes in the fracture toughness properties of ferritic materials in the reactor vessel beltline region of water-cooled reactors resulting from exposure to neutron irradiation and the thermal environment. Fracture toughness test data are obtained from material specimens contained in capsules that are periodically withdrawn from the reactor vessel. These data permit determination of the conditions under which the vessel can be operated with adequate safety margins against non-ductile fracture throughout its service life.

A method for guarding against non-ductile fracture in reactor vessels is described in Appendix G to the American Society of Mechanical Engineers (ASME) Boiler and Pressure Vessel (B&PV) Code, Section III, *"Rules for Construction of Nuclear Facility Components"*^[10] and Section XI, *"Rules for Inservice Inspection of Nuclear Power Plant Components"*^[11]. This method uses fracture mechanics concepts and the reference nil-ductility temperature, RT_{NDT} which is defined as the greater of the drop weight nil-ductility transition temperature (in accordance with ASTM E 208-91^[12]) or the temperature that is 60°F below that at which the material exhibits 50 ft-lbs and 35 mils lateral expansion. The RT_{NDT} of a given material is used to index that material to a reference stress intensity factor curve (K_{IR} curve), which appears in Appendix G of ASME B&PV Code Section III and Section XI. The K_{IR} curve is a lower bound of dynamic and crack arrest fracture toughness data obtained from several heats of pressure vessel steel. When a given material is indexed to the K_{IR} curve, allowable stress intensity factors can be obtained for the material as a function of temperature. The operating limits can then be determined using these allowable stress intensity factors.

The RT_{NDT} and, in turn, the operating limits of a nuclear power plant, are adjusted to account for the effects of irradiation on the fracture toughness of the reactor vessel materials. The irradiation embrittlement and the resultant changes in mechanical properties of a given pressure vessel steel can be monitored by a surveillance program in which surveillance capsules containing prepared specimens of the

reactor vessel materials are periodically removed from the operating nuclear reactor and the specimens are tested. The increase in the Charpy V-notch 30 ft-lb temperature is added to the original RT_{NDT} to adjust it for irradiation embrittlement. The adjusted RT_{NDT} is used to index the material to the K_{IR} curve which, in turn, is used to set operating limits for the nuclear power plant. These new limits take into account the effects of irradiation on the reactor vessel materials.

10 CFR 50, Appendix G, also requires a minimum initial CvUSE of 75 ft-lbs for all beltline region materials unless it is demonstrated that lower values of upper-shelf fracture energy will provide an adequate margin of safety against fracture equivalent to those required by ASME Section XI, Appendix G. No action is required for a material that does not meet the initial 75 ft-lbs requirement provided that the irradiation embrittlement does not cause the CvUSE to drop below 50 ft-lbs. The regulations specify that if the CvUSE drops below 50 ft-lbs, it must be demonstrated, in a manner approved by the Office of Nuclear Reactor Regulation, that the lower values will provide adequate margins of safety.

3.0 SURVEILLANCE PROGRAM DESCRIPTION

The reactor vessel surveillance program for HNP includes six capsules designed to monitor the effects of neutron and thermal environment on the materials of the reactor pressure vessel core region. The capsules, which were inserted into the reactor vessel before initial plant startup, were positioned inside the reactor vessel between the neutron shielding pads and the vessel wall at the locations shown in Figure 3-1. The six capsules, designed to be placed in holders attached to the neutron shield pads, are positioned near the peak axial and azimuthal neutron flux. WCAP-10502 includes a full description of the capsule locations and design. Capsule Z was irradiated in the 340° position during the time of irradiation in the reactor vessel (cycles 1 through 21).

Capsule Z was removed during the twenty-first refueling shutdown (EOC 21) of the HNP plant. The capsule contained Charpy V-notch (CVN) impact test specimens fabricated from one base metal plate (SA-533, Grade B, Class 1), heat-affected-zone (HAZ) material, and a weld metal representative of the HNP reactor vessel beltline region intermediate to lower shell circumferential weld. The tensile test specimens were fabricated from the same base metal plate and weld metal. In addition, specimens were included for determining the fracture toughness of both the base metal plate and the weld metal. The number of specimens of each material contained in Capsule Z is described in Table 3-1, and the location of the individual specimens within the capsule is shown in Figure 3-2. The chemical compositions of the surveillance materials in Capsule Z, obtained from the original surveillance program report^[1] are described in Table 3-2. In addition, six irradiated base metal and weld metal Charpy specimens from Capsule U were previously analyzed by emission spectrograph to determine the copper and nickel contents^[3]. The results of these analyses are presented in Table 3-3. The heat treatment of the surveillance materials in Capsule Z is presented in Table 3-4.

All base metal specimens were machined from the 1/4-thickness (1/4T) location of the plate material after stress relieving. The base metal, HAZ material, and weld metal specimens were oriented such that the longitudinal axis of the specimen was either parallel or perpendicular to the principal working direction of the plate.

Capsule Z contained dosimeter wires of copper, iron, nickel, and aluminum-0.15 weight percent cobalt (cadmium-shielded and unshielded) and cadmium-shielded neptunium-237 (²³⁷Np) and uranium-238 (²³⁸U). The location of these dosimeters within Capsule Z is shown in Figure 3-2.

Thermal monitors fabricated from two low-melting alloys were included in the capsule. The thermal monitors were sealed in Pyrex tubes and inserted in spacers located in Figure 3-2. The eutectic alloys and their melting points are listed below:

2.5% Ag, 97.5% Pb

Melting Point 579°F

1.5% Ag, 1.0% Sn, 97.5% Pb

Melting Point 590°F

Table 3-1. Test Specimens Contained in HNP Capsule Z

| Material Description | Number of Test Specimens | | | |
|---|--------------------------|------------|---------|----------|
| | Tension | CVN Impact | Compact | Bend Bar |
| Base Metal Plate (Heat No. B4197-2) | | | | |
| Longitudinal | 3 | 15 | 4 | -- |
| Transverse | 3 | 15 | 4 | 1 |
| HAZ Metal | -- | 15 | -- | -- |
| Weld Metal (Wire Ht. 5P6771/ Flux Lot 0342) | 3 | 15 | 4 | -- |
| Total | 9 | 60 | 12 | 1 |

Table 3-2. Chemical Composition of HNP Capsule Z Surveillance Materials

| Element | Chemical Composition, wt% | |
|----------------|--|---|
| | Base Metal Plate (Heat No. B4197-2) | Weld Metal (Wire Ht. 5P6771/ Flux Lot 0342) |
| C | 0.22 | 0.04 |
| Mn | 1.34 | 1.23 |
| P | 0.014 | 0.006 |
| S | 0.016 | 0.006 |
| Si | 0.37 | 0.41 |
| Ni | 0.49 | 0.87 |
| Mo | 0.50 | 0.48 |
| Cr | 0.095 | 0.068 |
| Cu | 0.073 | 0.023 |
| Al | 0.043 | 0.018 |
| Co | 0.011 | 0.009 |
| Pb | 0.001 | <0.005 |
| W | Not detected | 0.02 |
| Ti | 0.004 | <0.001 |
| Zr | Not detected | <0.001 |
| V | Not detected | <0.008 |
| Sn | 0.006 | 0.09 |
| As | 0.007 | <0.005 |
| Cb | Not detected | <0.005 |
| N ₂ | 0.007 | 0.005 |
| B | <0.001 | 0.011 |

**Table 3-3. Chemical Analysis Results of Selected Charpy Specimens
from HNP Capsule U for Copper and Nickel Contents**

| Material | Charpy Specimen | Copper, wt% | Nickel, wt% |
|---|------------------------|--------------------|--------------------|
| Base Metal Plate (Heat No. B4197-2) | QL1 | 0.090 | 0.52 |
| | QL8 | 0.095 | 0.51 |
| | QL12 | 0.088 | 0.50 |
| Weld Metal (Wire Ht. 5P6771/ Flux Lot 0342) | QW1 | 0.026 | 0.94 |
| | QW12 | 0.019 | 1.07 |
| | QW13 | 0.029 | 0.95 |

Table 3-4. Heat Treatment of the Surveillance Materials in Capsule Z

| Heat No. | Temp. (°F) | Time (h) | Cooling |
|-----------------|-------------------|-----------------|----------------|
| B4197-2 | 1575-1625 | 4 | Water quenched |
| | 1225-1275 | 4 | Air cooled |
| | 1050 | 4 | Air cooled |
| Weld metal | 1100-1175 | 35.75 | Furnace cooled |
| | 1100-1175 | 10.25 | Furnace cooled |

Figure 3-1. Reactor Vessel Cross Section Showing Location of Capsule Z in Shearon Harris Unit 1

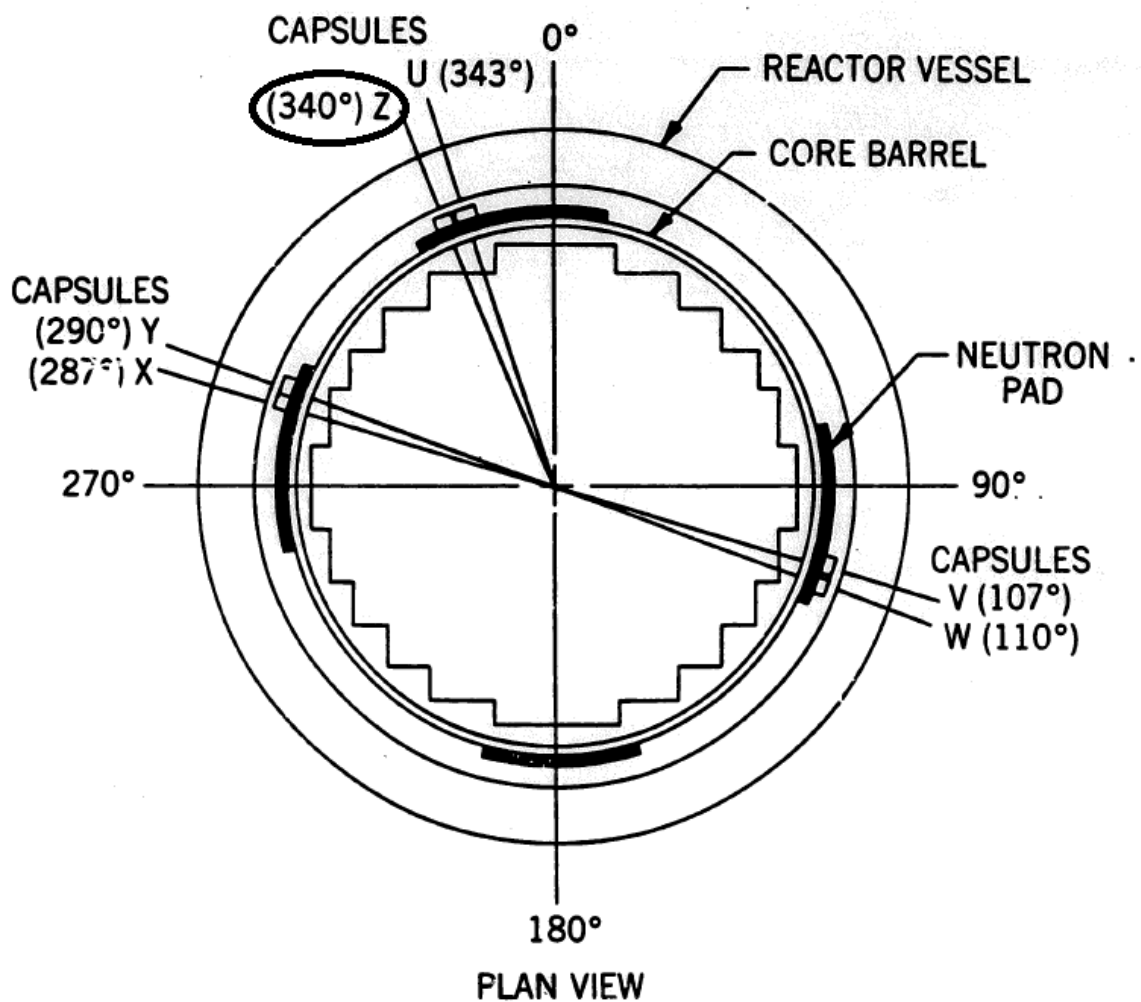
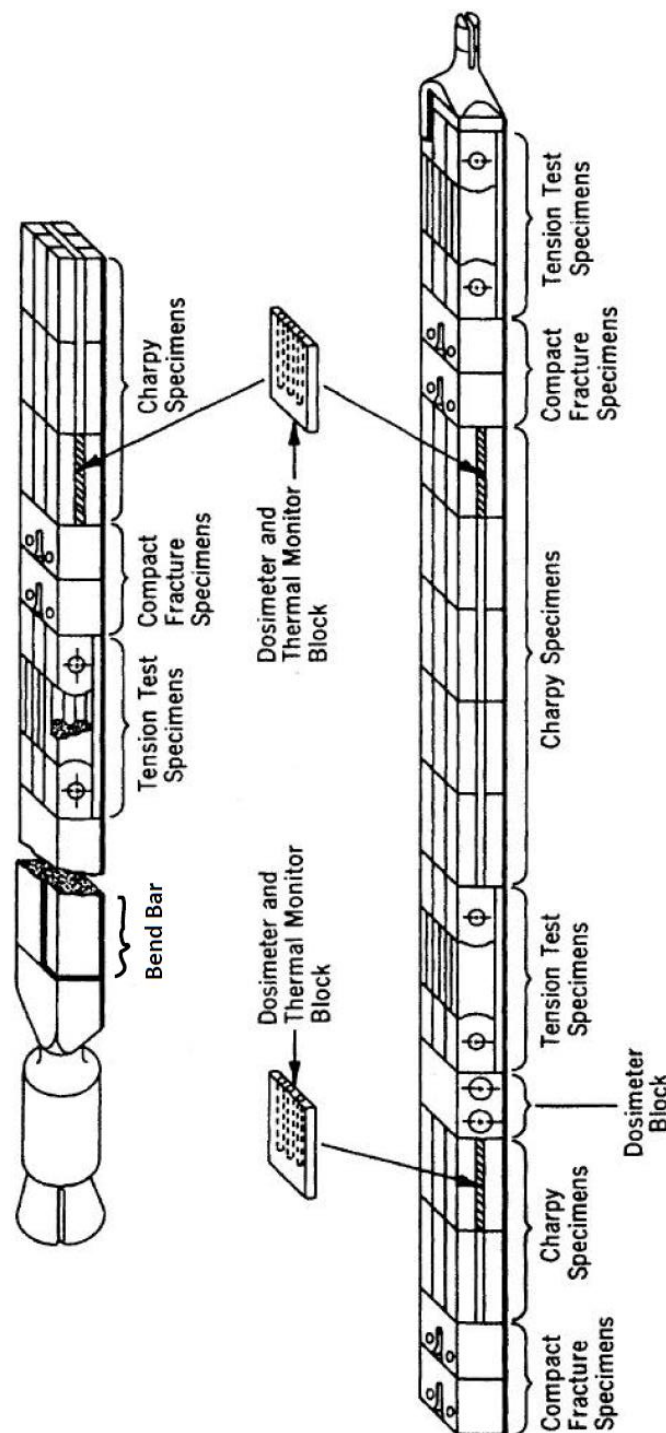


Figure 3-2. Surveillance Capsule Assembly Showing Location of Specimens and Monitors for HNP Capsule Z



4.0 TESTS OF UNIRRADIATED MATERIAL

Unirradiated material was evaluated for two purposes: (1) to establish baseline data to which irradiated properties data could be compared; and (2) to determine those material properties as required for compliance with 10 CFR 50, Appendices G and H.

Westinghouse Electric Corporation, as part of the development of the HNP RVSP, performed the testing of the unirradiated surveillance material. The details of the testing procedures are described in Westinghouse Electric Corporation Report WCAP-10502^[1]. The unirradiated mechanical properties for the HNP RVSP materials are summarized in Appendices B and C of this report.

The original unirradiated Charpy V-notch impact data were evaluated based on hand-fit Charpy curves generated using engineering judgment. These data were re-evaluated herein using a hyperbolic tangent curve-fitting program, and the results of the re-evaluation are presented in Appendix C. In addition, Appendix D contains a comparison of the Charpy V-notch shift results for each surveillance material, hand-fit versus hyperbolic tangent curve-fit.

5.0 POST-IRRADIATION TESTING

The post-irradiation testing of the tension test specimens, the Charpy V-notch impact specimens, thermal monitors, and dosimeters for the HNP Capsule Z was performed at the BWX Technologies, Inc. (BWXT) Lynchburg Technology Center (LTC)^[13].

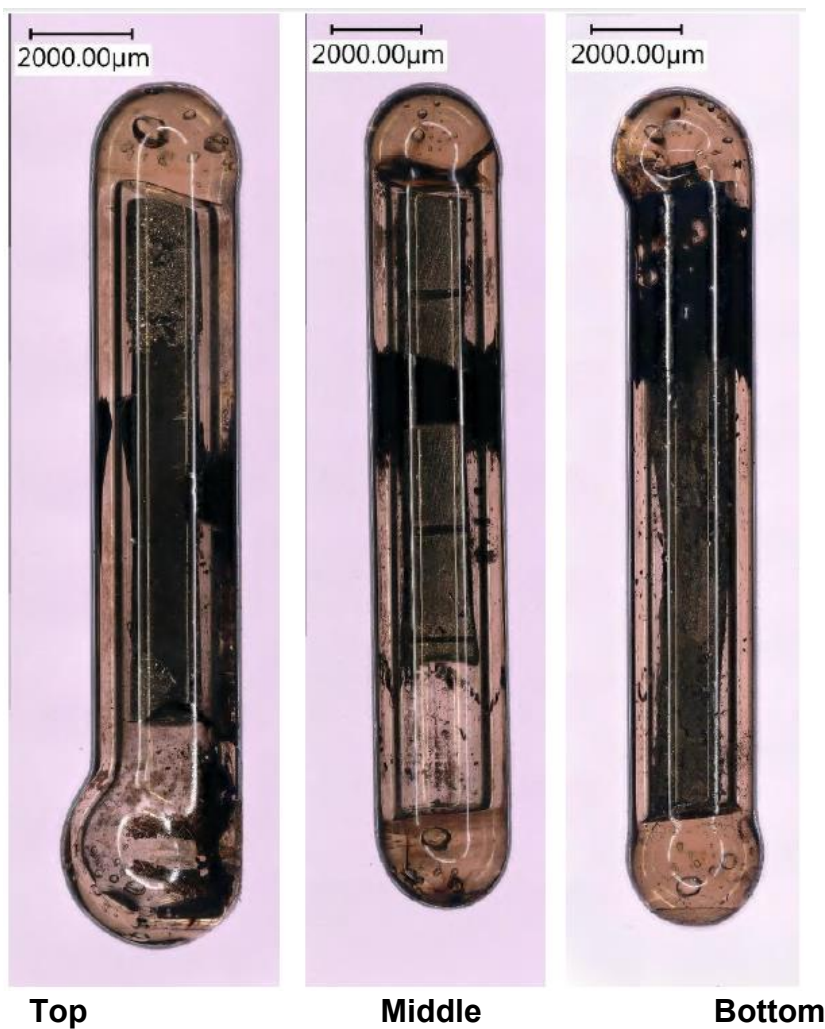
5.1 *Capsule Disassembly and Inventory*

After capsule disassembly, the contents of Capsule Z were inventoried and found to be consistent with the surveillance program report inventory (WCAP-10502). The capsule contained a total of 60 standard Charpy V-notch specimens, nine (9) tensile specimens, twelve (12) 0.5T compact fracture specimens, one (1) bend bar specimen, four (4) dosimetry blocks, and three (3) temperature monitors.

5.2 *Thermal Monitors*

The low-melting point (579°F and 590°F) eutectic alloys contained in Capsule Z were examined to reveal the shape of the monitors and examined for evidence of melting. No indication of melting was observed (see Figure 5-1). Therefore, based on this examination, the maximum temperature that the capsule test specimens were exposed to was less than 579°F.

**Figure 5-1. Photographs of Thermal Monitors Removed from the HNP
RVSP Capsule Z**



5.3 Tension Test Results

The results of the post-irradiation tension test are presented in Table 5-1, and the stress-strain curves are presented in Figures 5-2 through 5-10. Tests were performed at 100°F, 175°F, 200°F, 250°F, 275°F, 300°F, and the HNP operating temperature (550°F). The tests were performed using a MTS 25 ton/55 kip Model #312.31 Serial #435 servo-hydraulic test machine. The test machine was interfaced with the MTS FlexTest controller. The gripping devices used were a pin and clevis design fabricated specifically for RVSP tension specimens. A BWXT certified MTS program TestWare Elite was used to control the machine and acquire the data. All tension tests were run using a constant free running crosshead speed of 0.01875 inch per minute throughout the entirety of the test. The tension testing was performed in accordance with the applicable requirements of ASTM Standard E 8-96a^[14] and ASTM Standard E 21-92^[15]. Photographs of the tension test specimen fractured surfaces are shown in Figures 5-11 through 5-19.

Table 5-1. Tensile Properties of HNP Capsule Z Reactor Vessel Surveillance Materials, Irradiated to 9.45×10^{19} n/cm² (E>1.0 MeV)

| Material | Specimen No. | Test Temp. [°F] | Strength | | Fracture Properties | | | Elongation | | Reduction in Area [%] |
|--|--------------|-----------------|-------------|----------------|---------------------|--------------|----------------|-------------|-----------|-----------------------|
| | | | Yield [ksi] | Ultimate [ksi] | Load [lb] | Stress [ksi] | Strength [ksi] | Uniform [%] | Total [%] | |
| Base Metal Plate Heat No. B4197-2 Longitudinal | QL-18 | 176.3 | 83.1 | 103.1 | 2915 | 121.4 | 59.4 | 9.0 | 20.91 | 51.11 |
| | QL-17 | 275.2 | 78.5 | 99.8 | 3397 | 139.2 | 69.2 | 9.1 | 19.08 | 50.29 |
| | QL-16 | 550.0 | 76.6 | 104.0 | 4265 | 139.8 | 86.9 | 9.9 | 17.02 | 37.87 |
| Base Metal Plate Heat No. B4197-2 Transverse | QT-17 | 201.3 | 82.8 | 100.6 | 3707 | 154.4 | 75.5 | 9.0 | 18.97 | 51.11 |
| | QT-16 | 301.3 | 86.4 | 101.5 | 3455 | 134.4 | 70.4 | 7.2 | 16.26 | 47.64 |
| | QT-18 | 550.8 | 81.1 | 104.7 | 4202 | 136.0 | 85.6 | 8.3 | 16.48 | 37.05 |
| Weld Metal Wire Heat 5P6771/ Flux Lot 0342 | WQ-18 | 100.9 | 91.3 | 100.5 | 3342 | 172.2 | 68.1 | 9.5 | 23.35 | 60.48 |
| | WQ-16 | 250.4 | 77.3 | 95.2 | 3189 | 160.2 | 65.0 | 9.3 | 22.23 | 59.46 |
| | QW-17 | 550.9 | 80.4 | 97.3 | 3396 | 148.9 | 69.2 | 4.9 | 22.67 | 53.55 |

Figure 5-2. Tension Test Stress-Strain Curve for Base Metal Plate, Heat No. B4197-2, Longitudinal Orientation, Specimen No. QL18, Tested at 175°F

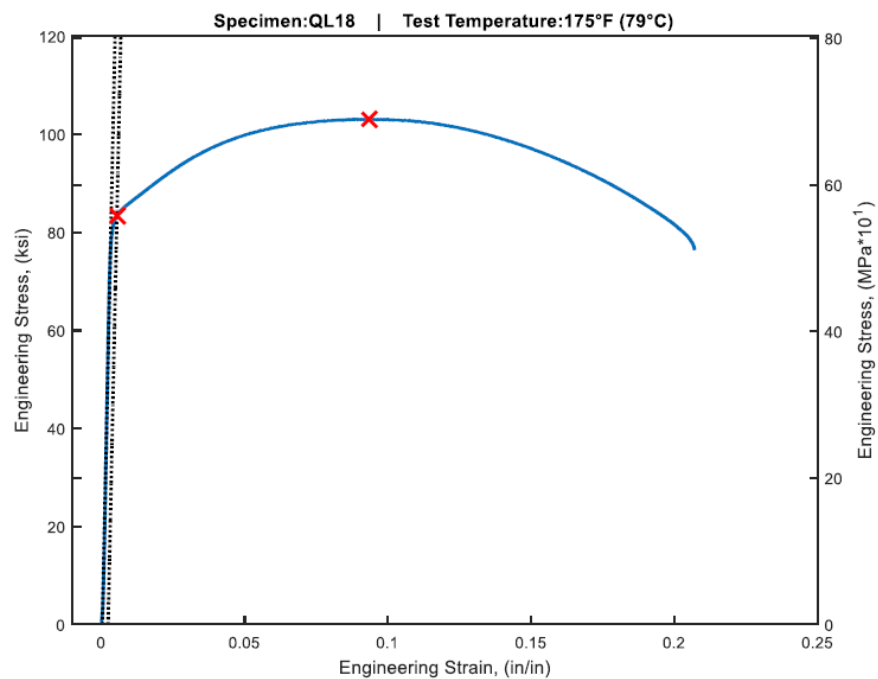


Figure 5-3. Tension Test Stress-Strain Curve for Base Metal Plate, Heat No. B4197-2, Longitudinal Orientation, Specimen No. QL17, Tested at 275°F

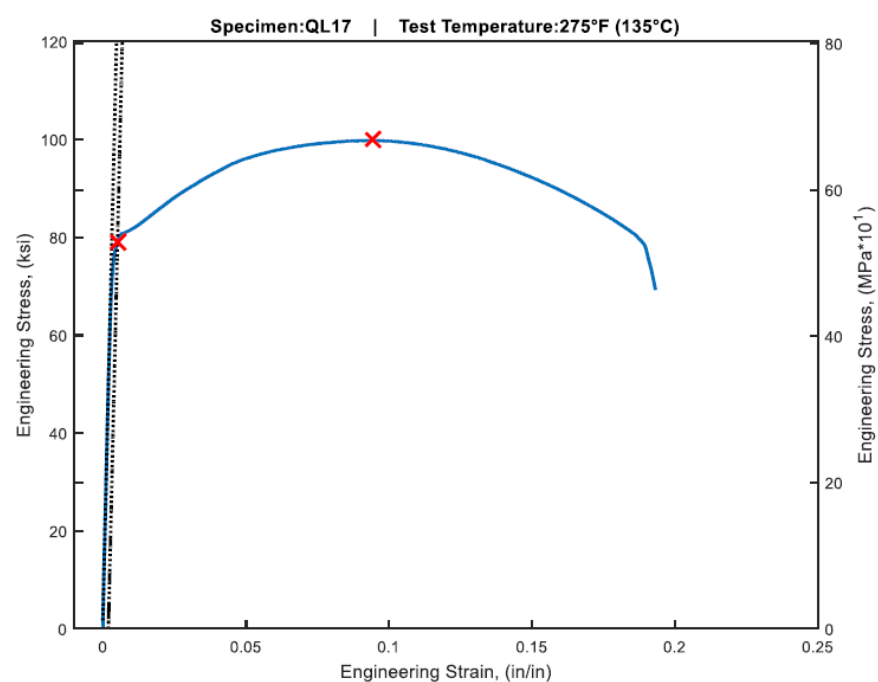


Figure 5-4. Tension Test Stress-Strain Curve for Base Metal Plate, Heat No. B4197-2, Longitudinal Orientation, Specimen No. QL16, Tested at 550°F

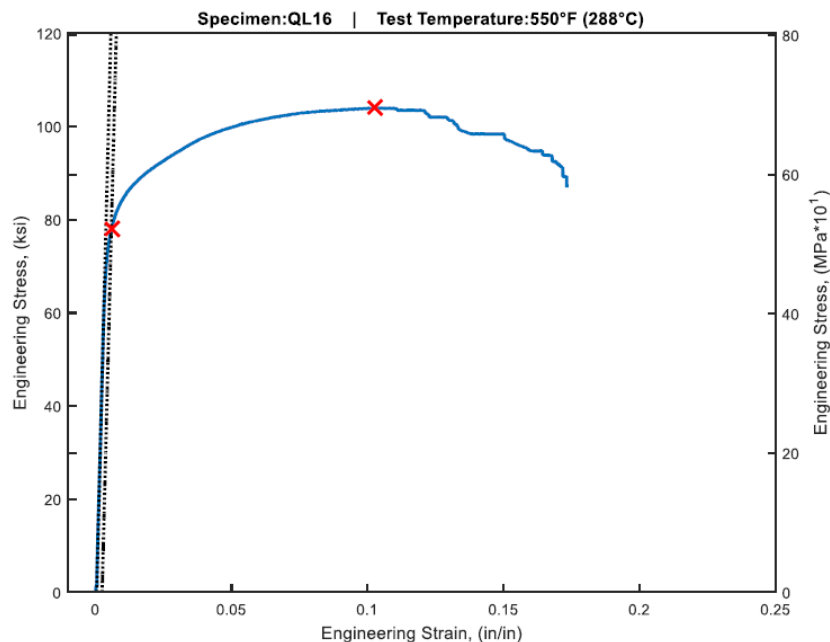


Figure 5-5. Tension Test Stress-Strain Curve for Base Metal Plate, Heat No. B4197-2, Transverse Orientation, Specimen No. QT17, Tested at 200°F

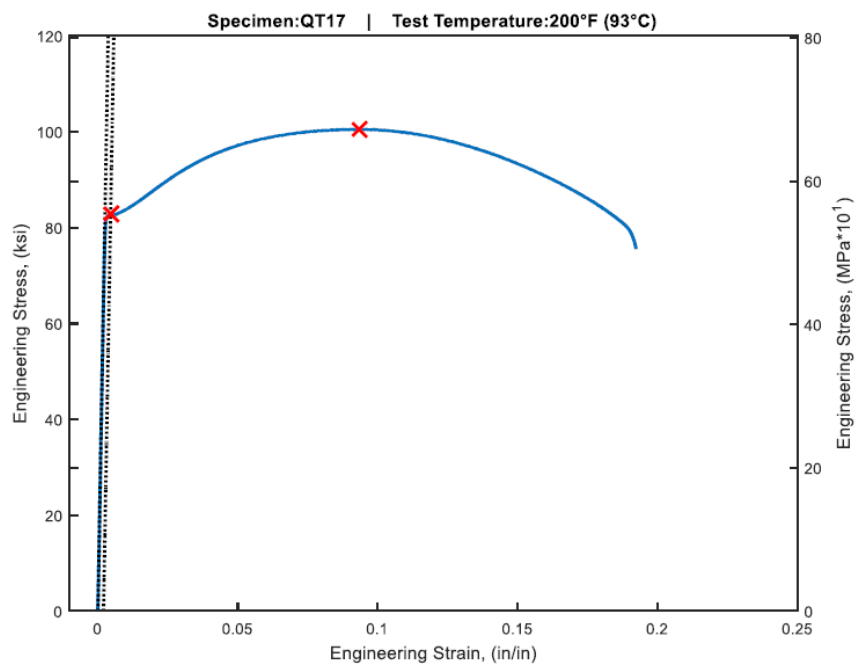


Figure 5-6. Tension Test Stress-Strain Curve for Base Metal Plate, Heat No. B4197-2, Transverse Orientation, Specimen No. QT16, Tested at 300°F

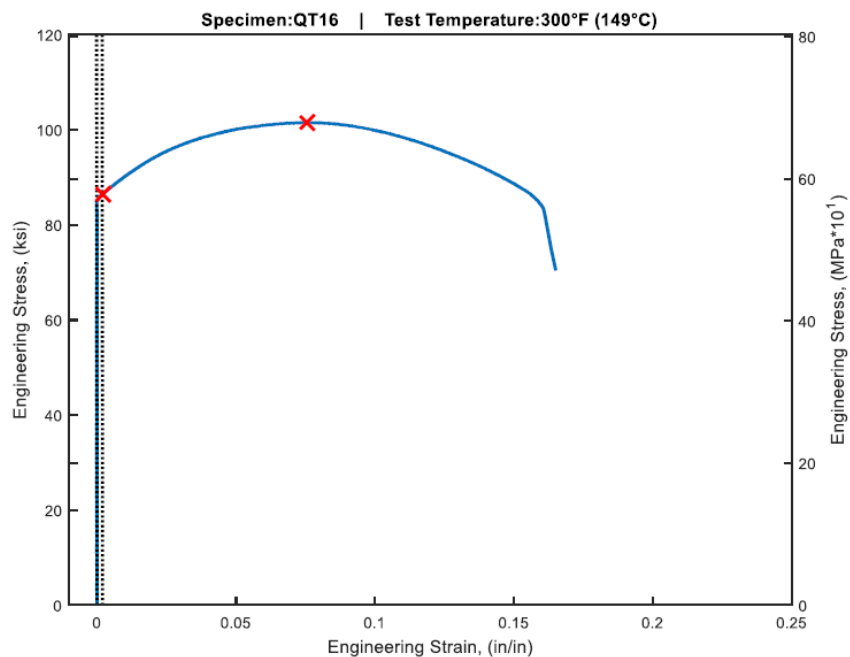


Figure 5-7. Tension Test Stress-Strain Curve for Base Metal Plate, Heat No. B4197-2, Transverse Orientation, Specimen No. QT18, Tested at 550°F

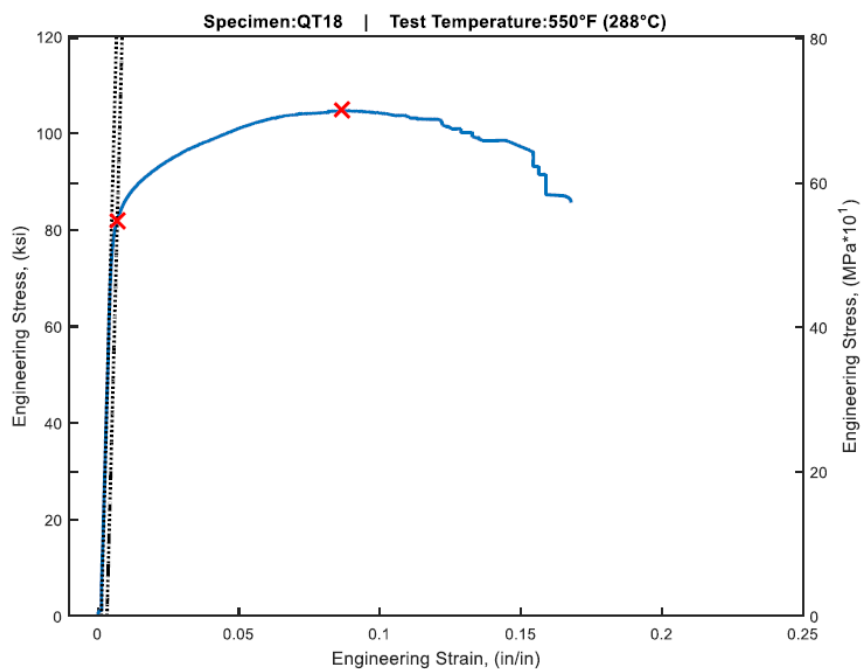


Figure 5-8. Tension Test Stress-Strain Curve for Weld Metal, Wire Heat 5P6771/Flux Lot 0342, Specimen No. QW18, Tested at 100°F

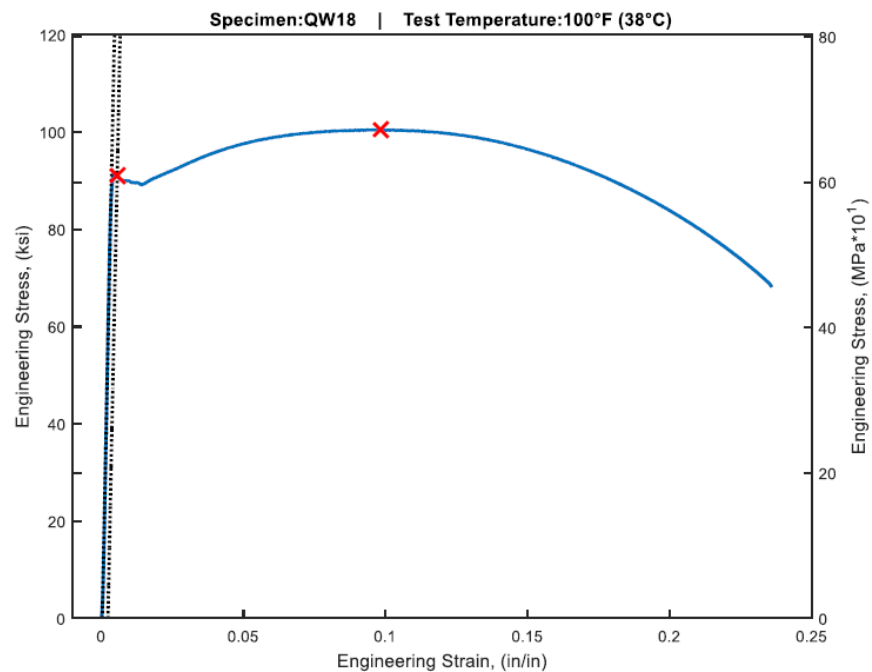


Figure 5-9. Tension Test Stress-Strain Curve for Weld Metal, Wire Heat 5P6771/Flux Lot 0342, Specimen No. QW16, Tested at 250°F

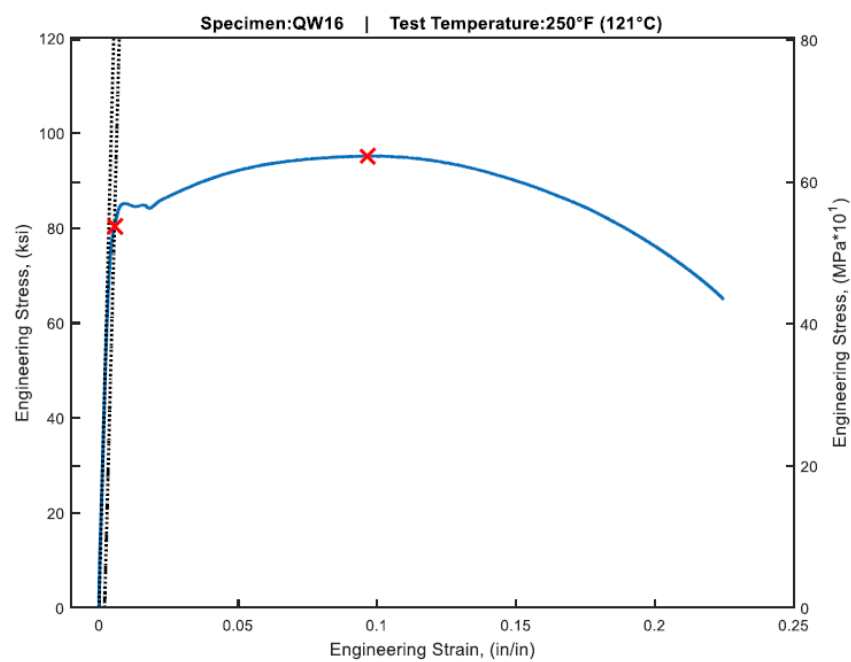


Figure 5-10. Tension Test Stress-Strain Curve for Weld Metal, Wire Heat 5P6771/Flux Lot 0342, Specimen No. QW17, Tested at 550°F

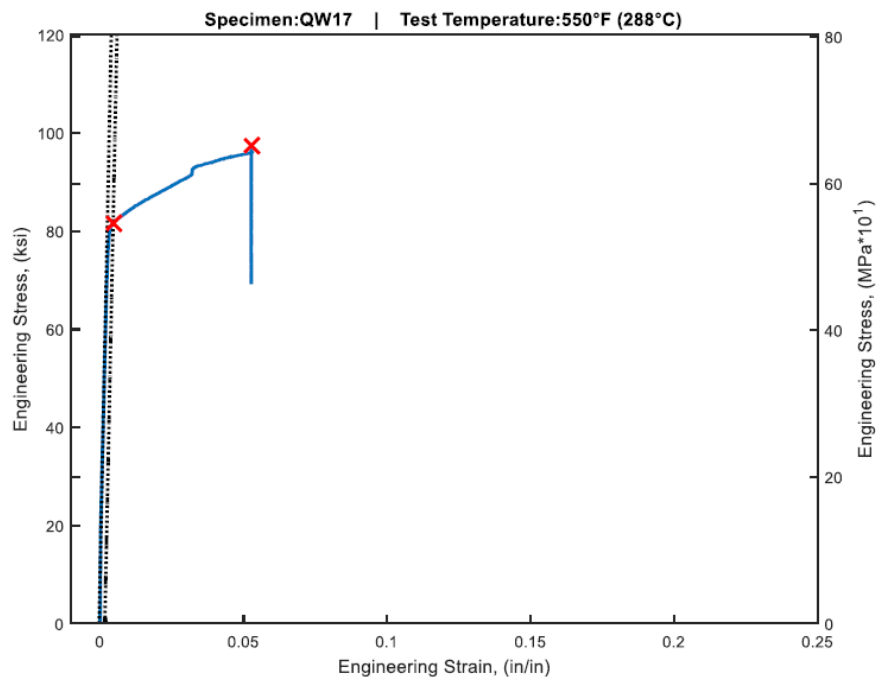


Figure 5-11. Photographs of Tested Tension Test Specimen QL-18 and Corresponding Fracture Surfaces – Base Metal Plate, Heat No. B4197-2, Longitudinal Orientation, 175°F

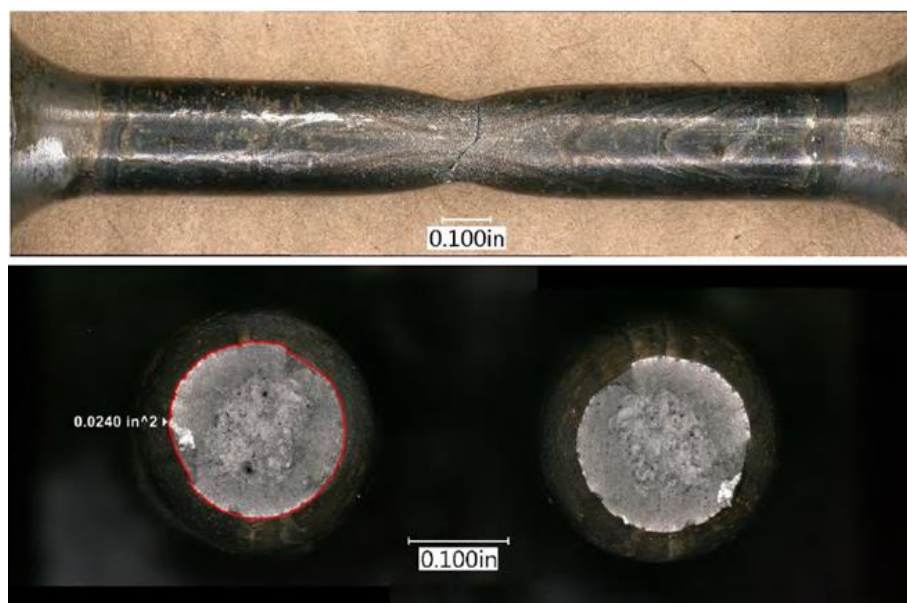


Figure 5-12. Photographs of Tested Tension Test Specimen QL-17 and Corresponding Fracture Surfaces – Base Metal Plate, Heat No. B4197-2, Longitudinal Orientation, 275°F

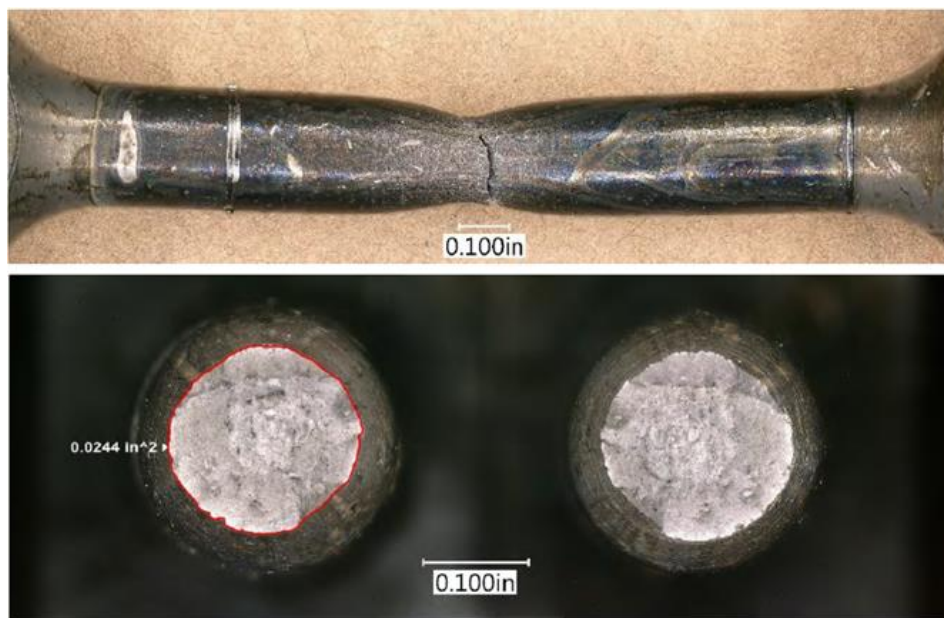


Figure 5-13. Photographs of Tested Tension Test Specimen QL-16 and Corresponding Fracture Surfaces – Base Metal Plate, Heat No. B4197-2, Longitudinal Orientation, 550°F

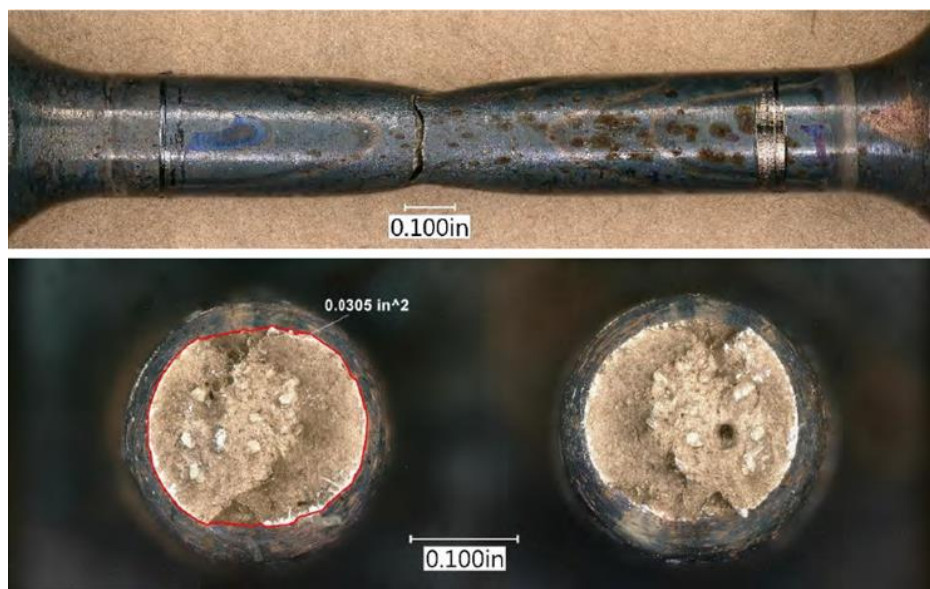


Figure 5-14. Photographs of Tested Tension Test Specimen QT-17 and Corresponding Fracture Surfaces – Base Metal Plate, Heat No. B4197-2, Transverse Orientation, 200°F

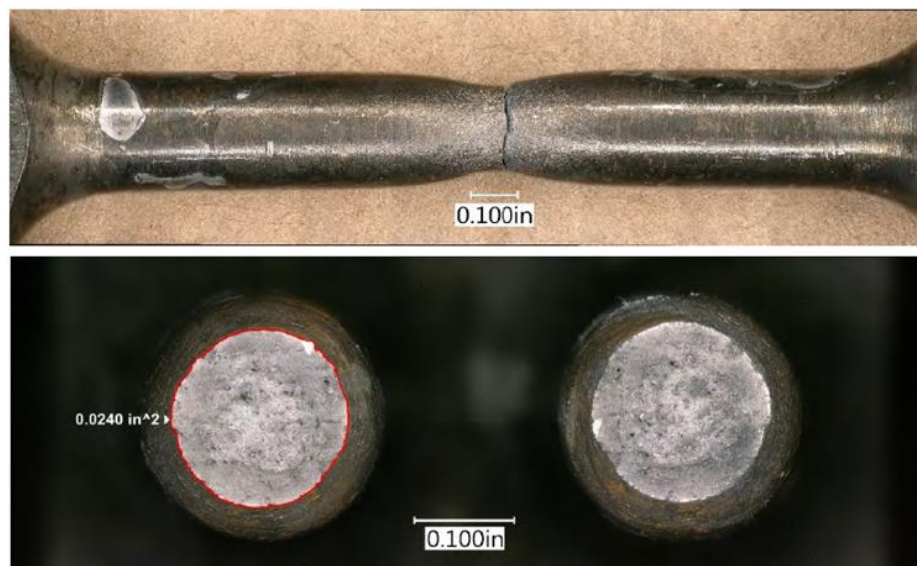


Figure 5-15. Photographs of Tested Tension Test Specimen QT-16 and Corresponding Fracture Surfaces – Base Metal Plate, Heat No. B4197-2, Transverse Orientation, 300°F

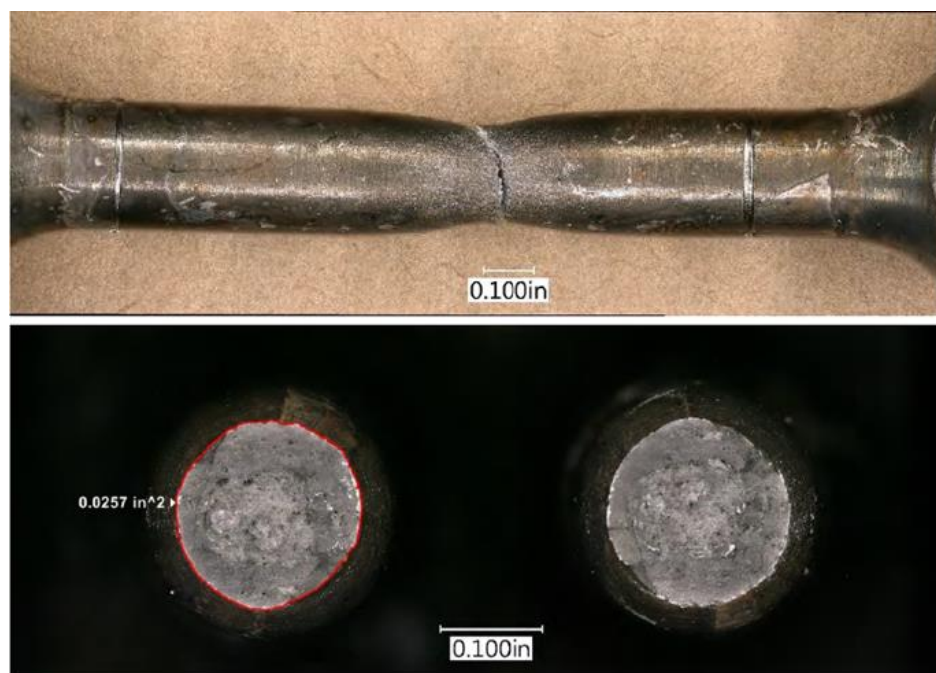


Figure 5-16. Photographs of Tested Tension Test Specimen QT-18 and Corresponding Fracture Surfaces – Base Metal Plate, Heat No. B4197-2, Transverse Orientation, 550°F



Figure 5-17. Photographs of Tested Tension Test Specimen QW-18 and Corresponding Fracture Surfaces – Weld Metal, Wire Heat 5P6771/Flux Lot 0342, 100°F

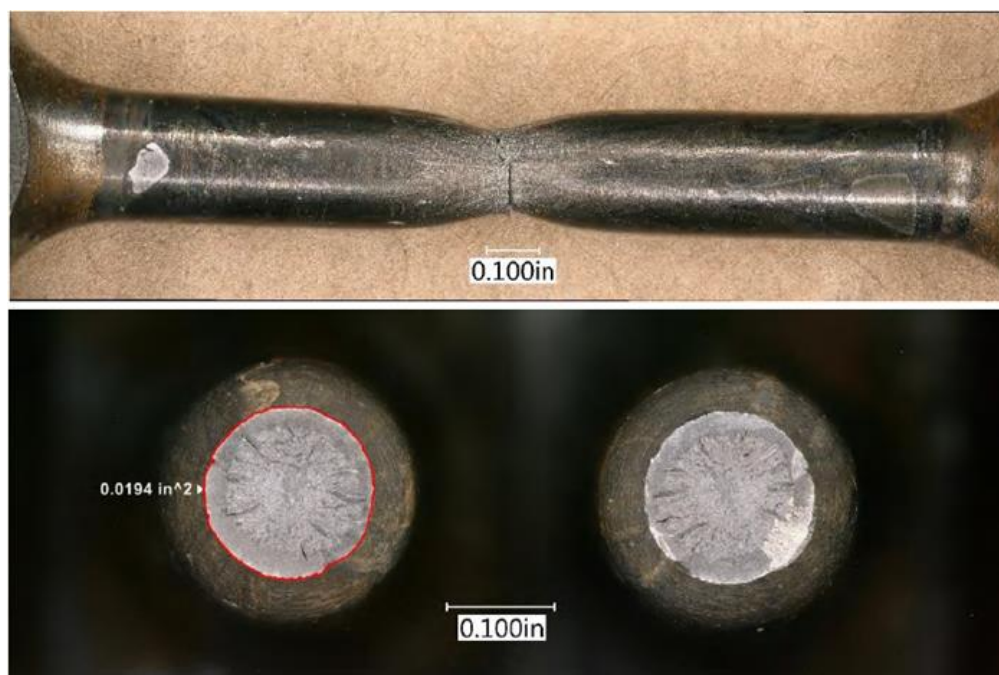


Figure 5-18. Photographs of Tested Tension Test Specimen QW-16 and Corresponding Fracture Surfaces – Weld Metal, Wire Heat 5P6771/Flux Lot 0342, 250°F

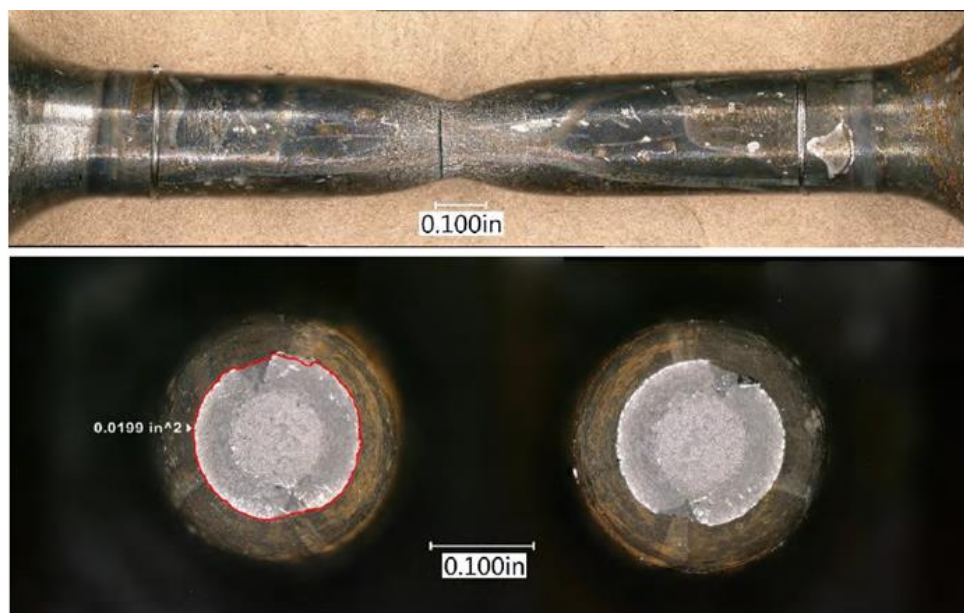
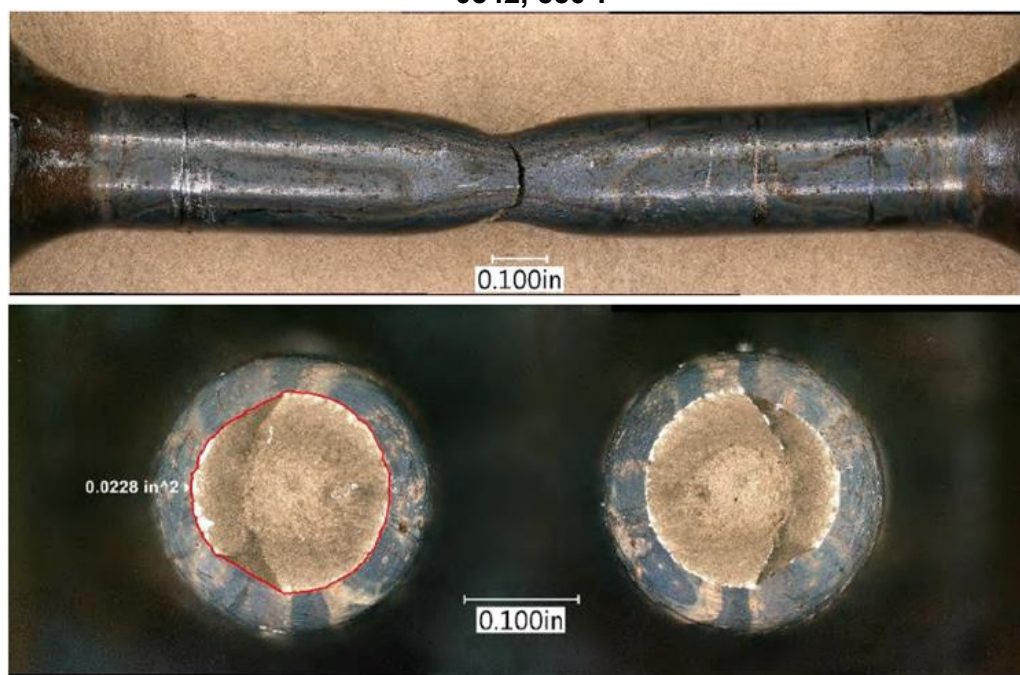


Figure 5-19. Photographs of Tested Tension Test Specimen QW-17 and Corresponding Fracture Surfaces – Weld Metal, Wire Heat 5P6771/Flux Lot 0342, 550°F



5.4 Charpy V-Notch Impact Test Results

The Charpy V-notch impact testing was performed in accordance with the applicable requirements of ASTM Standard E 23-91^[16]. Impact energy, lateral expansion, and percent shear fracture were measured at numerous test temperatures and recorded for each specimen. The impact energy was measured using a certified Satec SI-IK Impact tester (traceable to NIST Standard) with a striker velocity of 5.18 m/s (16.99 ft/sec) and 240 ft-lb of available energy and an accuracy of ± 1 ft-lb or 5% of the dial reading, whichever is larger. The lateral expansion was measured using a certified dial indicator. The specimen percent shear was estimated by examining high resolution fracture face images taken on a certified digital microscope and comparison with the visual standards presented in ASTM Standard E 23-91. Test temperatures were controlled to within $\pm 2^\circ\text{F}$ per ASTM E23 within circulating oil heating and alcohol cooling baths using thermocouples certified to ASTM E230. Charpy verification specimens, along with a completed questionnaire are shipped to the National Institute of Standards and Technology (NIST). The specimen's results are analyzed by NIST and average values were found to be within acceptable ranges at the energy levels tested, in accordance with ASTM E23 standards.

The results of the Charpy V-notch impact testing are shown in Tables 5-2 through 5-5 and Figures 5-20 through 5-23. The curves were generated using a hyperbolic tangent curve-fitting program, CVGRAPH, Version 5.0.1, a certified hyperbolic tangent curve-fitting program, to produce the best-fit curve through the data. The hyperbolic tangent (TANH) function (test response, i.e., absorbed energy, lateral expansion, and percent shear fracture, "R," as a function of test temperature, "T") used to evaluate the surveillance data is as follows:

$$R = A + B * \tanh \left[\frac{T - T_0}{C} \right]$$

The Charpy V-notch data was entered, and the coefficients A , B , T_0 , and C are determined by the program minimizing the sum of the errors squared (least-squares fit) of the data points about the fitted curve. Using these coefficients and the above TANH function, a smooth curve is generated through the data for interpretation of the material transition region behavior. The coefficients determined for irradiated materials in Capsule Z are shown in Table 5-6.

Photographs of the Charpy V-notch specimen fracture surfaces are presented in Figures 5-24 through 5-27.

Table 5-2. Charpy V-Notch Impact Results for HNP Capsule Z Base Metal Plate, Heat No. B4197-2, Irradiated to 9.45×10^{19} n/cm² (E>1.0 MeV) Longitudinal (LT) Orientation

| Specimen No. | Test Temp. [°F] | Impact Energy [ft-lbs] | Lateral Expansion [mils] | Shear Fracture [%] |
|--------------|-----------------|------------------------|--------------------------|--------------------|
| QL-83 | 67.4 | 6.0 | 3.5 | 10 |
| QL-87 | 100.7 | 15.5 | 12.5 | 20 |
| QL-81 | 125.1 | 20.0 | 18.5 | 30 |
| QL-78 | 150.6 | 22.0 | 18.0 | 40 |
| QL-84 | 175.6 | 30.5 | 27.5 | 45 |
| QL-82 | 200.3 | 34.0 | 30.5 | 60 |
| QL-86 | 224.9 | 45.0 | 42.0 | 75 |
| QL-76 | 249.8 | 57.0 | 51.0 | 90 |
| QL-89 | 275.0 | 54.0 | 47.0 | 100 |
| QL-85 | 300.0 | 63.0 | 54.5 | 100 |
| QL-79 | 350.5 | 59.0 | 51.0 | 100 |
| QL-88 | 399.9 | 64.0 | 60.0 | 100 |
| QL-77 | 425.0 | 66.0 | 56.0 | 100 |
| QL-90 | 450.2 | 64.0 | 54.0 | 100 |
| QL-80 | 475.0 | 69.0 | 53.0 | 100 |

Table 5-3. Charpy V-Notch Impact Results for HNP Capsule Z Base Metal Plate, Heat No. B4197-2, Irradiated to 9.45×10^{19} n/cm² (E>1.0 MeV) Transverse (TL) Orientation

| Specimen No. | Test Temp. [°F] | Impact Energy [ft-lbs] | Lateral Expansion [mils] | Shear Fracture [%] |
|--------------|-----------------|------------------------|--------------------------|--------------------|
| QT-78 | 67.4 | 5.0 | 4.5 | 10 |
| QT-90 | 100.9 | 13.0 | 8.5 | 15 |
| QT-82 | 125.4 | 15.5 | 13.0 | 25 |
| QT-87 | 150.5 | 16.0 | 15.0 | 40 |
| QT-89 | 175.7 | 24.5 | 23.0 | 45 |
| QT-83 | 200.2 | 30.0 | 23.5 | 50 |
| QT-80 | 224.8 | 34.5 | 32.0 | 70 |
| QT-84 | 249.6 | 45.0 | 38.0 | 80 |
| QT-88 | 275.0 | 46.5 | 42.0 | 95 |
| QT-79 | 300.1 | 52.0 | 43.0 | 100 |
| QT-76 | 350.5 | 49.0 | 44.0 | 100 |
| QT-77 | 401.0 | 54.0 | 53.0 | 100 |
| QT-86 | 425.0 | 49.0 | 47.0 | 100 |
| QT-85 | 450.2 | 54.5 | 49.0 | 100 |
| QT-81 | 475.0 | 54.5 | 46.0 | 100 |

Table 5-4. Charpy V-Notch Impact Results for HNP Capsule Z Weld Metal, Wire Heat No. 5P6771/Flux Lot 0342, Irradiated to 9.45×10^{19} n/cm² (E>1.0 MeV)

| Specimen No. | Test Temp. [°F] | Impact Energy [ft-lbs] | Lateral Expansion [mils] | Shear Fracture [%] |
|--------------|-----------------|------------------------|--------------------------|--------------------|
| QW-90 | -25.0 | 4.5 | 1.0 | 10 |
| QW-78 | 24.1 | 10.0 | 13.5 | 20 |
| QW-88 | 49.2 | 17.5 | 17.0 | 40 |
| QW-81 | 67.3 | 14.0 | 17.5 | 35 |
| QW-89 | 67.4 | 31.0 | 25.0 | 45 |
| QW-80 | 100.8 | 29.5 | 34.0 | 50 |
| QW-77 | 124.9 | 42.0 | 39.0 | 65 |
| QW-76 | 150.3 | 41.5 | 34.5 | 60 |
| QW-85 | 175.6 | 52.0 | 45.5 | 80 |
| QW-79 | 200.5 | 57.0 | 35.5 | 90 |
| QW-83 | 249.9 | 59.5 | 53.5 | 100 |
| QW-82 | 300.3 | 63.5 | 44.5 | 100 |
| QW-86 | 350.6 | 65.5 | 45.0 | 100 |
| QW-87 | 400.1 | 64.5 | 44.5 | 100 |
| QW-84 | 449.5 | 65.0 | 57.5 | 100 |

Table 5-5. Charpy V-Notch Impact Results for HNP Capsule Z Base Metal Plate, Heat-Affected-Zone, Irradiated to 9.45×10^{19} n/cm² (E>1.0 MeV)

| Specimen No. | Test Temp. [°F] | Impact Energy [ft-lbs] | Lateral Expansion [mils] | Shear Fracture [%] |
|--------------|-----------------|------------------------|--------------------------|--------------------|
| QH-77 | -74.7 | 3.0 | 3.5 | 0 |
| QH-76 | -25.9 | 15.0 | 6.0 | 10 |
| QH-83 | 24.3 | 27.5 | 18.5 | 30 |
| QH-86 | 67.4 | 24.0 | 18.5 | 40 |
| QH-84 | 100.5 | 34.0 | 27.0 | 45 |
| QH-82 | 125.6 | 39.0 | 31.5 | 50 |
| QH-79 | 151.2 | 43.0 | 34.5 | 50 |
| QH-90 | 159.8 | 48.0 | 38.5 | 80 |
| QH-89 | 175.5 | 61.0 | 44.5 | 100 |
| QH-88 | 200.4 | 64.0 | 46.0 | 100 |
| QH-78 | 250.1 | 54.0 | 38.0 | 100 |
| QH-85 | 300.0 | 57.0 | 43.0 | 100 |
| QH-87 | 350.3 | 64.0 | 43.5 | 100 |
| QH-80 | 400.7 | 55.0 | 43.5 | 100 |
| QH-81 | 450.2 | 64.0 | 58.0 | 100 |

**Table 5-6. Hyperbolic Tangent Curve Fit Coefficients for the HNP
Capsule Z Surveillance Materials**

| Material Description | Hyperbolic Tangent Curve Fit Coefficients | | | |
|---|---|-----------------|-------------------|------------------------|
| | Variable | Absorbed Energy | Lateral Expansion | Percent Shear Fracture |
| Base Metal Plate B4197-2 (LT) | A | 32.45 | 27.94 | 50 |
| | B | 30.25 | 27.94 | 50 |
| | C | 94.41 | 97.45 | 88.02 |
| | T0 | 179.37 | 175.69 | 171.84 |
| Base Metal Plate B4197-2 (TL) | A | 27.2 | 24.47 | 50 |
| | B | 25 | 24.47 | 50 |
| | C | 93.59 | 109.16 | 93.52 |
| | T0 | 184.65 | 189.52 | 181.86 |
| Weld Metal Wire Ht. 5P6771/ Flux Lot 0342 | A | 32.9 | 23.97 | 50 |
| | B | 30.7 | 23.97 | 50 |
| | C | 97.68 | 93.62 | 118.76 |
| | T0 | 106.31 | 75.3 | 94.18 |
| HAZ Metal | A | 31.05 | 23.76 | 50 |
| | B | 28.85 | 23.76 | 50 |
| | C | 118.25 | 125 | 104.3 |
| | T0 | 73.6 | 77.91 | 100.59 |

Figure 5-20. Charpy Impact Data for Irradiated Base Metal Plate, Heat No. B4197-2, Longitudinal (LT) Orientation

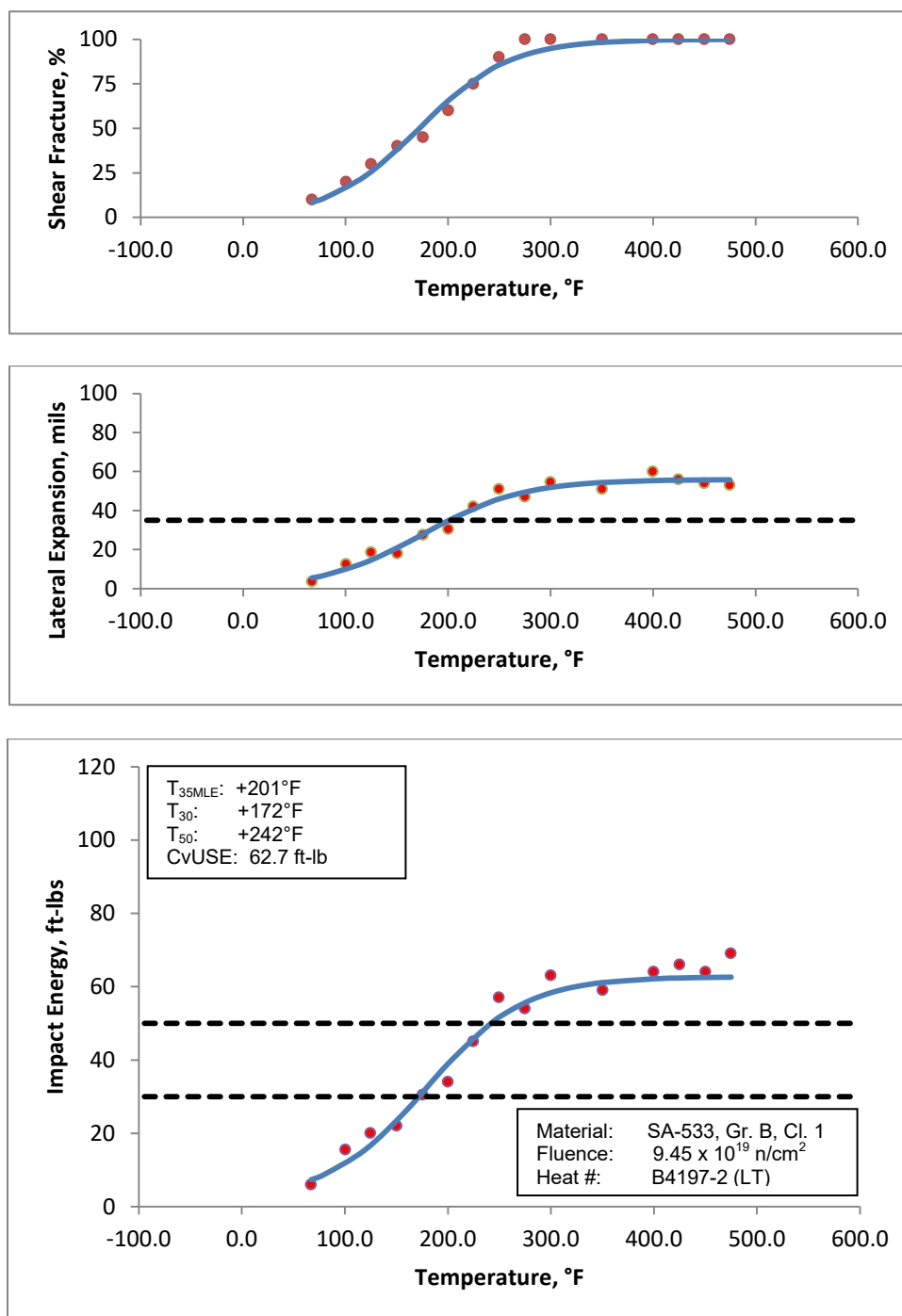


Figure 5-21. Charpy Impact Data for Irradiated Base Metal Plate, Heat No. B4197-2, Transverse (TL) Orientation

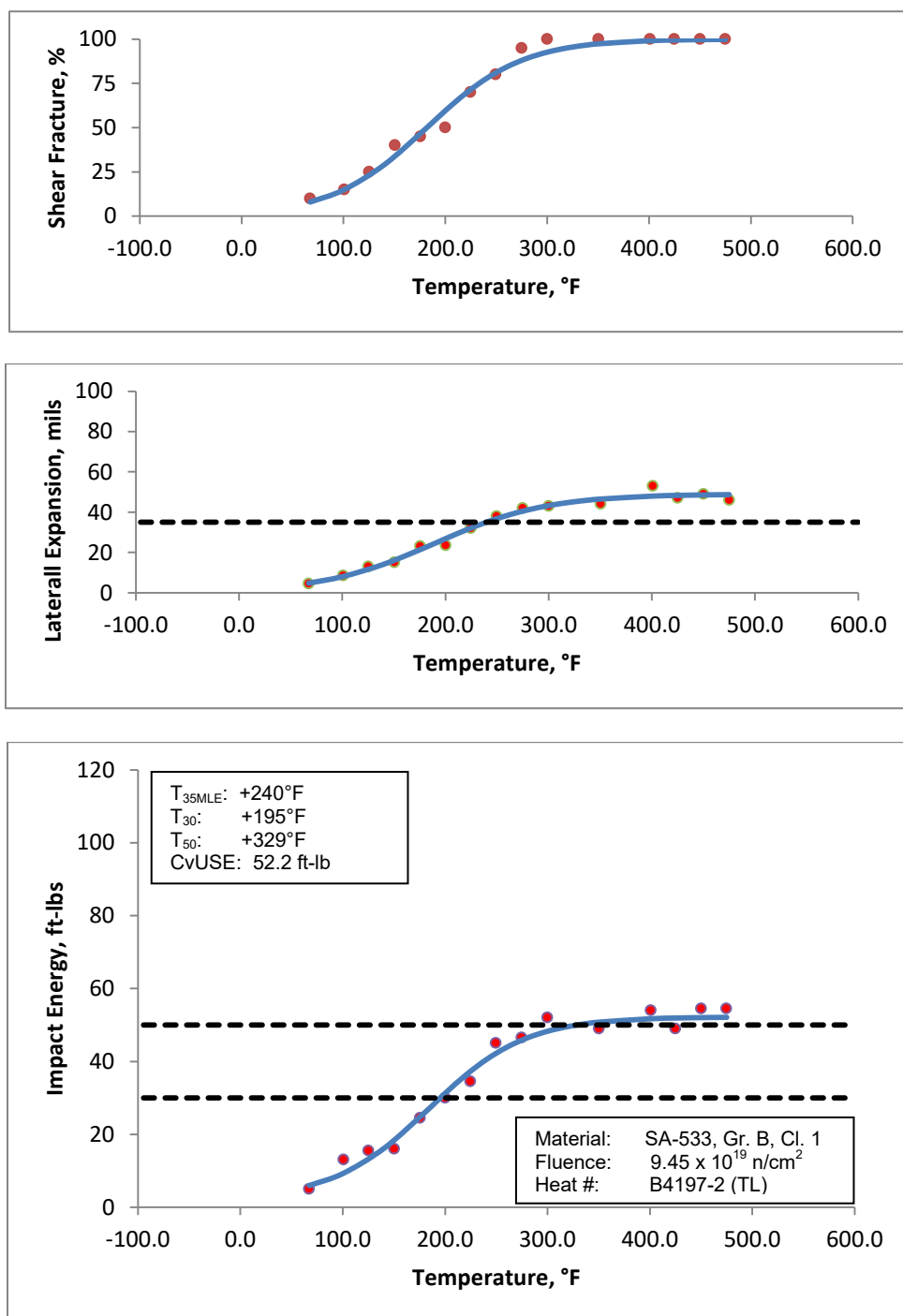


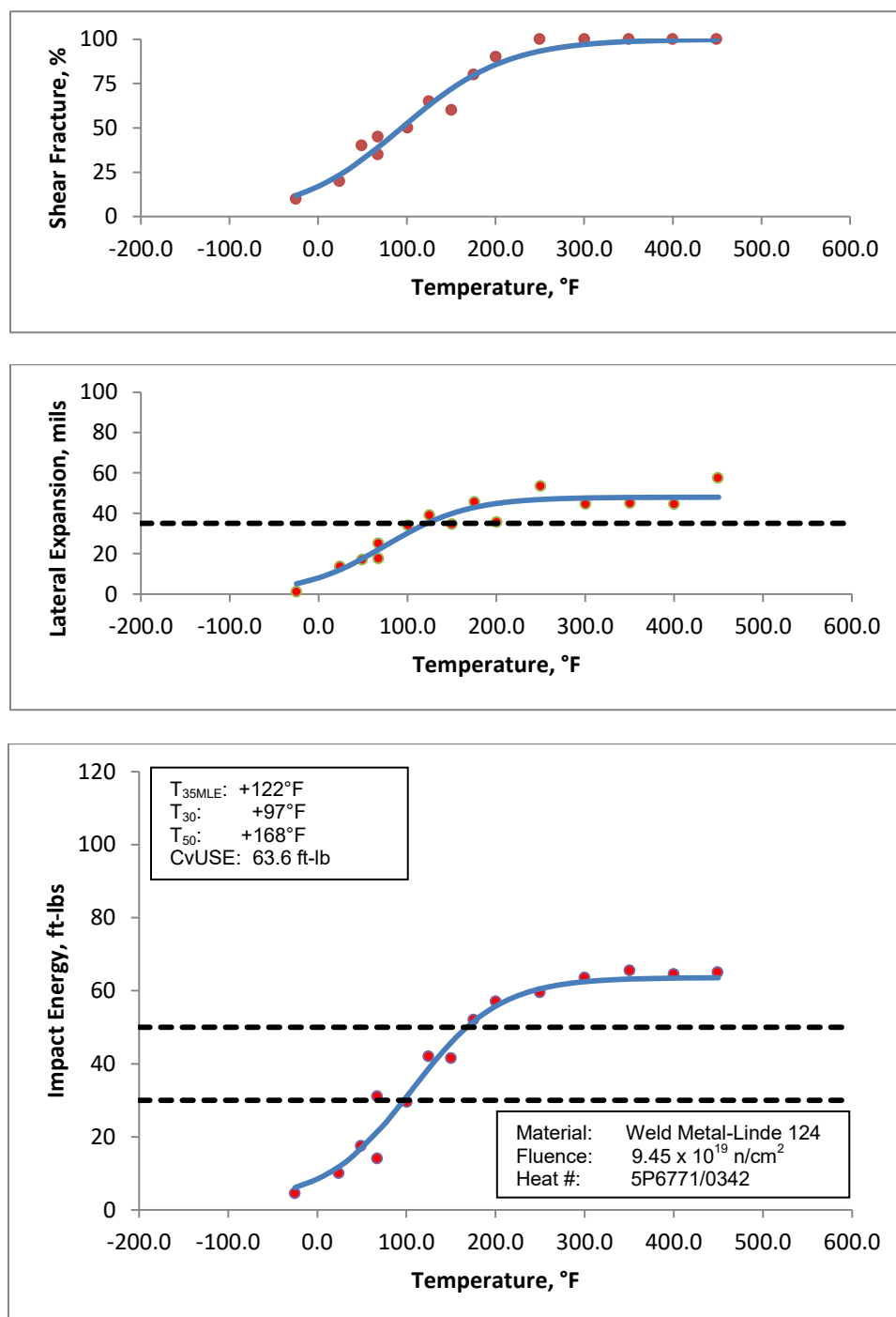
Figure 5-22. Charpy Impact Data for Irradiated Weld Metal Wire Heat 5P6771/Flux Lot 0342

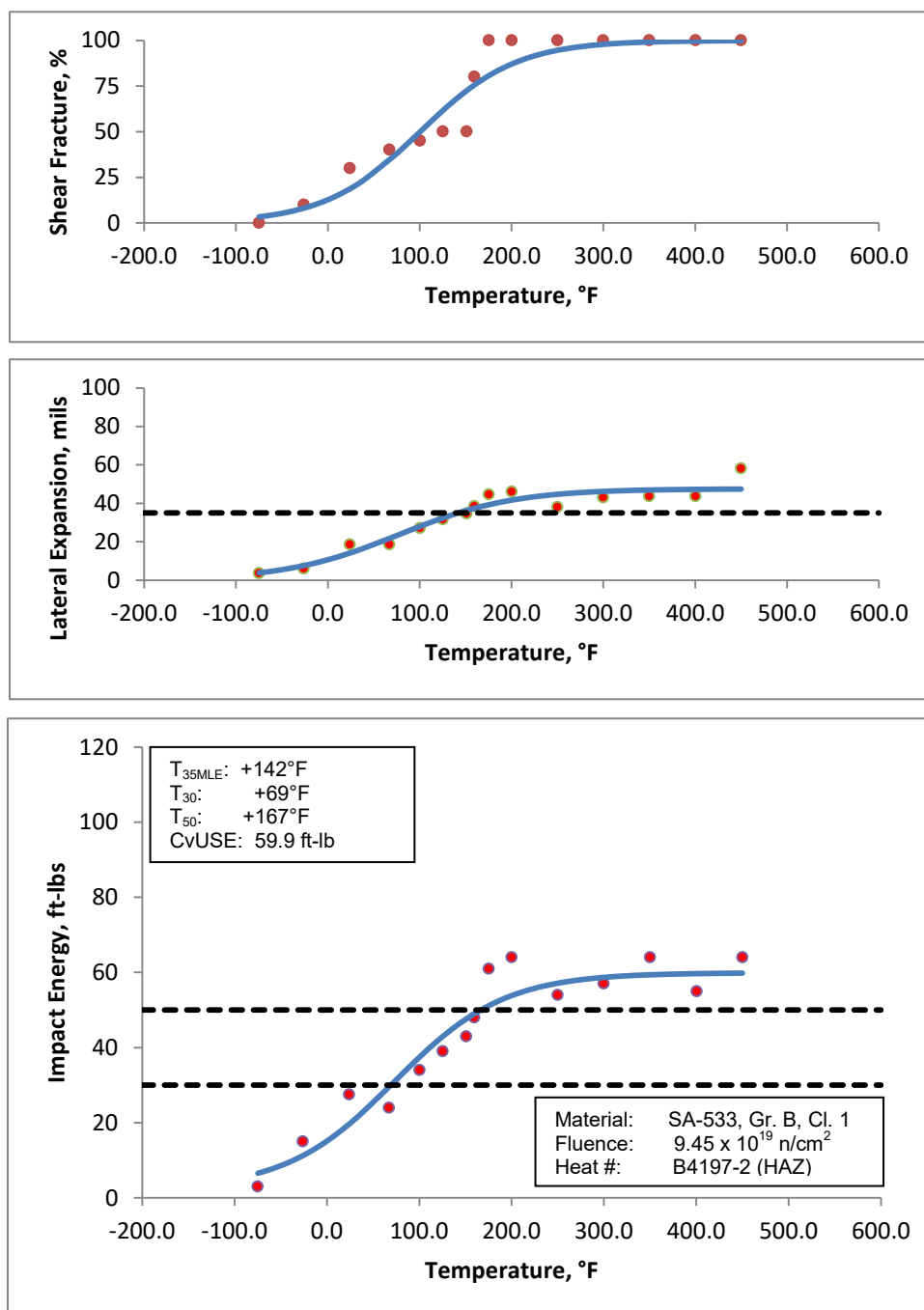
Figure 5-23. Charpy Impact Data for Irradiated Base Metal Plate Heat-Affected-Zone

Figure 5-24. Photographs of Charpy Impact Specimen Fracture Surfaces, Base Metal Plate, Heat No. B4197-2, Longitudinal (LT) Orientation



Figure 5-24, (Cont'd). Photographs of Charpy Impact Specimen Fracture Surfaces, Base Metal Plate, Heat No. B4197-2, Longitudinal (LT) Orientation



Figure 5-24, (Cont'd). Photographs of Charpy Impact Specimen Fracture Surfaces, Base Metal Plate, Heat No. B4197-2, Longitudinal (LT) Orientation

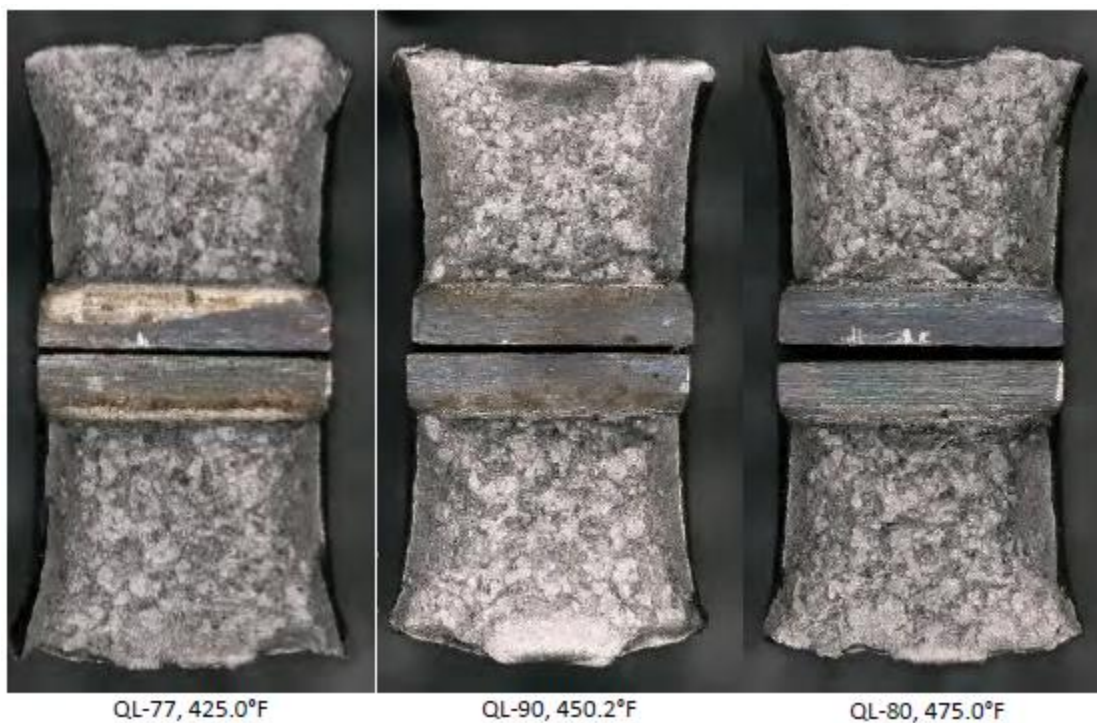


Figure 5-25. Photographs of Charpy Impact Specimen Fracture Surfaces, Base Metal Plate, Heat No. B4197-2, Transverse (TL) Orientation

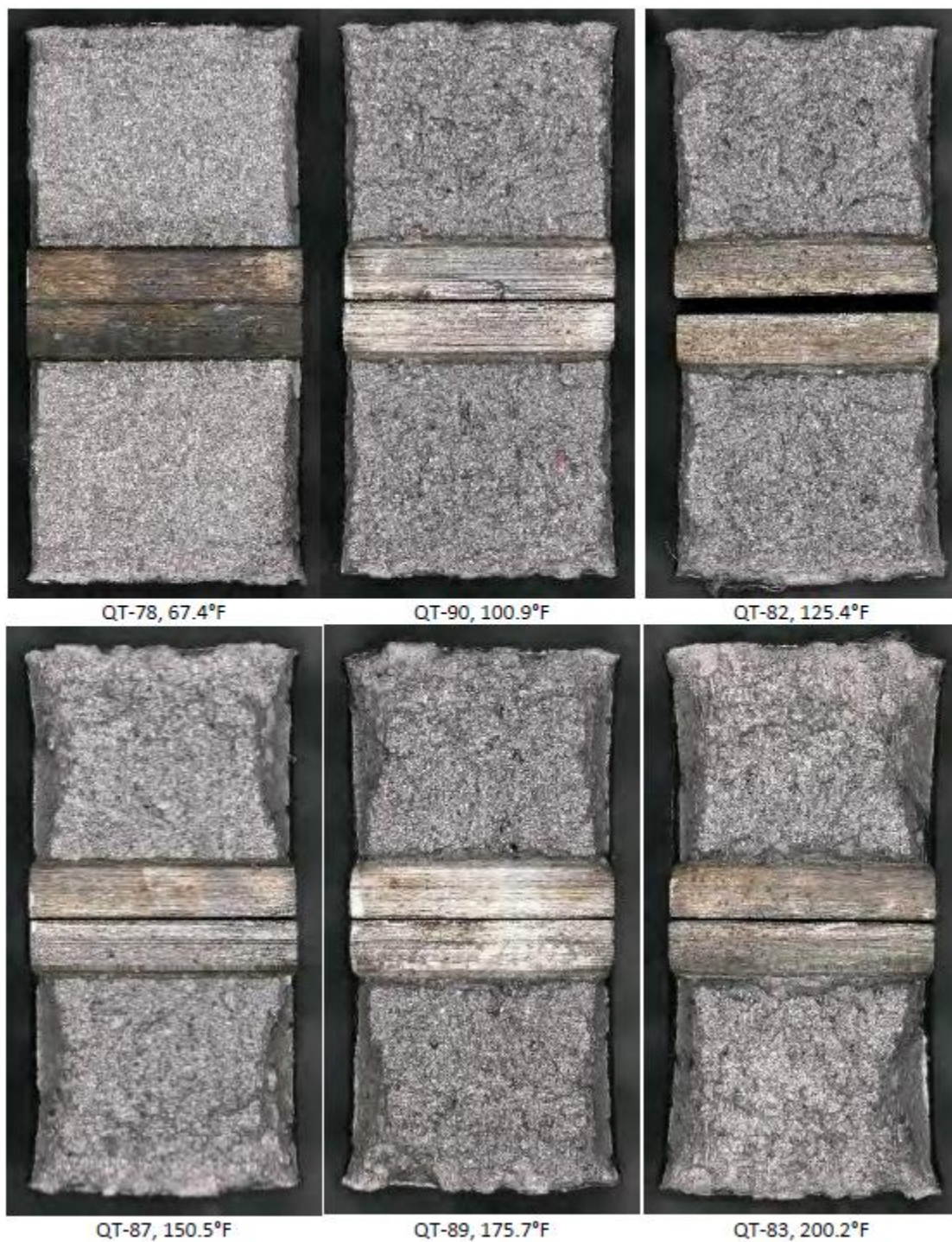
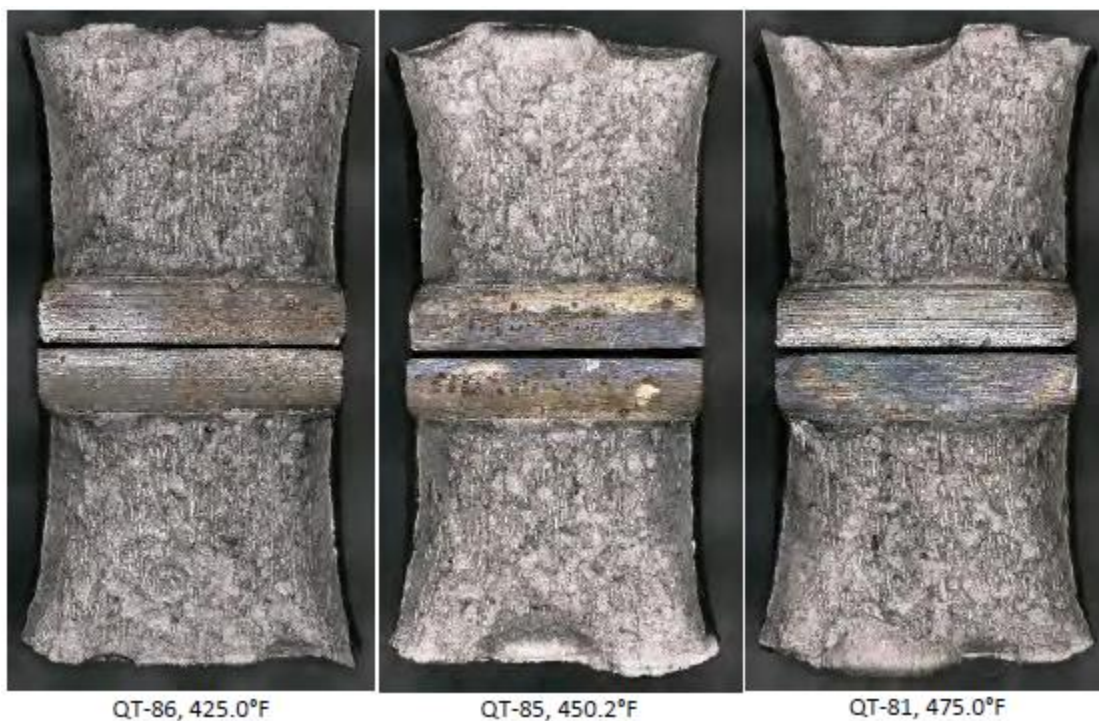


Figure 5-25, (Cont'd). Photographs of Charpy Impact Specimen Fracture Surfaces, Base Metal Plate, Heat No. B4197-2, Transverse (TL) Orientation



Figure 5-25, (Cont'd). Photographs of Charpy Impact Specimen Fracture Surfaces, Base Metal Plate, Heat No. B4197-2, Transverse (TL) Orientation



**Figure 5-26. Photographs of Charpy Impact Specimen Fracture Surfaces,
Weld Metal Wire Heat 5P6771/Flux Lot 0342**



Figure 5-26 (Cont'd). Photographs of Charpy Impact Specimen Fracture Surfaces, Weld Metal Wire Heat 5P6771/Flux Lot 0342



**Figure 5-26 (Cont'd). Photographs of Charpy Impact Specimen Fracture Surfaces, Weld
Metal Wire Heat 5P6771/Flux Lot 0342**



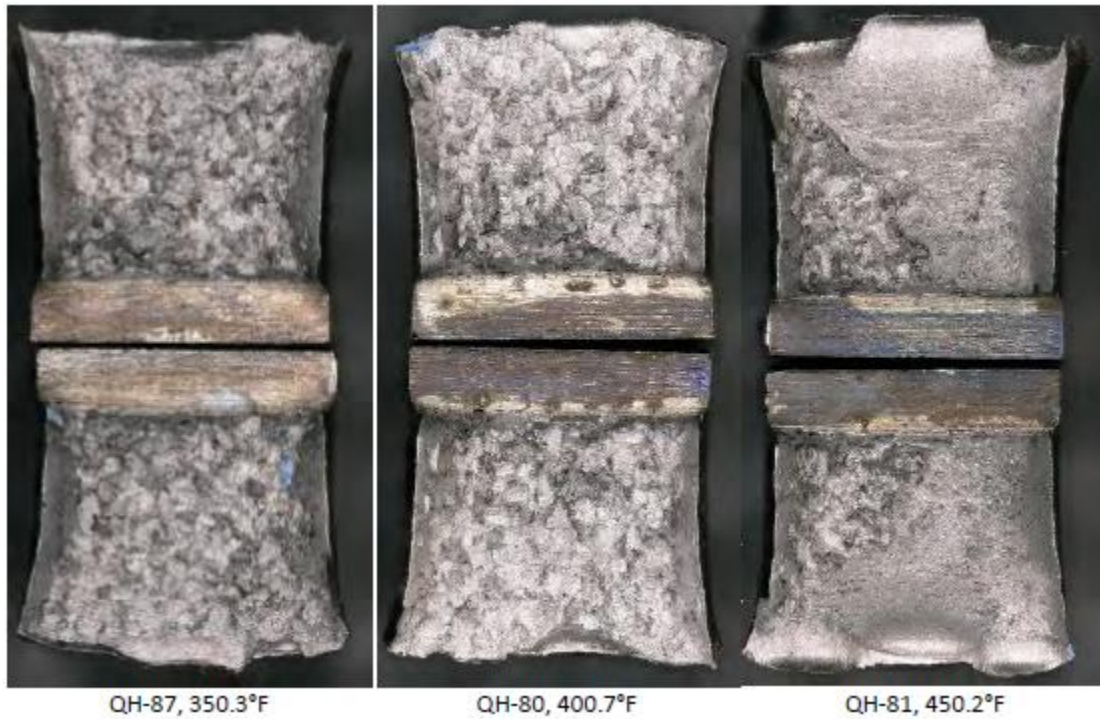
Figure 5-27. Photographs of Charpy Impact Specimen Fracture Surfaces, Base Metal Plate, Heat-Affected-Zone



Figure 5-27 (Cont'd). Photographs of Charpy Impact Specimen Fracture Surfaces, Base Metal Plate, Heat-Affected-Zone



Figure 5-27 (Cont'd). Photographs of Charpy Impact Specimen Fracture Surfaces, Base Metal Plate, Heat-Affected-Zone



5.5 Compact Fracture Toughness and Bend Bar Specimens

The 0.5T compact fracture toughness specimens and the bend bar specimen were not tested at the request of Duke Energy. The specimens are to be stored at the BWXT LTC Long Term RVSP Specimen Storage facility for possible future testing.

6.0 NEUTRON FLUENCE

6.1 *Objectives and Background*

Framatome Inc. has developed a calculation based fluence analysis methodology that can be used to accurately predict the fast neutron fluence in the reactor vessel using surveillance capsule dosimetry, cavity dosimetry, or both to verify the uncertainties in the fluence predictions.^[17] The methodology was developed through a full-scale benchmark experiment that was performed at the Davis-Besse Unit 1 reactor.^[17] The results of the benchmark experiment demonstrated that the accuracy of a fluence analysis that employs the Framatome methodology was unbiased and has a precision well within the NRC-suggested limit of 20%.^{[17],[18]}

The Framatome methodology was used to calculate the neutron fluence exposure to the pressure vessel, certain vessel welds in the beltline region, and surveillance Capsule Z of the HNP reactor vessel. The fast neutron fluences ($E > 1 \text{ Me V}$) at those points were calculated in accordance with the requirements of the U.S. NRC Regulatory Guide 1.190,^[18] as described in detail in the Framatome fluence topical report, BAW-2241P, Revision 1.^[17]

The energy-dependent flux at the capsule was used to determine the calculated activity of each dosimeter. The calculated activities were adjusted to account for known biases (photofission and U-235 impurity in the U-238), and compared directly to the measured activities. It is noted that the measurements are not used in any way to determine the magnitude of the flux or the fluence. The measurements are used only to show that the calculational results are reasonable and to show that the HNP results are consistent with the Framatome benchmark database of uncertainties.

Explicit values of the fast fluence were computed for the following locations:

- Surveillance Capsule
- "Wetted" Surface for the HNP Reactor Vessel Beltline Materials
- Clad-Base Metal Interface for the HNP Reactor Vessel Beltline Materials
- Clad-Base Metal Interface Maximum Peak Location
- $\frac{1}{4}T$ and $\frac{3}{4}T$ at Maximum Peak Location where T is the reactor vessel thickness.

The multi-cycle-average full power flux at each of these locations was calculated for cycles 9 through 21, and the corresponding fluence at each location was then calculated by computing the product of each flux by the appropriate effective full power time, in seconds.

Reactor vessel fluence can be projected to longer time periods in order to estimate the total fluence on the locations of interest. This projection is performed by assuming that the average fluence at the location of interest for the projected time is at equilibrium at the average fluence rate (flux) of the last cycle analyzed for a given location of interest. This assumption is acceptable as long as future core configurations are equivalent to the core design of the last cycle analyzed. The end of life (license) fluences are determined by taking the cumulative fluence and then projecting forward by utilizing the fluence rate (flux) of the last cycle analyzed for a given location of interest.

6.2 Results

The numerical and graphical results are presented in the following Tables and Figures:

- Calculation to Measurement Ratios are provided in Table 6-1
- Fluence results at all points of interest are provided in Tables 6-2 and 6-3

Table 6-1. C/M Ratios for HNP Capsule Z

| Dosimeter | C ($\mu\text{Ci/g}$) | M ($\mu\text{Ci/g}$) | C/M | C/M by Dosimeter |
|-----------|------------------------|------------------------|-----------------|------------------|
| Fe (Top) | 1810 | 1550 | 1.17 | |
| Fe (Mid) | 1760 | 1450 | 1.21 | 1.19 |
| Fe (Bot) | 1760 | 1470 | 1.20 | |
| Ni (Top) | 2470 | 2040 | 1.21 | |
| Ni (Mid) | 2470 | 1940 | 1.27 | 1.25 |
| Ni (bot) | 2460 | 1920 | 1.28 | |
| Cu (Top) | 15.2 | 14.0 | 1.09 | |
| Cu (mid) | 14.8 | 13.4 | 1.10 | 1.11 |
| Cu (Bot) | 14.8 | 12.9 | 1.15 | |
| U-238 | 77.2 | 85.0 | 0.91 | 0.91 |
| Np-237 | 609 | 565 | 1.08 | 1.08 |
| | | | Avg. C/M = 1.11 | |

Table 6-2. Fast Neutron Fluence ($E > 1 \text{ MeV}$) for the HNP Reactor Vessel "Wetted" Inside Surface

| Description | Cycle 21 Fluence (n/cm^2) | 36 EFPY Fluence (n/cm^2) | 55 EFPY Fluence (n/cm^2) |
|--|--------------------------------------|-------------------------------------|-------------------------------------|
| Forgings/Plates (original 40 year beltline) | | | |
| Inter. Shell Plates (ISP) | 3.33E+19 | 4.49E+19 | 6.97E+19 |
| Lower Shell Plates (LSP) | 3.25E+19 | 4.38E+19 | 6.79E+19 |
| Wetted Surface Max | 3.33E+19 | 4.49E+19 | 6.97E+19 |
| Welds (original 40 year beltline) | | | |
| USP to ISP Circ. Weld | 1.77E+18 | 2.32E+18 | 3.49E+18 |
| ISP to LSP Circ. Weld | 3.23E+19 | 4.36E+19 | 6.77E+19 |
| ISP Long. Weld | 1.28E+19 | 1.70E+19 | 2.60E+19 |
| LSP Long. Weld | 1.24E+19 | 1.66E+19 | 2.53E+19 |
| Additional Locations* | | | |
| Upper Shell Plates (USP) | 1.54E+18 | 2.02E+18 | 3.04E+18 |
| USP Long. Weld | 1.77E+18 | 2.32E+18 | 3.49E+18 |
| Inlet Nozzle Lower Weld | 1.96E+17 | 2.57E+17 | 3.87E+17 |
| Outlet Nozzle Lower Weld | 9.42E+16 | 1.23E+17 | 1.86E+17 |
| LSP to Bot. Head Circ. Weld | 8.79E+17 | 1.13E+18 | 1.65E+18 |

* Best estimate values. Methodology not approved by NRC for locations beyond "original 40 year beltline".

Table 6-3. Fast Neutron Fluence ($E > 1$ MeV) for the HNP Reactor Vessel Clad-Base Metal Interface

| Description | Cycle 21 Fluence (n/cm ²) | 36 EFPY Fluence (n/cm ²) | 55 EFPY Fluence (n/cm ²) |
|--|--|---|---|
| Forgings/Plates (original 40 year beltline) | | | |
| Inter. Shell Plates (ISP) | 3.28E+19 | 4.43E+19 | 6.87E+19 |
| Lower Shell Plates (LSP) | 3.20E+19 | 4.32E+19 | 6.70E+19 |
| Wetted Surface Max | 3.28E+19 | 4.43E+19 | 6.87E+19 |
| Welds (original 40 year beltline) | | | |
| USP to ISP Circ. Weld | 1.75E+18 | 2.30E+18 | 3.46E+18 |
| ISP to LSP Circ. Weld | 3.18E+19 | 4.30E+19 | 6.68E+19 |
| ISP Long. Weld | 1.26E+19 | 1.68E+19 | 2.57E+19 |
| LSP Long. Weld | 1.23E+19 | 1.64E+19 | 2.51E+19 |
| Additional Locations* | | | |
| Upper Shell Plates (USP) | 1.52E+18 | 1.99E+18 | 3.00E+18 |
| USP Long. Weld | 1.75E+18 | 2.30E+18 | 3.46E+18 |
| Inlet Nozzle Lower Weld | 1.94E+17 | 2.55E+17 | 3.83E+17 |
| Outlet Nozzle Lower Weld | 9.34E+16 | 1.22E+17 | 1.84E+17 |
| LSP to Bot. Head Circ. Weld | 8.79E+17 | 1.13E+18 | 1.65E+18 |
| ¼T | 1.92E+19 | 2.60E+19 | 4.04E+19 |
| ¾T | 4.77E+18 | 6.44E+18 | 9.99E+18 |

* Best estimate values. Methodology not approved by NRC for locations beyond "original 40 year beltline".

As shown in Tables 6-2 and 6-3, the peak location is at the intermediate shell plate.

Table 6-4. HNP Capsule Z Fast Neutron Fluence ($E > 1$ MeV) and Lead Factors at EOC 21

| | |
|---|----------------------------|
| Exposure at EOC 21 | 9875.67 EFPD |
| Capsule Average Neutron Fluence ($E > 1.0$ MeV) | 9.45E+19 n/cm ² |
| Lead Factor (Capsules Y & Z to I.S. Maximum Location) | 2.84 |
| Lead Factor (Capsules Y & Z to ¼T Location) | 4.91 |

7.0 DISCUSSION OF CAPSULE RESULTS

7.1 *Unirradiated Material Property Data*

The base metal and weld metal were selected for inclusion in the HNP surveillance program in accordance with the criteria in effect at the time the program was designed. The applicable selection criterion was based on the unirradiated properties only. A review of the original unirradiated material properties of the reactor vessel core beltline region materials indicated no significant deviation from expected properties except in the case of the upper-shelf energy properties of the RVSP base metal in the transverse (TL) orientation which was below the required minimum initial Charpy upper-shelf energy (CvUSE) of 75 ft-lbs. No action is required for a material that does not meet the initial 75 ft-lbs requirement provided that the irradiation embrittlement does not cause the CvUSE to drop below 50 ft-lbs. Based on the predicted end-of-service peak neutron fluence value at the 1/4T vessel wall location and the copper content of the RVSP base metal, it was predicted that the end-of-service CvUSE would not be below 50 ft-lbs for the RVSP base metal.

The unirradiated mechanical properties for the HNP RVSP materials are summarized in Appendices B and C of this report.

7.2 *Irradiated Property Data*

7.2.1 Tensile Properties

Table 7-1 compares the irradiated and unirradiated tensile properties. Review of the surveillance tensile test data indicates that the ultimate strength and yield strength changes in the base metal plate as a result of irradiation and the corresponding changes in ductility are consistent with the expected trends in irradiated materials. The changes in tensile properties for the surveillance weld metal, as a result of irradiation, are also consistent with the expected trends in irradiated materials.

The general behavior of the tensile properties as a function of neutron irradiation is an increase in both ultimate and yield strength and a decrease in ductility as measured by both total elongation and reduction in area. The most significant observation from these data is that the base metal with the transverse orientation exhibited slightly greater sensitivity to neutron irradiation than the weld metal.

Analysis of Capsule Z

Duke Energy Shearon Harris Nuclear Power Plant

Reactor Vessel Material Surveillance Program

Page 7-2

Table 7-1. Summary of HNP Reactor Vessel Surveillance Capsules Tensile Test Results

| Material | Fluence [10 ¹⁹ n/cm ²] | Test Temp [°F] | Strength [ksi] | | | | Ductility [%] | | | |
|--|---|----------------------|---------------------|------------------|---------------------|------------------|---------------------|------------------|----------------------|------------------|
| | | | Ultimate | % ^(a) | Yield | % ^(a) | Total Elong. | % ^(a) | Reduction of Area | % ^(a) |
| Base Metal Plate, B4197-2 (Longitudinal) | 0.000 | 75 | 94.0 ^(b) | --- | 75.5 ^(b) | --- | 26.0 ^(b) | --- | 61.5 ^(b) | --- |
| | | 300 | 87.5 ^(b) | --- | 74.5 ^(b) | --- | 21.5 ^(b) | --- | 63.5 ^(b) | --- |
| | | 600 | 88.0 ^(b) | --- | 73.5 ^(b) | --- | 19.0 ^(b) | --- | 54.0 ^(b) | --- |
| | 0.552 | 70 | 96.7 ^(b) | 2.9 | 72.4 ^(b) | -4.1 | 23.3 ^(b) | -10.4 | 62.6 ^(b) | 1.8 |
| | | 550 | 93.6 | 6.4 | 65.7 | 10.6 | 19.3 | 1.6 | 52.7 | -2.4 |
| | 1.32 | 70 | 97.7 ^(b) | 3.9 | 73.9 ^(b) | -2.1 | 22.1 ^(b) | -15.0 | 62.5 ^(b) | 1.6 |
| | | 550 | 93.8 | 6.6 | 69.0 | -6.1 | 15.9 | -16.3 | 42.4 | -21.5 |
| | 3.25 | 70 | 101.2 | 7.7 | 79.6 | 5.4 | 22.9 | -11.9 | 60.2 | -2.1 |
| | | 300 | 92.6 | 5.8 | 71.7 | -3.8 | 20.3 | -5.6 | 60.3 | -5.0 |
| | | 550 | 99.0 | 12.5 | 72.8 | -1.0 | 17.0 | -10.5 | 43.8 | -18.9 |
| | 9.45 | 176.3 | 103.1 | 9.7 | 83.1 | 10.1 | 20.9 | -19.6 | 51.1 | -16.9 |
| | | 275.2 | 99.8 | 14.1 | 78.5 | 5.4 | 19.1 | -11.3 | 50.3 | -20.8 |
| | | 550 | 104.0 | 18.2 | 76.6 | 4.2 | 17.0 | -10.4 | 37.9 | -29.9 |
| Base Metal Plate, B4197-2 (Transverse) | 0.000 | 75 | 91.0 ^(b) | --- | 68.5 ^(b) | --- | 26.0 ^(b) | --- | 61.5 ^(b) | --- |
| | | 300 | 83.0 ^(b) | --- | 61.0 ^(b) | --- | 23.0 ^(b) | --- | 58.5 ^(b) | --- |
| | | 600 | 86.5 ^(b) | --- | 60.0 ^(b) | --- | 20.5 ^(b) | --- | 54.5 ^(b) | --- |
| | 0.552 | 70.0 | 96.6 ^(b) | 6.2 | 72.3 ^(b) | 5.5 | 23.7 ^(b) | -8.8 | 57.5 ^(b) | -6.5 |
| | | 550.0 | 93.7 | 8.3 | 69.3 | 15.5 | 17.4 | -15.1 | 50.4 | -7.5 |
| | 1.32 | 70.0 | 97.4 ^(b) | 7.0 | 76.0 ^(b) | 10.9 | 21.7 ^(b) | -16.5 | 58.4 ^(b) | -5.0 |
| | | 550.0 | 92.7 | 7.2 | 66.6 | 11.0 | 17.3 | -15.6 | 44.2 | -18.9 |
| | 3.25 | 70.0 | 101.0 | 11.0 | 80.0 | 16.8 | 22.5 | -13.5 | 60.1 | -2.3 |
| | | 300.0 | 92.8 | 11.8 | 72.6 | 19.0 | 19.4 | -15.7 | 55.6 | -5.0 |
| | | 550.0 | 95.8 | 10.8 | 70.4 | 17.3 | 17.8 | -13.2 | 53.2 | -2.4 |
| | 9.45 | 201.3 | 100.6 | 10.5 | 82.8 | 20.9 | 19.0 | -27.0 | 51.1 | -16.9 |
| | | 301.3 | 101.5 | 22.3 | 86.4 | 41.6 | 16.3 | -29.3 | 47.6 | -18.6 |
| | | 550.8 | 104.7 | 21.0 | 81.1 | 35.2 | 16.5 | -19.6 | 37.1 | -32.0 |
| Weld Metal (Wire Ht. SP6771/ Flux Lot 0342) | 0.000 | 75 | 89.0 ^(b) | --- | 74.0 ^(b) | --- | 27.5 ^(b) | --- | 67.5 ^(b) | --- |
| | | 300 | 81.0 ^(b) | --- | 65.0 ^(b) | --- | 23.5 ^(b) | --- | 66.0 ^(b) | --- |
| | | 600 | 83.5 ^(b) | --- | 63.0 ^(b) | --- | 22.5 ^(b) | --- | 64.5 ^(b) | --- |
| | 0.552 | 70.0 | 91.1 ^(b) | 2.4 | 76.3 ^(b) | 3.1 | 25.8 ^(b) | -6.2 | 67.1 ^(b) | -0.6 |
| | | 550.0 | 87.5 | 4.8 | 69.0 | 9.5 | 20.9 | -7.1 | 62.5 | -3.1 |
| | 1.32 | 70.0 | 91.8 ^(b) | 3.1 | 76.0 ^(b) | 2.7 | 22.5 ^(b) | -18.2 | 61.9 ^(b) | -8.3 |
| | | 550.0 | 88.3 | 5.7 | 70.3 | 11.6 | 18.6 | -17.3 | 61.6 | -4.5 |
| | 3.25 | 70.0 | 95.4 | 7.2 | 82.8 | 11.9 | 24.8 | -9.8 | 63.0 | -6.7 |
| | | 300.0 | 88.2 | 8.9 | 76.0 | 16.9 | 22.3 | -5.1 | 64.5 | -2.3 |
| | | 550.0 | 93.0 | 11.4 | 75.6 | 20 | 21.1 | -6.2 | 61.1 | -5.3 |
| | 9.45 | 100.9 | 100.5 | 12.9 | 91.3 | 23.4 | 23.4 | -15.1 | 60.5 | -10.4 |
| | | 250.4 | 95.2 | 17.5 | 77.3 | 18.9 | 22.2 | -5.4 | 59.5 | -9.9 |
| | | 550.9 | 97.3 | 16.5 | 80.4 | 27.6 | 22.7 | 0.8 | 53.6 | -17.0 |

(a) Change relative to unirradiated material property

(b) Mean value of available test data

7.2.2 Impact Properties

Tables 7-2 and 7-3 compare the measured changes in irradiated Charpy V-notch impact properties from Capsule Z with the predicted changes in accordance with Regulatory Guide 1.99, Revision 2^[19].

The measured 30 ft-lb transition temperature shifts for the surveillance materials are greater than the values predicted using Regulatory Guide 1.99, Revision 2. When the margin (2σ) is added to these predicted shifts, the predicted 30 ft-lb transition temperature shift values are non-conservative for the Base Metal longitudinal and transverse surveillance materials and the Weld metal surveillance material (see Table 7-2).

Table 7-2. Measured vs. Predicted 30 ft-lb Transition Temperature Changes for HNP Capsule Z Surveillance Materials – 9.45×10^{19} n/cm²

| Material | Measured 30 ft-lb Transition Temperature, °F | | | 30 ft-lb Transition Temperature Shift Predicted in Accordance With Regulatory Guide 1.99, Rev. 2, °F | | | |
|---|--|------------|------------|--|-------------------|----------------------|-----------------------------|
| | Unirradiated | Irradiated | Difference | Chemistry Factor ^(a) | ΔRT_{NDT} | Margin (2σ) | $\Delta RT_{NDT} + 2\sigma$ |
| Base Metal Plate, B4197-2 (Longitudinal) | 51 | 171.8 | 120.8 | 55.9 ^(b) | 84.2 | 34 | 118.2 |
| Base Metal Plate, B4197-2 (Transverse) | 72 | 195.2 | 123.2 | 55.9 ^(b) | 84.2 | 34 | 118.2 |
| Weld Metal (Wire Ht. 5P6771/Flux Lot 0342) | -34 | 97.1 | 131.1 | 32.6 ^(b) | 49.1 | 49.1 | 98.2 |
| Base Metal Plate, B4197-2 Heat-Affected-Zone Material | -44 | 69.3 | 113.3 | 55.9 ^(b) | 84.2 | 34 | 118.2 |

(a) Chemistry factor determined using Tables 1 and 2 of Regulatory Guide 1.99, Revision 2.

(b) Chemistry factor based on mean copper and nickel contents calculated using data in Tables 3-2 and 3-3.

Table 7-3. Measured vs. Predicted Upper-Shelf Energy Decreases for HNP Capsule Z Surveillance Materials – 9.45×10^{19} n/cm²

| Material | Measured Upper-Shelf Energy, ft-lb | | | % Decrease Predicted in Accordance With Regulatory Guide 1.99, Rev. 2, Figure 2 |
|---|------------------------------------|------------|------------|---|
| | Unirradiated | Irradiated | % Decrease | |
| Base Metal Plate, B4197-2 (Longitudinal) | 87 | 63 | 27.6 | 30.0 ^(a) |
| Base Metal Plate, B4197-2 (Transverse) | 70 | 52 | 25.7 | 30.0 ^(a) |
| Weld Metal (Wire Ht. 5P6771/Flux Lot 0342) | 94 | 64 | 31.9 | 28.0 ^(a) |
| Base Metal Plate, B4197-2 Heat-Affected-Zone Material | 85 | 60 | 29.4 | 30.0 ^(a) |

(a) Based on mean copper content calculated using data in Tables 3-2 and 3-3.

Analysis of Capsule Z
Duke Energy Shearon Harris Nuclear Power Plant
Reactor Vessel Material Surveillance Program

Page 7-4

The measured percent decrease in CvUSE for the surveillance weld metal is slightly greater than the value predicted using Regulatory Guide 1.99, Revision 2 (3.9%). However, the measured irradiated CvUSE value for the weld metal remains above the required 50 ft-lb limit. The measured percent reduction in CvUSE for the base metal surveillance data in the longitudinal (LT) and transverse (TL) orientations and the heat-affected-zone material are less than the Regulatory Guide 1.99, Revision 2 predictions.

The radiation-induced changes in toughness of all the HNP surveillance materials are summarized in Table 7-4. The original unirradiated and Capsule U and V Charpy impact data were evaluated based on hand-fit Charpy curves generated using engineering judgement. These data were replotted and re-evaluated in the Capsule X report^[5] using a hyperbolic tangent curve-fitting program to be consistent with the Capsule X Charpy curves and evaluations. The results of the re-evaluations are presented in Appendix C. In addition, Appendix D contains a comparison of the Charpy V-notch transition shift results for each surveillance material, hand-fit versus hyperbolic tangent curve-fit. Comparisons of the unirradiated and irradiated Charpy V-notch impact curves are presented in Figures 7-1 through 7-4.

Table 7-4. Summary of HNP Reactor Vessel Surveillance Capsules Charpy Impact Test Results

| Material | Capsule | Fluence, n/cm ² | Measured Transition Temperature | | Measured Upper- Shelf | |
|--|----------|-------------------------------|------------------------------------|-----------------------|--------------------------|---------------|
| | | | ΔC_{v30} , °F | ΔC_{v50} , °F | Energy, ft-lb | % Decrease |
| Base Metal Plate, B4197-2 (Longitudinal) | Baseline | --- | --- | --- | 87 | --- |
| | U | 5.52E+18 | 30 | 37 | 92 | -5.7 |
| | V | 1.32E+19 | 43 | 53 | 84 | 3.4 |
| | X | 3.25E+19 | 94 | 93 | 66 | 24.1 |
| | Z | 9.45E+19 | 120.8 | 143.0 | 63 | 27.6 |
| Base Metal Plate, B4197-2 (Transverse) | Baseline | --- | --- | --- | 70 | --- |
| | U | 5.52E+18 | 38 | 33 | 68 | 2.9 |
| | V | 1.32E+19 | 35 | 47 | 65 | 7.1 |
| | X | 3.25E+19 | 79 | 111 | 55 | 21.4 |
| | Z | 9.45E+19 | 123.2 | 189.8 | 52 | 25.7 |
| Weld Metal (Wire Ht. 5P6771/Flux Lot 0342) | Baseline | --- | --- | --- | 94 | --- |
| | U | 5.52E+18 | 20 | 29 | 83 | 9.8 |
| | V | 1.32E+19 | 18 | 27 | 82 | 10.9 |
| | X | 3.25E+19 | 79 | 94 | 67 | 27.2 |
| | Z | 9.45E+19 | 131.1 | 165.8 | 64 | 31.9 |
| Base Metal Plate, B4197-2 Heat-Affected- Zone Material | Baseline | --- | --- | --- | 85 | --- |
| | U | 5.52E+18 | 44 | 59 | 76 | 10.6 |
| | V | 1.32E+19 | 53 | 57 | 80 | 5.9 |
| | X | 3.25E+19 | 68 | 87 | 66 | 22.4 |
| | Z | 9.45E+19 | 113.3 | 169.7 | 60 | 29.4 |

Figure 7-1. Comparison of Unirradiated and Irradiated Charpy Impact Data Curves for Base Metal Plate, Heat No. B4197-2, Longitudinal (LT) Orientation

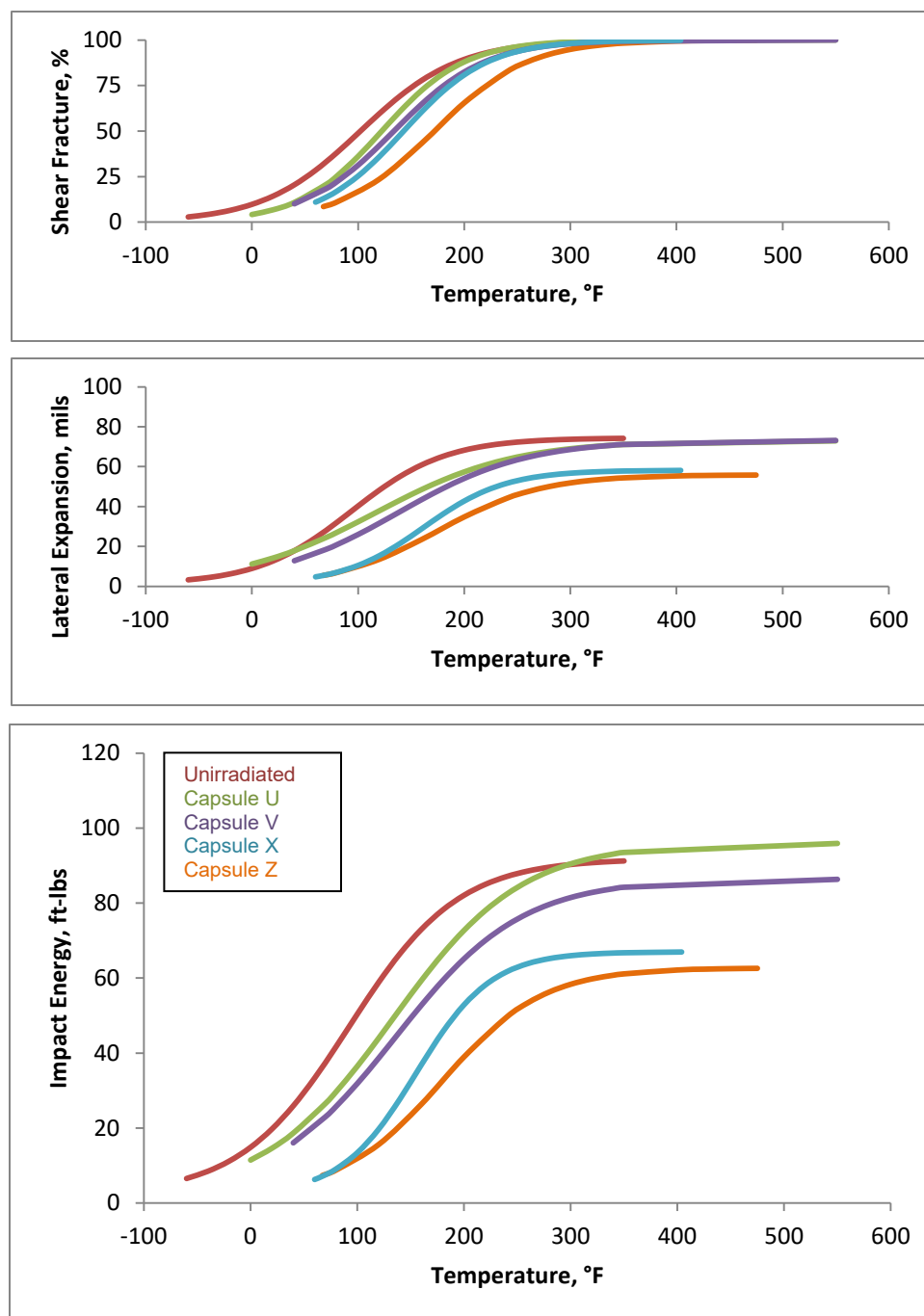


Figure 7-2. Comparison of Unirradiated and Irradiated Charpy Impact Data Curves for Base Metal Plate, Heat No. B4197-2, Transverse (TL) Orientation

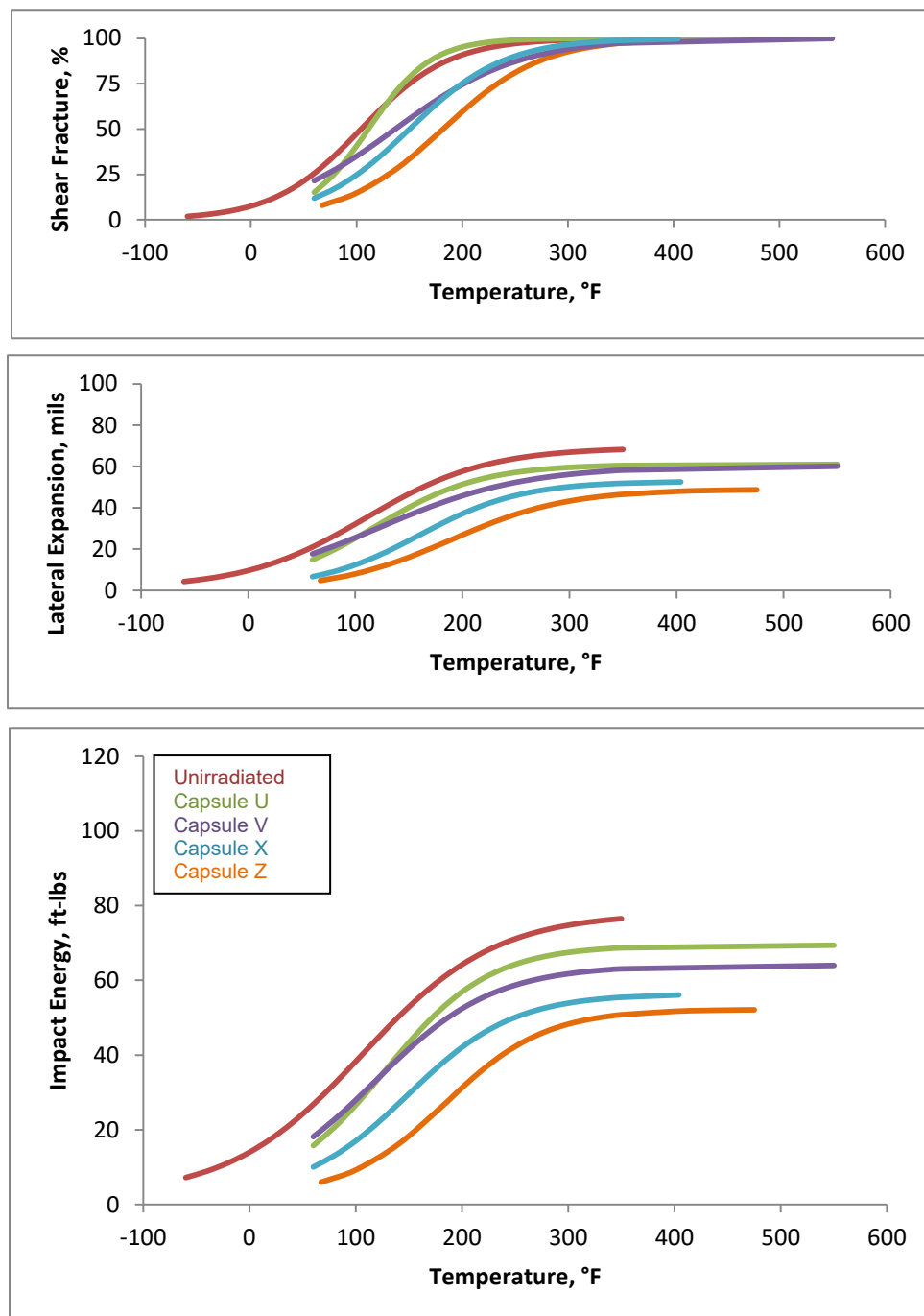


Figure 7-3. Comparison of Unirradiated and Irradiated Charpy Impact Data Curves for Weld Metal (Wire Heat 5P6771/Flux Lot 0342)

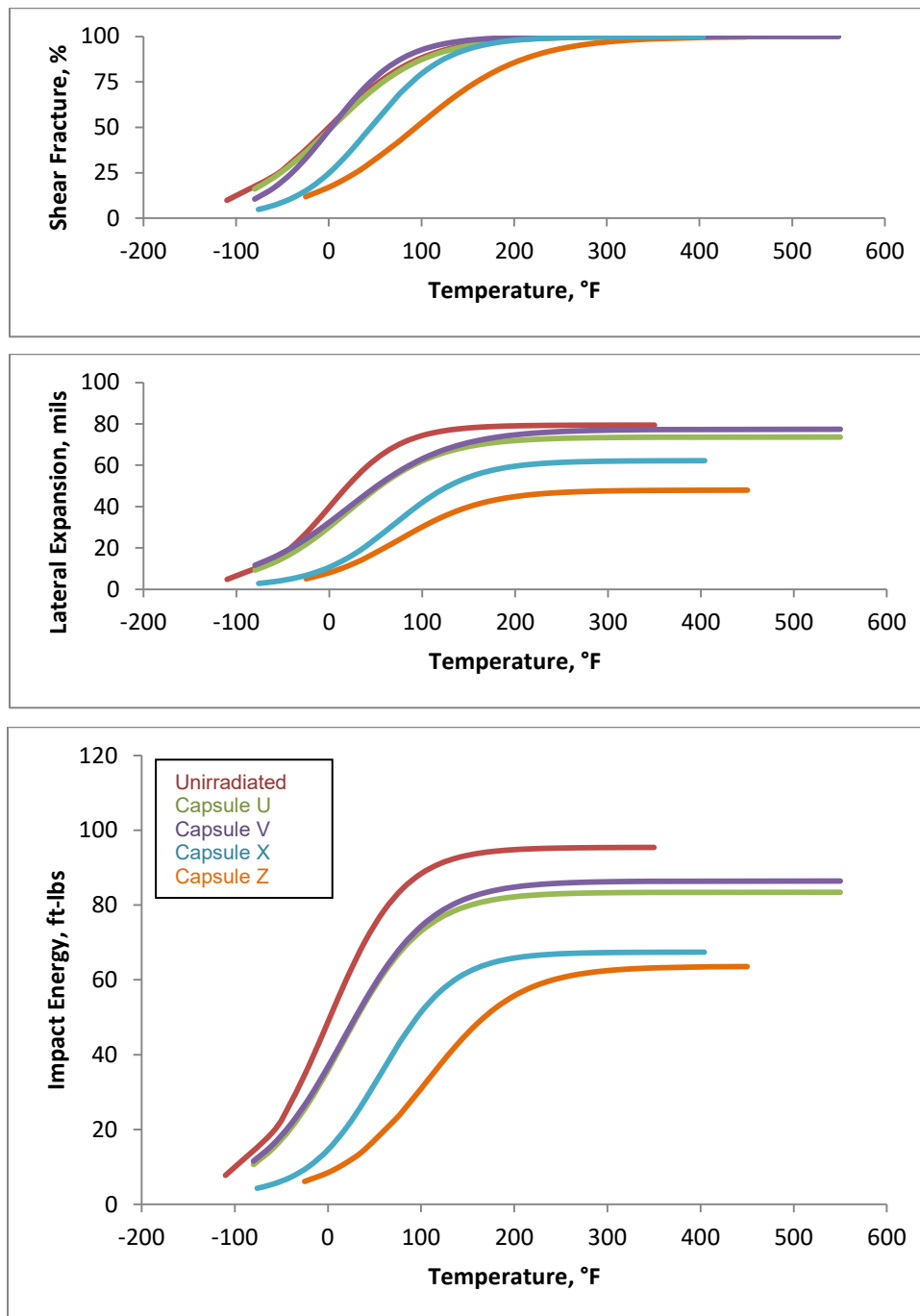
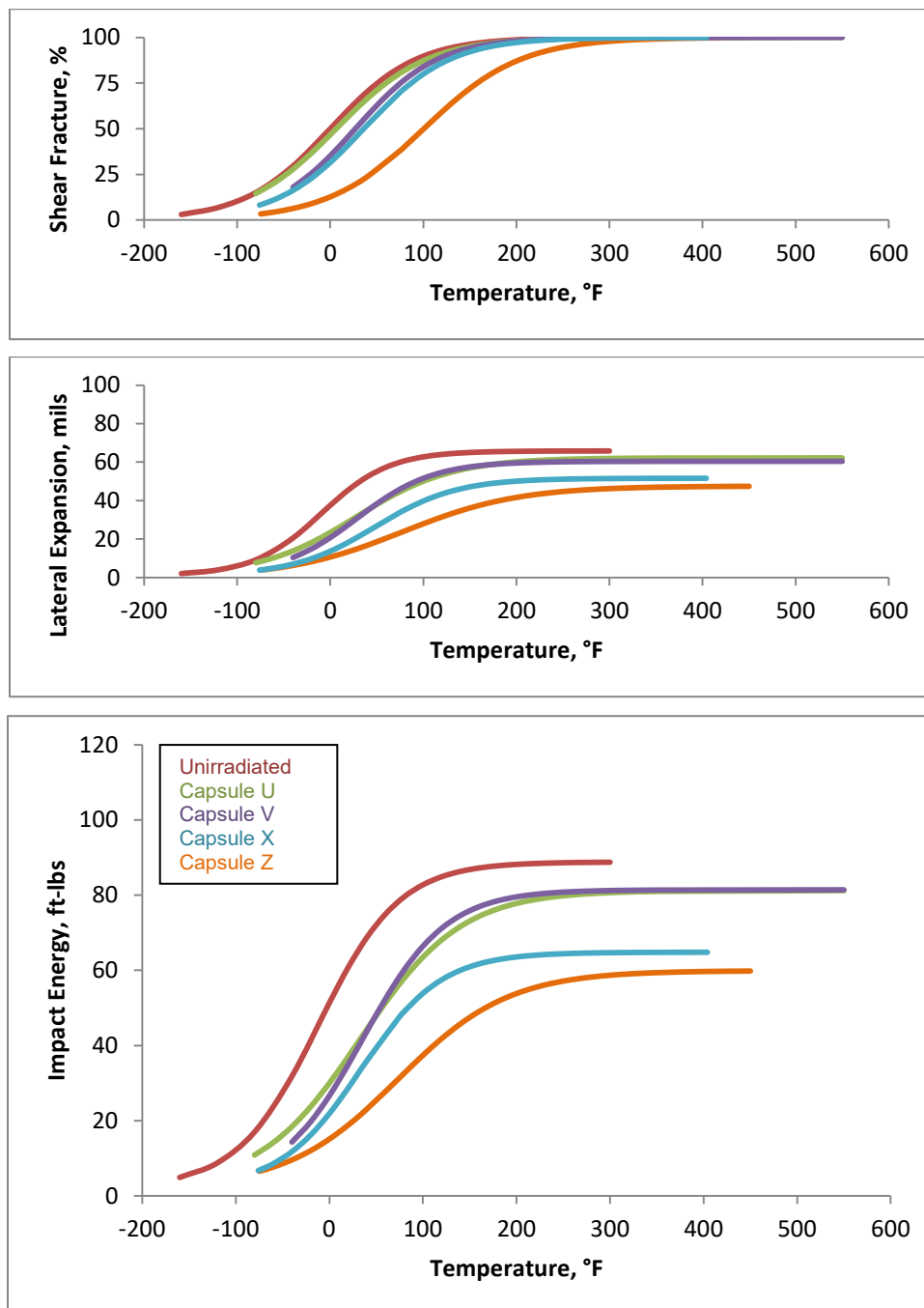


Figure 7-4. Comparison of Unirradiated and Irradiated Charpy Impact Data Curves for Heat-Affected-Zone Material

8.0 SUMMARY OF RESULTS

The analysis of the reactor vessel material contained in the fifth surveillance capsule, Capsule Z, removed for evaluation as part of the HNP Reactor Vessel Surveillance Program, led to the following conclusions:

1. The capsule received an average fast neutron fluence of $9.45 \times 10^{19} \text{ n/cm}^2$ ($E > 1.0 \text{ MeV}$).
2. Based on the calculated 21-cycle-average full power flux, the projected end-of-life (55 EFPY) peak fast fluence at the base metal-clad interface of the HNP reactor vessel is $6.87 \times 10^{19} \text{ n/cm}^2$ ($E > 1.0 \text{ MeV}$). The corresponding fluence at the outside surface vessel wall in this peak location is $4.22 \times 10^{19} \text{ n/cm}^2$ ($E > 1.0 \text{ MeV}$).
3. The 30 ft-lb transition temperature for the base metal plate, heat no. B4197-2, longitudinal (LT) orientation, increased 120.8°F after the irradiation to $9.45 \times 10^{19} \text{ n/cm}^2$ ($E > 1.0 \text{ MeV}$). In addition, the CvUSE for this material decreased by 27.6%.
4. The 30 ft-lb transition temperature for the base metal plate, heat no. B4197-2, transverse (TL) orientation, increased 123.2°F after the irradiation to $9.45 \times 10^{19} \text{ n/cm}^2$ ($E > 1.0 \text{ MeV}$). In addition, the CvUSE for this material decreased by 25.7%.
5. The 30 ft-lb transition temperature for the weld metal, weld wire heat 5P6771/flux lot 0342, increased 131.1°F after the irradiation to $9.45 \times 10^{19} \text{ n/cm}^2$ ($E > 1.0 \text{ MeV}$). In addition, the CvUSE for this material decreased by 31.9%.
6. The measured 30 ft-lb transition temperature shifts for the surveillance materials are greater than the values predicted using Regulatory Guide 1.99, Revision 2. When the margin (2σ) is added to the predicted shifts, the predicted 30 ft-lb transition temperature shift values are non-conservative for the Base Metal longitudinal and transverse surveillance materials and the Weld metal surveillance material.
7. The measured percent decrease in CvUSE for the surveillance weld metal is slightly greater than the values predicted using Regulatory Guide 1.99, Revision 2 (3.9%). However, this value remains above the required 50 ft-lb limit.
8. The measured percent decrease in CvUSE for the surveillance base metal in the longitudinal (LT) and transverse (TL) orientations were less than the Regulatory Guide 1.99, Revision 2 prediction.

9.0 SURVEILLANCE CAPSULE REMOVAL SCHEDULE

Based on the post-irradiation test results of Capsule Z, the following schedule is recommended for the examination of the remaining capsules in the HNP reactor vessel surveillance program:

| Withdrawal/Evaluation Schedule^(a) | | | | |
|---|-------------------------------------|----------------------------|----------------------|---|
| Capsule Identification | Location of Capsules ^(b) | Lead Factor ^(c) | Removal Time | Expected Capsule Fluence (n/cm ²) |
| W ^(d) | 110° | ---- | ---- | ----- |
| Y | 290° | 2.84 | Standby ^c | ----- |

- (a) In accordance with ASTM Standard E 185-82.
- (b) Reference reactor vessel irradiation locations, Figure 3-1.
- (c) The factor by which the capsule fluence leads the vessels maximum inner wall fluence.
- (d) Capsule W was removed at the end-of-cycle 16 (EOC-16), when the neutron fluence on Capsule W was expected to be roughly equal to the maximum neutron fluence on the clad-vessel interface at EOL (55 EFPY). Capsule W is currently in storage, held ready for testing or reconstitution and reinsertion into the vessel in accordance with the Harris renewed license NPF-62, Condition 2.K.^[8]
- (e) Capsule Y shall be left in place and maintained in readiness should it become necessary at a future date.^[8]

10.0 REFERENCES

1. L. R. Singer, *"Carolina Power & Light Company Shearon Harris Unit No. 1 Reactor Vessel Radiation Surveillance Program,"* WCAP-10502, Westinghouse Electric Corporation, Pittsburgh, Pennsylvania, May 1984.
2. Materials Reliability Program: Coordinated PWR Reactor Vessel Surveillance Program (CRVSP) Guidelines (MRP-326), EPRI, Palo Alto, CA: 2011. 1022871.
3. A. L. Lowe, Jr., et al., *"Analysis of Capsule U Carolina Power & Light Company Shearon Harris Unit No. 1 - Reactor Vessel Material Surveillance Program --,"* BAW-2083, Babcock & Wilcox, Lynchburg, Virginia, August 1989.
4. A. L. Lowe, Jr., et al., *"Analysis of Capsule V Carolina Power & Light Company Shearon Harris Unit No. 1 - Reactor Vessel Material Surveillance Program --,"* BAW-2154, B&W Nuclear Technologies, Lynchburg, Virginia, March 1992.
5. M. J. DeVan, et al., *"Analysis of Capsule X Carolina Power & Light Company Shearon Harris Unit No. 1 - Reactor Vessel Material Surveillance Program --,"* BAW-2355, Framatome Technologies, Lynchburg, Virginia, October 1999.
6. ASTM Standard E 185-82, *"Standard Practice for Conducting Surveillance Tests for Light-Water Cooled Nuclear Power Reactor Vessels, E 706 (IF)"* American Society for Testing and Materials, Philadelphia, Pennsylvania.
7. Code of Federal Regulation, Title 10, Part 50, *"Domestic Licensing of Production and Utilization Facilities,"* Appendix H, Reactor Vessel Material Surveillance Program Requirements, [60 FR 65476, Dec. 19, 1995; 68 FR 75390, Dec. 31, 2003; 73 FR 5723, Jan. 31, 2008].
8. NRC Letter, Subject: "Shearon Harris Nuclear Plant – Safety Evaluation for Revision to Reactor Vessel Surveillance Capsule Withdrawal Schedule (TAC No. ME6998)", dated October 21, 2011. (NRC Accession No. ML 11293A076)
9. Code of Federal Regulation, Title 10, Part 50, *"Domestic Licensing of Production and Utilization Facilities,"* Appendix G, Fracture Toughness Requirements, [60 FR 65474, Dec. 19, 1995; 73 FR 5723, Jan. 31, 2008; 78 FR 34248, Jun. 7, 2013; 78 FR 75450, Dec. 12, 2013].
10. American Society of Mechanical Engineers (ASME) Boiler and Pressure Vessel Code, Section III, *"Rules for Construction of Nuclear Facility Components,"* Appendix G, Fracture Toughness Criteria for Protection Against Failure, 2013 Edition.
11. American Society of Mechanical Engineers (ASME) Boiler and Pressure Vessel Code, Section XI, *"Rules for Inservice Inspection of Nuclear Power Plant Components,"* Appendix G, Fracture Toughness Criteria for Protection Against Failure, 2013 Edition.
12. ASTM Standard E 208-91, *"Method for Conducting Drop-Weight Test to Determine Nil-Ductility Transition Temperature of Ferritic Steels,"* American Society for Testing and Materials, Philadelphia, Pennsylvania.
13. C. Williams, *"Evaluation of Shearon Harris RVSP Capsule Z Sample Retrieval, Dosimetry, and Mechanical Testing,"* L-2005-015, BWX Technologies, Inc., Lynchburg, Virginia, June 2019.
14. ASTM Standard E 8-96a, *"Standard Test Methods for Tension Testing of Metallic Materials,"* American Society for Testing and Materials, Philadelphia, Pennsylvania.

15. ASTM Standard E 21-92, *"Standard Test Methods for Elevated Temperature Tension Tests of Metallic Materials,"* American Society for Test and Materials, Philadelphia, Pennsylvania.
16. ASTM Standard E 23-91, *"Standard Test Methods for Notched Bar Impact Testing of Metallic Materials,"* American Society for Test and Materials, Philadelphia, Pennsylvania.
17. J. R. Worsham III, *"Fluence and Uncertainty Methodologies,"* BAW-2241P, Revision 1, Framatome Inc., Lynchburg, Virginia, April 1999.
18. U.S. Nuclear Regulatory Commission, *"Calculational and Dosimetry Methods for Determining Pressure Vessel Neutron Fluence,"* Draft Regulatory Guide DG-1053, June 1996.
19. U.S. Nuclear Regulatory Commission, *"Radiation Embrittlement of Reactor Vessel Materials,"* Regulatory Guide 1.99, Revision 2, May 1988.

APPENDIX A REACTOR VESSEL SURVEILLANCE PROGRAM BACKGROUND DATA AND INFORMATION

A.1 *Capsule Identification*

The capsules used in the HNP reactor vessel surveillance program are identified in Table A-1 by identification, location, and designed lead factors. The capsule locations within the HNP reactor vessel are shown in Figure A-3.

A.2 *HNP Reactor Pressure Vessel*

The HNP reactor pressure vessel was fabricated by the Chicago Bridge & Iron Company. The HNP reactor vessel beltline region consists of two shells, containing four heats of base metal plate, four longitudinal weld seams, and one circumferential weld seam. Table A-2 presents a description of the HNP reactor vessel beltline materials including their copper and nickel chemical contents and their unirradiated mechanical properties. The heat treatments of the beltline materials are presented in Table A-3. The locations of the materials within the reactor vessel beltline region are shown in Figures A-1 and A-2.

A.3 *Surveillance Material Data Selection*

The data used to select the materials for the specimens in the surveillance program, in accordance with ASTM Standard E 185-82, are shown in Table A-2. Based on the initial RT_{NDT} value, copper and nickel contents and the projected end-of-life fluences, the reactor vessel intermediate shell plate B4197-2 is considered to be the limiting reactor vessel beltline material and has been used in the HNP reactor vessel surveillance program (RVSP). The surveillance weld used in the HNP RVSP was fabricated using the wire heat 5P6771 and Linde 124 flux lot 0342 which is identical to the intermediate to lower shell circumferential weld in the HNP reactor vessel.

Table A-1. HNP Surveillance Capsule Identifications, Original Locations, and Design Lead Factors

| Capsule Identification | Capsule Location ^(a) | Design Lead Factor ^(b) |
|------------------------|---------------------------------|-----------------------------------|
| U | 343° | 3.12 |
| V | 107° | 3.12 |
| X | 287° | 3.12 |
| W | 110° | 2.7 |
| Y | 290° | 2.7 |
| Z | 340° | 2.7 |

(a) Reference irradiation capsule locations as shown in Figure A-3.

(b) The factor by which the capsule fluence leads the vessel's maximum inner wall fluence

Framatome Inc.

ANP-3798NP

Revision 0

Analysis of Capsule Z

Duke Energy Shearon Harris Nuclear Power Plant

Reactor Vessel Material Surveillance Program

Page A-2

Table A-2. Description of the HNP Reactor Vessel Beltline Region Materials^{[A-1],[A-2]}

| Material Heat No. | Material Type | Beltline Region Location | Chemical Composition | | Unirradiated Toughness Properties | | | | | |
|----------------------------|------------------------|---|----------------------|---------|-----------------------------------|--------------|------------|---------------|-----------------------|------------------------|
| | | | Cu, wt% | Ni, wt% | 30 ft-lb, °F | 50 ft-lb, °F | 35 MLE, °F | CvUSE, ft-lbs | T _{NDT} , °F | RT _{NDT} , °F |
| A9153-1 | SA-533 Gr. B1 | Intermediate Shell | 0.09 | 0.46 | ---- | ---- | ---- | 83 | -10 | 60 |
| B4197-2 | SA-533 Gr. B1 | Intermediate Shell | 0.09 | 0.50 | ---- | ---- | ---- | 71 | -10 | 91 |
| C9924-1 | SA-533 Gr. B1 | Lower Shell | 0.08 | 0.47 | ---- | ---- | ---- | 98 | -10 | 54 |
| C9924-2 | SA-533 Gr. B1 | Lower Shell | 0.08 | 0.47 | ---- | ---- | ---- | 88 | -20 | 57 |
| 4P4784/3930 ^(a) | ASA Weld/ Linde 124 | Intermediate Shell Longitudinal Welds | 0.05 | 0.91 | ---- | ---- | ---- | 94 | -20 | -20 |
| 5P6771/0342 ^(a) | ASA Weld/ Linde 124 | Intermediate to Lower Shell Circ. Weld | 0.03 | 0.94 | ---- | ---- | ---- | 80 | -80 | -20 |
| 4P4784/3930 ^(a) | ASA Weld/ Linde 124 | Lower Shell Longitudinal Welds | 0.05 | 0.91 | ---- | ---- | ---- | 94 | -20 | -20 |

(a) Weld wire heat number and flux lot identifiers.

Table A-3. Heat Treatment of the HNP Reactor Vessel Beltline Region Materials

| Material | Heat Treatment^(a) |
|--|--|
| Intermediate Shell Plates A9153-1 and B4197-2 (Core Ring No. 2) | Austenitizing: 1600 ± 25°F for 4 hours; water quenched Tempered: 1250 ± 25°F for 4 hours; air cooled Stress Relief: 1050°F for 4 hours; air cooled Post Weld: 1150 + 25°F/ -50°F for 35-3/4 hours; furnace cooled |
| Lower Shell Plates C9924-1 and C9924-2 (Core Ring No. 1) | Austenitizing: 1600 ± 25°F for 4 hours; water quenched Tempered: 1250 ± 25°F for 4 hours; air cooled Stress Relief: 1075°F for 4 hours; air cooled Post Weld: 1150 + 25°F/ -50°F for 43 hours; furnace cooled |
| Intermediate Shell Longitudinal Seam Welds (Wire Heat 4P4784/ Flux Lot 3930) | Post Weld: 1150 + 25°F/ -50°F for 33-3/4 hours; furnace cooled ^(b) |
| Lower Shell Longitudinal Seam Welds (Wire Heat 4P4784/ Flux Lot 3930) | Post Weld: 1150 + 25°F/ -50°F for 36-1/4 hours; furnace cooled ^(b) |
| Intermediate to Lower Shell Girth Seam Weld (Wire Heat 5P6771/ Flux Lot 0342) | Local Heat Treat: 1150 + 25°F/ -50°F for 10-1/4 hours; furnace cooled |

(a) Austenitizing, tempering, and stress relief times are from Lukens Steel Company Test Certificates. The post weld heat treatment times are from Chicago Bridge & Iron Company thermal history records.

(b) The post weld heat treatment includes the PWHT for the Intermediate to Lower Shell Girth Seam Weld.

Figure A-1. Locations and Identifications of Materials Used in the Fabrication of the HNP Reactor Pressure Vessel

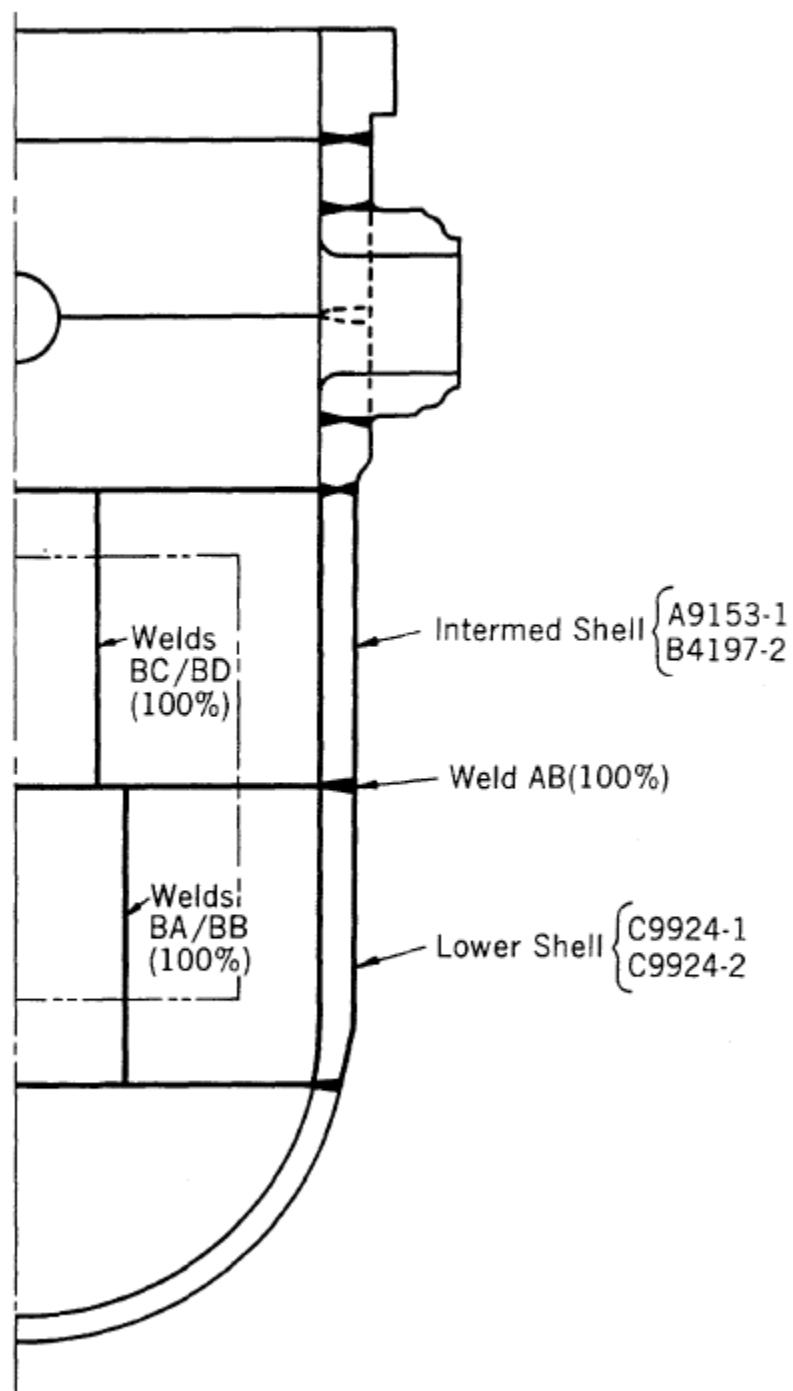


Figure A-2. Locations of Longitudinal Welds in HNP Reactor Pressure Vessel Upper and Lower Shell Courses

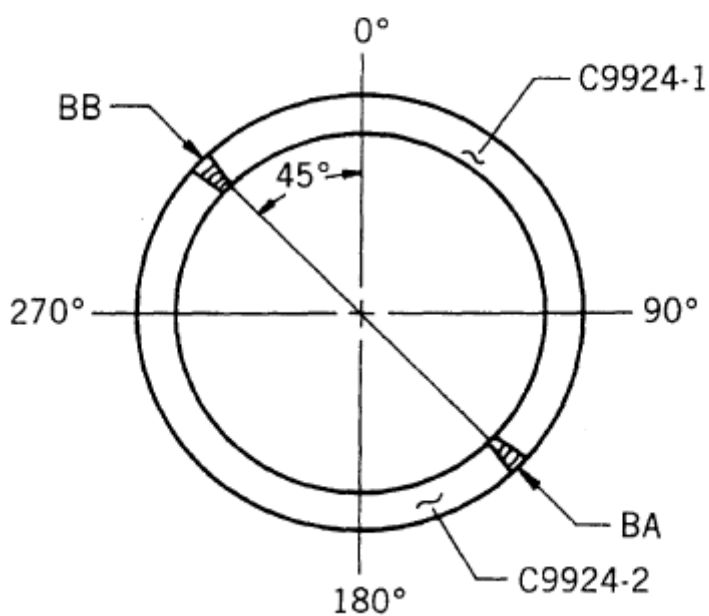
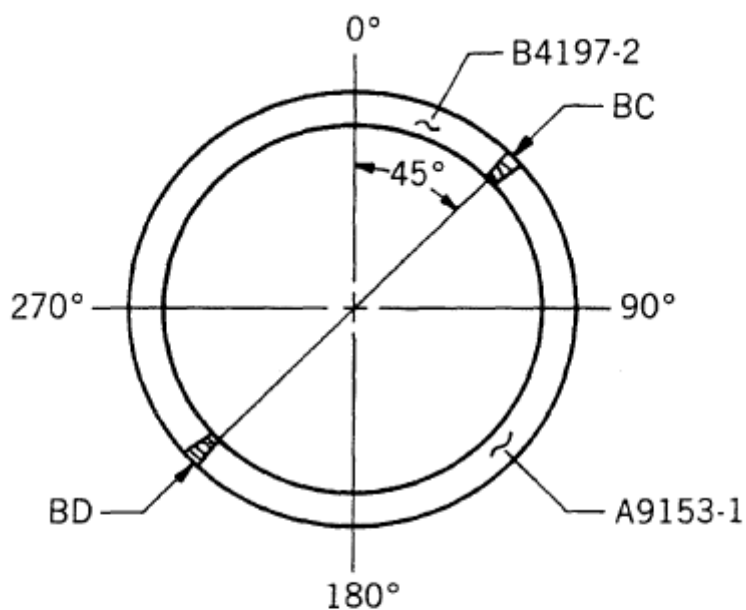
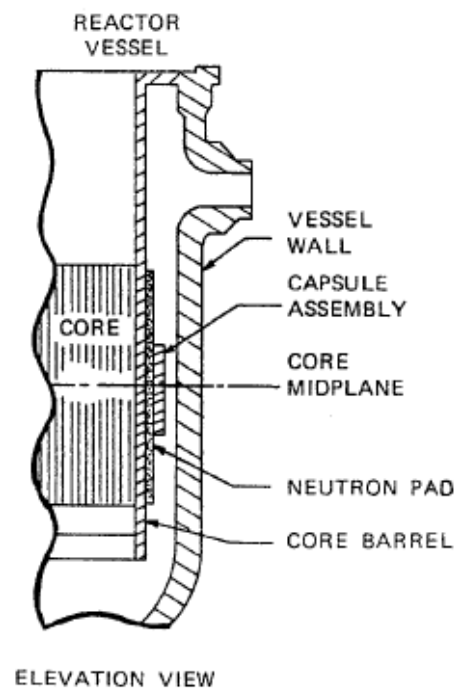
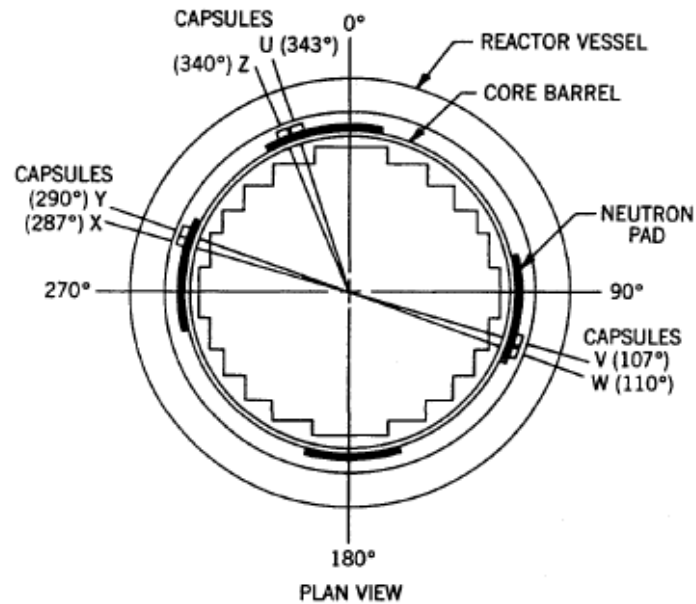


Figure A-3. Locations of Surveillance Capsule Irradiation Sites in the HNP Reactor Pressure Vessel



A.4 References

- A-1. Letter from W. R. Robinson (CP&L) to U.S. Nuclear Regulatory Commission, Attention: Document Control Desk, "*Shearon Harris Nuclear Power Plant Docket No. 50-400/License No. NPF-63 Request for License Amendment RCS Pressure/Temperature Limits,*" Serial: HNP-96-206, dated December 30, 1996.
- A-2. Letter from James Scarola (CP&L) to U.S. Nuclear Regulatory Commission, Attention: Document Control Desk, "*Shearon Harris Nuclear Power Plant Docket No. 50-400/License No. NPF-63 Response to Request for Additional Information Regarding Generic Letter 92-01, Revision 1, Supplement 1,*" Serial: HNP-98-129, dated September 16, 1998.

APPENDIX B UNIRRADIATED AND IRRADIATED TENSILE DATA FOR THE HNP RVSP MATERIALS

**Table B-1. Unirradiated Surveillance Tensile Properties of HNP
Base Metal Plate, Heat No. B4197-2, Longitudinal Orientation**

| Specimen No. | Test Temp., °F | Strength, ksi | | Elongation, % | | Reduction of Area % |
|--------------|----------------|---------------|----------|---------------|-------|---------------------|
| | | Yield | Ultimate | Uniform | Total | |
| --- | 75 | 71.0 | 94.0 | 8 | 25 | 61 |
| --- | 75 | 80.0 | 94.0 | 8 | 27 | 62 |
| --- | 300 | 74.0 | 88.0 | 6 | 22 | 64 |
| --- | 300 | 75.0 | 87.0 | 6 | 21 | 63 |
| --- | 550 | 74.0 | 88.0 | 6 | 19 | 54 |
| --- | 550 | 73.0 | 88.0 | 7 | 19 | 54 |

**Table B-2. Unirradiated Surveillance Tensile Properties of HNP
Base Metal Plate, Heat No. B4197-2, Transverse Orientation**

| Specimen No. | Test Temp., °F | Strength, ksi | | Elongation, % | | Reduction of Area % |
|--------------|----------------|---------------|----------|---------------|-------|---------------------|
| | | Yield | Ultimate | Uniform | Total | |
| --- | 75 | 69.0 | 91.0 | 10 | 26 | 63 |
| --- | 75 | 68.0 | 91.0 | 11 | 26 | 60 |
| --- | 300 | 61.0 | 83.0 | 10 | 24 | 59 |
| --- | 300 | 61.0 | 83.0 | 9 | 23 | 58 |
| --- | 550 | 60.0 | 87.0 | 9 | 21 | 54 |
| --- | 550 | 60.0 | 86.0 | 9 | 20 | 55 |

**Table B-3. Unirradiated Surveillance Tensile Properties of HNP
Weld Metal, Wire Heat 5P6771 / Flux Lot 034**

| Specimen No. | Test Temp., °F | Strength, ksi | | Elongation, % | | Reduction of Area % |
|--------------|----------------|---------------|----------|---------------|-------|---------------------|
| | | Yield | Ultimate | Uniform | Total | |
| --- | 75 | 74.0 | 89.0 | 10 | 29 | 68 |
| --- | 75 | 74.0 | 89.0 | 10 | 26 | 67 |
| --- | 300 | 66.0 | 82.0 | 8 | 23 | 65 |
| --- | 300 | 64.0 | 80.0 | 7 | 24 | 67 |
| --- | 550 | 63.0 | 84.0 | 9 | 23 | 65 |
| --- | 550 | 63.0 | 83.0 | 8 | 22 | 64 |

Table B-4. HNP Capsule U Surveillance Tensile Properties of Base Metal Plate, Heat No. B4197-2, Irradiated to 5.52×10^{18} n/cm² (E>1.0 MeV) Longitudinal Orientation

| Specimen No. | Test Temp., °F | Strength, ksi | | Elongation, % | | Reduction of Area % |
|--------------|----------------|---------------|----------|---------------|-------|---------------------|
| | | Yield | Ultimate | Uniform | Total | |
| QL2 | 70 | 72.4 | 97.0 | 10.1 | 23.7 | 63.0 |
| QL3 | 70 | 72.3 | 96.4 | 10.4 | 22.8 | 62.1 |
| QL1 | 550 | 65.7 | 93.6 | 9.6 | 19.3 | 52.7 |

Table B-5. HNP Capsule U Surveillance Tensile Properties of Base Metal Plate, Heat No. B4197-2, Irradiated to 5.52×10^{18} n/cm² (E>1.0 MeV) Transverse Orientation

| Specimen No. | Test Temp., °F | Strength, ksi | | Elongation, % | | Reduction of Area % |
|--------------|----------------|---------------|----------|---------------|-------|---------------------|
| | | Yield | Ultimate | Uniform | Total | |
| QT2 | 70 | 72.2 | 97.3 | 11.1 | 23.2 | 55.9 |
| QT3 | 70 | 72.3 | 95.8 | 11.3 | 24.1 | 59.0 |
| QT1 | 550 | 69.3 | 93.7 | 8.5 | 17.4 | 50.4 |

Table B-6. HNP Capsule U Surveillance Tensile Properties of Weld Metal, Wire Heat 5P6771 / Flux Lot 0342, Irradiated to 5.52×10^{18} n/cm² (E>1.0 MeV)

| Specimen No. | Test Temp., °F | Strength, ksi | | Elongation, % | | Reduction of Area % |
|--------------|----------------|---------------|----------|---------------|-------|---------------------|
| | | Yield | Ultimate | Uniform | Total | |
| QW3 | 70 | 76.3 | 91.0 | 11.2 | 25.6 | 66.8 |
| QW1 | 70 | 76.3 | 91.1 | 11.3 | 25.9 | 67.3 |
| QW2 | 550 | 69.0 | 87.5 | 9.2 | 20.9 | 62.5 |

Table B-7. HNP Capsule V Surveillance Tensile Properties of Base Metal Plate, Heat No. B4197-2, Irradiated to 1.32×10^{19} n/cm² (E>1.0 MeV) Longitudinal Orientation

| Specimen No. | Test Temp., °F | Strength, ksi | | Elongation, % | | Reduction of Area % |
|--------------|----------------|---------------|----------|---------------|-------|---------------------|
| | | Yield | Ultimate | Uniform | Total | |
| QL4 | 70 | 73.6 | 97.4 | 10.1 | 23.2 | 62.4 |
| QL5 | 70 | 74.3 | 98.0 | 8.7 | 21.0 | 62.5 |
| QL6 | 550 | 69.0 | 93.8 | 8.1 | 15.9 | 42.4 |

Table B-8. HNP Capsule V Surveillance Tensile Properties of Base Metal Plate, Heat No. B4197-2, Irradiated to 1.32×10^{19} n/cm² (E>1.0 MeV) Transverse Orientation

| Specimen No. | Test Temp., °F | Strength, ksi | | Elongation, % | | Reduction of Area % |
|--------------|----------------|---------------|----------|---------------|-------|---------------------|
| | | Yield | Ultimate | Uniform | Total | |
| QT4 | 70 | 73.7 | 96.2 | 9.6 | 22.9 | 58.5 |
| QT5 | 70 | 78.3 | 98.5 | 8.2 | 20.5 | 58.3 |
| QT6 | 550 | 66.6 | 92.7 | 8.8 | 17.3 | 44.2 |

Table B-9. HNP Capsule V Surveillance Tensile Properties of Weld Metal, Wire Heat 5P6771 / Flux Lot 0342, Irradiated to 1.32×10^{19} n/cm² (E>1.0 MeV)

| Specimen No. | Test Temp., °F | Strength, ksi | | Elongation, % | | Reduction of Area % |
|--------------|----------------|---------------|----------|---------------|-------|---------------------|
| | | Yield | Ultimate | Uniform | Total | |
| QW4 | 70 | 75.3 | 91.6 | 9.3 | 22.4 | 64.0 |
| QW5 | 70 | 76.6 | 91.9 | 9.4 | 22.6 | 59.8 |
| QW6 | 550 | 70.3 | 88.3 | 7.6 | 18.6 | 61.6 |

Table B-10. HNP Capsule X Surveillance Tensile Properties of Base Metal Plate, Heat No. B4197-2, Irradiated to 3.25×10^{19} n/cm² (E>1.0 MeV) Longitudinal Orientation

| Specimen No. | Test Temp., °F | Strength, ksi | | Elongation, % | | Reduction of Area % |
|--------------|----------------|---------------|----------|---------------|-------|---------------------|
| | | Yield | Ultimate | Uniform | Total | |
| QL11 | 70 | 79.6 | 101.2 | 10.2 | 22.9 | 60.2 |
| QL12 | 300 | 71.7 | 92.6 | 9.2 | 20.3 | 60.3 |
| QL10 | 550 | 72.8 | 99.0 | 8.7 | 17.0 | 43.8 |

Table B-11. HNP Capsule X Surveillance Tensile Properties of Base Metal Plate, Heat No. B4197-2, Irradiated to 3.25×10^{19} n/cm² (E>1.0 MeV) Transverse Orientation

| Specimen No. | Test Temp., °F | Strength, ksi | | Elongation, % | | Reduction of Area % |
|--------------|----------------|---------------|----------|---------------|-------|---------------------|
| | | Yield | Ultimate | Uniform | Total | |
| QT11 | 70 | 80.0 | 101.0 | 9.8 | 22.5 | 60.1 |
| QT12 | 300 | 72.6 | 92.8 | 9.3 | 19.4 | 55.6 |
| QT10 | 550 | 70.4 | 95.8 | 9.9 | 17.8 | 53.2 |

Table B-12. HNP Capsule X Surveillance Tensile Properties of Weld Metal, Wire Heat 5P6771 / Flux Lot 0342, Irradiated to 3.25×10^{19} n/cm² (E>1.0 MeV)

| Specimen No. | Test Temp., °F | Strength, ksi | | Elongation, % | | Reduction of Area % |
|--------------|----------------|---------------|----------|---------------|-------|---------------------|
| | | Yield | Ultimate | Uniform | Total | |
| QW11 | 70 | 82.8 | 95.4 | 10.2 | 24.8 | 63.0 |
| QW10 | 300 | 76.0 | 88.2 | 10.0 | 22.3 | 64.5 |
| QW12 | 550 | 75.6 | 93.0 | 9.4 | 21.1 | 61.1 |

APPENDIX C UNIRRADIATED AND IRRADIATED CHARPY V-NOTCH IMPACT SURVEILLANCE DATA FOR THE HNP RVSP MATERIALS USING HYPERBOLIC TANGENT CURVE-FITTING METHOD

**Table C-1. Unirradiated Surveillance Charpy V-Notch Impact Data
for HNP Base Metal Plate, Heat No. B4197-2, Longitudinal (LT)
Orientation**

| Specimen | Test Temp (°F) | Impact Energy (ft-lb) | Lateral Expansion (mils) | Shear Fracture (%) |
|-----------------|-------------------------------|--------------------------------------|---|-----------------------------------|
| -- | -60 | 5.0 | 0.0 | 5 |
| -- | -60 | 8.0 | 2.0 | 5 |
| -- | 0 | 14.0 | 8.0 | 15 |
| -- | 0 | 18.0 | 10.0 | 15 |
| -- | 30 | 19.0 | 12.0 | 25 |
| -- | 30 | 27.0 | 18.0 | 20 |
| -- | 30 | 38.0 | 30.0 | 30 |
| -- | 75 | 31.0 | 23.0 | 30 |
| -- | 75 | 36.0 | 29.0 | 30 |
| -- | 75 | 37.0 | 29.0 | 33 |
| -- | 120 | 52.0 | 45.0 | 45 |
| -- | 120 | 52.0 | 43.0 | 50 |
| -- | 120 | 55.0 | 46.0 | 55 |
| -- | 160 | 78.0 | 64.0 | 90 |
| -- | 160 | 83.0 | 68.0 | 90 |
| -- | 200 | 84.0 | 67.0 | 95 |
| -- | 200 | 85.0 | 75.0 | 95 |
| -- | 250 | 92.0 | 75.0 | 100 |
| -- | 250 | 94.0 | 71.0 | 100 |
| -- | 350 | 74.0 | 65.0 | 100 |

Table C-2. HNP Capsule U Surveillance Charpy Impact Data for Base Metal Plate, Heat No. B4197-2, Irradiated to 5.52×10^{18} n/cm² (E>1.0 MeV) Longitudinal (LT) Orientation

| Specimen | Test Temp (°F) | Impact Energy (ft-lb) | Lateral Expansion (mils) | Shear Fracture (%) |
|-----------------|-----------------------|------------------------------|---------------------------------|---------------------------|
| QL1 | 0 | 11.5 | 8.0 | 0 |
| QL3 | 40 | 21.0 | 17.0 | 20 |
| QL10 | 70 | 22.5 | 21.0 | 30 |
| QL11 | 90 | 40.0 | 45.0 | 30 |
| QL12 | 110 | 37.0 | 30.0 | 30 |
| QL15 | 125 | 43.5 | 38.0 | 50 |
| QL6 | 140 | 49.0 | 43.0 | 60 |
| QL14 | 175 | 66.0 | 49.0 | 85 |
| QL2 | 225 | 80.5 | 64.0 | 100 |
| QL4 | 275 | 89.5 | 67.0 | 100 |
| QL8 | 325 | 90.0 | 72.0 | 100 |
| QL9 | 375 | 99.0 | 69.0 | 100 |
| QL5 | 425 | 89.0 | 71.0 | 100 |
| QL7 | 475 | 92.5 | 69.0 | 100 |
| QL13 | 550 | 100.0 | 79.0 | 100 |

Table C-3. HNP Capsule V Surveillance Charpy Impact Data for Base Metal Plate, Heat No. B4197-2, Irradiated to 1.32×10^{19} n/cm² (E>1.0 MeV) Longitudinal (LT) Orientation

| Specimen | Test Temp (°F) | Impact Energy (ft-lb) | Lateral Expansion (mils) | Shear Fracture (%) |
|----------|----------------|-----------------------|--------------------------|--------------------|
| QL30 | 40 | 17.0 | 14.0 | 5 |
| QL28 | 70 | 22.0 | 17.0 | 20 |
| QL26 | 90 | 32.0 | 25.0 | 30 |
| QL18 | 110 | 32.0 | 26.0 | 45 |
| QL29 | 140 | 45.0 | 38.0 | 50 |
| QL22 | 170 | 55.0 | 46.0 | 50 |
| QL23 | 200 | 66.5 | 57.0 | 95 |
| QL21 | 225 | 75.0 | 59.0 | 95 |
| QL20 | 275 | -- | 66.0 | 100 |
| QL27 | 275 | 76.0 | 63.0 | 100 |
| QL19 | 325 | 87.5 | 70.0 | 100 |
| QL16 | 375 | 87.0 | 73.0 | 100 |
| QL24 | 425 | 84.0 | 71.0 | 100 |
| QL25 | 475 | 84.0 | 71.0 | 100 |
| QL17 | 550 | 86.0 | 76.0 | 100 |

Table C-4. HNP Capsule X Surveillance Charpy Impact Data for Base Metal Plate, Heat No. B4197-2, Irradiated to 3.25×10^{19} n/cm² (E>1.0 MeV) Longitudinal (LT) Orientation

| Specimen | Test Temp (°F) | Impact Energy (ft-lb) | Lateral Expansion (mils) | Shear Fracture (%) |
|-----------------|-----------------------|------------------------------|---------------------------------|---------------------------|
| QL49 | 74 | 13.5 | 9.0 | 10 |
| QL50 | 104 | 15.5 | 12.0 | 30 |
| QL51 | 129 | 21.0 | 18.0 | 50 |
| QL47 | 154 | 28.5 | 22.0 | 55 |
| QL48 | 154 | 30.5 | 23.0 | 55 |
| QL46 | 179 | 42.5 | 36.0 | 65 |
| QL56 | 179 | 47.5 | 39.0 | 65 |
| QL60 | 204 | 61.0 | 48.0 | 90 |
| QL52 | 229 | 53.0 | 45.0 | 85 |
| QL57 | 254 | 67.5 | 57.0 | 100 |
| QL58 | 254 | 68.5 | 53.0 | 100 |
| QL54 | 304 | 64.5 | 56.0 | 100 |
| QL55 | 304 | 61.0 | 53.0 | 100 |
| QL53 | 354 | 63.5 | 59.0 | 100 |
| QL59 | 404 | 68.5 | 59.0 | 100 |

Table C-5. Hyperbolic Tangent Curve Fit Coefficients for HNP Base Metal Plate, Heat No. B4197-2, Longitudinal (LT) Orientation

| | Hyperbolic Tangent Curve Fit Coefficients | | | |
|--------------|---|-----------------|-------------------|------------------------|
| | Coefficient | Absorbed Energy | Lateral Expansion | Percent Shear Fracture |
| Unirradiated | A | 47.0 | 37.7 | 50.0 |
| | B | 44.8 | 36.7 | 50.0 |
| | C | 102.3 | 88.9 | 91.9 |
| | T0 | 92.3 | 93.9 | 102.3 |
| Capsule U | A | 49.1 | 37.0 | 50.0 |
| | B | 46.9 | 36.0 | 50.0 |
| | C | 120.5 | 129.7 | 78.1 |
| | T0 | 133.3 | 117.0 | 122.4 |
| Capsule V | A | 44.3 | 37.1 | 50.0 |
| | B | 42.1 | 36.1 | 50.0 |
| | C | 118.1 | 120.6 | 85.6 |
| | T0 | 136.0 | 138.5 | 133.8 |
| Capsule X | A | 34.6 | 29.6 | 50.0 |
| | B | 32.4 | 28.6 | 50.0 |
| | C | 70.4 | 76.6 | 79.3 |
| | T0 | 155.1 | 162.0 | 143.0 |

**Table C-6. Unirradiated Surveillance Charpy V-Notch Impact Data
for HNP Base Metal Plate, Heat No. B4197-2, Transverse (TL)
Orientation**

| Specimen | Test Temp (°F) | Impact Energy (ft-lb) | Lateral Expansion (mils) | Shear Fracture (%) |
|-----------------|-------------------------------|--------------------------------------|---|-----------------------------------|
| -- | -60 | 4.0 | 0.0 | 2 |
| -- | -60 | 4.0 | 0.0 | 5 |
| -- | 0 | 12.0 | 7.0 | 10 |
| -- | 0 | 14.0 | 8.0 | 15 |
| -- | 40 | 23.0 | 19.0 | 30 |
| -- | 40 | 27.0 | 22.0 | 25 |
| -- | 75 | 29.0 | 22.0 | 35 |
| -- | 75 | 29.0 | 26.0 | 30 |
| -- | 75 | 37.0 | 28.0 | 30 |
| -- | 120 | 39.0 | 35.0 | 40 |
| -- | 120 | 42.0 | 36.0 | 55 |
| -- | 120 | 48.0 | 43.0 | 50 |
| -- | 160 | 56.0 | 52.0 | 90 |
| -- | 160 | 61.0 | 52.0 | 90 |
| -- | 200 | 63.0 | 56.0 | 100 |
| -- | 200 | 65.0 | 58.0 | 100 |
| -- | 250 | 67.0 | 60.0 | 100 |
| -- | 250 | 69.0 | 60.0 | 100 |
| -- | 350 | 65.0 | 62.0 | 100 |
| -- | 350 | 93.0 | 82.0 | 100 |

**Table C-7. HNP Capsule U Surveillance Charpy Impact Data for
Base Metal Plate, Heat No. B4197-2, Irradiated to 5.52×10^{18} n/cm²
(E>1.0 MeV) Transverse (TL) Orientation**

| Specimen | Test Temp (°F) | Impact Energy (ft-lb) | Lateral Expansion (mils) | Shear Fracture (%) |
|-----------------|-------------------------------|--------------------------------------|---|-----------------------------------|
| QT10 | 70 | 17.0 | 18.0 | 20 |
| QT15 | 70 | 15.0 | 15.0 | 20 |
| QT9 | 90 | 29.5 | 25.0 | 35 |
| QT6 | 110 | 29.5 | 26.0 | 40 |
| QT1 | 140 | 47.0 | 46.0 | 100 |
| QT14 | 140 | 32.0 | 30.0 | 60 |
| QT5 | 175 | 51.5 | 47.0 | 80 |
| QT8 | 175 | 50.0 | 45.0 | 85 |
| QT11 | 225 | 62.0 | 56.0 | 100 |
| QT13 | 275 | 66.0 | 57.0 | 100 |
| QT12 | 325 | 70.0 | 62.0 | 100 |
| QT2 | 375 | 68.0 | 59.0 | 100 |
| QT3 | 425 | 68.0 | 61.0 | 100 |
| QT4 | 475 | 71.5 | 64.0 | 100 |
| QT7 | 550 | 68.5 | 59.0 | 100 |

Table C-8. HNP Capsule V Surveillance Charpy Impact Data for Base Metal Plate, Heat No. B4197-2, Irradiated to 1.32×10^{19} n/cm² (E>1.0 MeV) Transverse (TL) Orientation

| Specimen | Test Temp (°F) | Impact Energy (ft-lb) | Lateral Expansion (mils) | Shear Fracture (%) |
|----------|----------------|-----------------------|--------------------------|--------------------|
| QT22 | 70 | 18.0 | 16.0 | 10 |
| QT29 | 90 | 27.0 | 24.0 | 40 |
| QT27 | 110 | 32.5 | 31.0 | 50 |
| QT26 | 140 | 38.0 | 36.0 | 50 |
| QT21 | 170 | 47.5 | 40.0 | 70 |
| QT28 | 170 | 48.0 | 40.0 | 50 |
| QT18 | 200 | 50.0 | 45.0 | 75 |
| QT23 | 200 | 49.5 | 44.0 | 50 |
| QT30 | 225 | 60.0 | 52.0 | 50 |
| QT19 | 275 | 60.0 | 53.0 | 55 |
| QT24 | 325 | 63.5 | 58.0 | 100 |
| QT20 | 375 | 60.0 | 56.0 | 60 |
| QT25 | 425 | 66.0 | 60.0 | 100 |
| QT17 | 475 | 61.5 | 59.0 | 100 |
| QT16 | 550 | 67.0 | 63.0 | 100 |

Table C-9. HNP Capsule X Surveillance Charpy Impact Data for Base Metal Plate, Heat No. B4197-2, Irradiated to 3.25×10^{19} n/cm² (E>1.0 MeV) Transverse (TL) Orientation

| Specimen | Test Temp (°F) | Impact Energy (ft-lb) | Lateral Expansion (mils) | Shear Fracture (%) |
|-----------------|-----------------------|------------------------------|---------------------------------|---------------------------|
| QT56 | 74 | 13.5 | 8.0 | 10 |
| QT55 | 104 | 19.5 | 16.0 | 30 |
| QT50 | 129 | 20.5 | 16.0 | 40 |
| QT49 | 154 | 24.5 | 20.0 | 50 |
| QT52 | 154 | 32.0 | 25.0 | 60 |
| QT57 | 179 | 43.5 | 37.0 | 50 |
| QT60 | 179 | 36.5 | 34.0 | 65 |
| QT58 | 204 | 47.5 | 39.0 | 95 |
| QT46 | 229 | 42.5 | 38.0 | 70 |
| QT47 | 254 | 43.5 | 40.0 | 85 |
| QT54 | 254 | 55.0 | 53.0 | 100 |
| QT48 | 304 | 50.0 | 47.0 | 100 |
| QT51 | 304 | 60.5 | 55.0 | 100 |
| QT53 | 354 | 54.5 | 51.0 | 100 |
| QT59 | 404 | 56.5 | 53.0 | 100 |

Table C-10. Hyperbolic Tangent Curve Fit Coefficients for HNP Base Metal Plate, Heat No. B4197-2, Transverse (TL) Orientation

| | Hyperbolic Tangent Curve Fit Coefficients | | | |
|--------------|---|-----------------|-------------------|------------------------|
| | Coefficient | Absorbed Energy | Lateral Expansion | Percent Shear Fracture |
| Unirradiated | A | 40.1 | 35.1 | 50.0 |
| | B | 37.9 | 34.1 | 50.0 |
| | C | 125.2 | 113.4 | 83.1 |
| | T0 | 105.9 | 110.0 | 104.3 |
| Capsule U | A | 35.8 | 31.0 | 50.0 |
| | B | 33.6 | 30.0 | 50.0 |
| | C | 98.2 | 97.9 | 59.4 |
| | T0 | 127.5 | 119.2 | 111.2 |
| Capsule V | A | 33.1 | 30.6 | 50.0 |
| | B | 30.9 | 29.6 | 50.0 |
| | C | 110.9 | 135.2 | 118.4 |
| | T0 | 118.6 | 123.4 | 136.6 |
| Capsule X | A | 29.3 | 26.9 | 50.0 |
| | B | 27.1 | 25.9 | 50.0 |
| | C | 99.9 | 95.1 | 90.0 |
| | T0 | 148.8 | 160.5 | 150.1 |

**Table C-11. Unirradiated Surveillance Charpy V-Notch Impact Data
for HNP Weld Metal, Wire Heat 5P6771/Flux Lot 0342**

| Specimen | Test Temp (°F) | Impact Energy (ft-lb) | Lateral Expansion (mils) | Shear Fracture (%) |
|-----------------|-------------------------------|--------------------------------------|---|-----------------------------------|
| -- | -110 | 7.0 | 1.0 | 15 |
| -- | -110 | 8.0 | 2.0 | 15 |
| -- | -60 | 21.0 | 16.0 | 35 |
| -- | -60 | 25.0 | 18.0 | 40 |
| -- | -30 | 28.0 | 20.0 | 55 |
| -- | -30 | 31.0 | 26.0 | 45 |
| -- | -30 | 33.0 | 26.0 | 45 |
| -- | 0 | 42.0 | 36.0 | 50 |
| -- | 0 | 46.0 | 41.0 | 55 |
| -- | 0 | 52.0 | 45.0 | 65 |
| -- | 40 | 65.0 | 58.0 | 80 |
| -- | 40 | 75.0 | 60.0 | 85 |
| -- | 75 | 78.0 | 64.0 | 90 |
| -- | 75 | 89.0 | 73.0 | 97 |
| -- | 75 | 90.0 | 72.0 | 95 |
| -- | 160 | 91.0 | 78.0 | 100 |
| -- | 160 | 92.0 | 84.0 | 100 |
| -- | 250 | 92.0 | 79.0 | 100 |
| -- | 250 | 96.0 | 75.0 | 100 |
| -- | 350 | 97.0 | 81.0 | 100 |

Table C-12. HNP Capsule U Surveillance Charpy Impact Data for Weld Metal, Wire Heat 5P6771/Flux Lot 0342, Irradiated to 5.52×10^{18} n/cm² (E>1.0 MeV) Transverse (TL) Orientation

| Specimen | Test Temp (°F) | Impact Energy (ft-lb) | Lateral Expansion (in) | Lateral Expansion (mils) | Shear Fracture (%) |
|----------|----------------|-----------------------|------------------------|--------------------------|--------------------|
| QW6 | -80 | 7.5 | 0.005 | 5.0 | 20 |
| QW2 | -40 | 19.0 | 0.017 | 17.0 | 40 |
| QW12 | -20 | 28.0 | 0.025 | 25.0 | 30 |
| QW11 | 0 | 42.0 | 0.035 | 35.0 | 50 |
| QW5 | 20 | 40.0 | 0.035 | 35.0 | 60 |
| QW15 | 40 | 64.0 | 0.051 | 51.0 | 75 |
| QW3 | 70 | 62.0 | 0.052 | 52.0 | 70 |
| QW8 | 70 | 60.5 | 0.053 | 53.0 | 85 |
| QW9 | 110 | 74.0 | 0.063 | 63.0 | 90 |
| QW10 | 140 | 81.0 | 0.069 | 69.0 | 100 |
| QW13 | 175 | 80.5 | 0.070 | 70.0 | 100 |
| QW4 | 225 | 83.0 | 0.074 | 74.0 | 100 |
| QW1 | 275 | 80.0 | 0.073 | 73.0 | 100 |
| QW7 | 375 | 83.0 | 0.071 | 71.0 | 100 |
| QW14 | 550 | 89.0 | 0.078 | 78.0 | 100 |

**Table C-13. HNP Capsule V Surveillance Charpy Impact Data for
Weld Metal, Wire Heat 5P6771/Flux Lot 0342, Irradiated to 1.32×10^{19}
 n/cm^2 ($E > 1.0$ MeV) Transverse (TL) Orientation**

| Specimen | Test Temp (°F) | Impact Energy (ft-lb) | Lateral Expansion (in) | Lateral Expansion (mils) | Shear Fracture (%) |
|-----------------|-------------------------------|--------------------------------------|---------------------------------------|---|-----------------------------------|
| QW23 | -80 | 12.0 | 0.010 | 10.0 | 15 |
| QW28 | -40 | 23.0 | 0.021 | 21.0 | 30 |
| QW27 | 0 | 34.0 | 0.031 | 31.0 | 50 |
| QW30 | 20 | 42.0 | 0.039 | 39.0 | 50 |
| QW19 | 40 | 58.5 | 0.050 | 50.0 | 65 |
| QW25 | 70 | 70.0 | 0.060 | 60.0 | 100 |
| QW16 | 110 | 74.0 | 0.056 | 56.0 | 100 |
| QW24 | 110 | 74.0 | 0.066 | 66.0 | 95 |
| QW18 | 140 | 80.0 | 0.071 | 71.0 | 100 |
| QW22 | 170 | 85.0 | 0.073 | 73.0 | 100 |
| QW21 | 225 | 88.0 | 0.078 | 78.0 | 100 |
| QW29 | 275 | 82.0 | 0.072 | 72.0 | 100 |
| QW26 | 325 | 81.5 | 0.074 | 74.0 | 100 |
| QW17 | 375 | 90.0 | 0.081 | 81.0 | 100 |
| QW20 | 550 | 90.0 | 0.081 | 81.0 | 100 |

**Table C-14. HNP Capsule X Surveillance Charpy Impact Data for
Weld Metal, Wire Heat 5P6771/Flux Lot 0342, Irradiated to 3.25×10^{19}
 n/cm^2 ($E > 1.0$ MeV) Transverse (TL) Orientation**

| Specimen | Test Temp (°F) | Impact Energy (ft-lb) | Lateral Expansion (in) | Lateral Expansion (mils) | Shear Fracture (%) |
|-----------------|-----------------------|------------------------------|-------------------------------|---------------------------------|---------------------------|
| QW59 | -76 | 4.5 | 0.005 | 5.0 | 0 |
| QW56 | -36 | 11.0 | 0.006 | 6.0 | 5 |
| QW58 | 4 | 11.5 | 0.007 | 7.0 | 25 |
| QW49 | 24 | 21.5 | 0.017 | 17.0 | 45 |
| QW54 | 44 | 31.0 | 0.024 | 24.0 | 50 |
| QW52 | 74 | 43.5 | 0.033 | 33.0 | 70 |
| QW48 | 104 | 52.0 | 0.045 | 45.0 | 80 |
| QW53 | 104 | 50.5 | 0.041 | 41.0 | 75 |
| QW55 | 129 | 58.5 | 0.051 | 51.0 | 85 |
| QW57 | 154 | 63.5 | 0.052 | 52.0 | 95 |
| QW51 | 204 | 67.0 | 0.061 | 61.0 | 100 |
| QW47 | 254 | 68.5 | 0.063 | 63.0 | 100 |
| QW46 | 304 | 70.0 | 0.065 | 65.0 | 100 |
| QW50 | 304 | 65.5 | 0.061 | 61.0 | 100 |
| QW60 | 404 | 64.0 | 0.059 | 59.0 | 100 |

**Table C-15. Hyperbolic Tangent Curve Fit Coefficients for HNP Weld
Metal, Wire Heat 5P6771/Flux Lot 0342**

| | Hyperbolic Tangent Curve Fit Coefficients | | | |
|--------------|---|-----------------|-------------------|------------------------|
| | Coefficient | Absorbed Energy | Lateral Expansion | Percent Shear Fracture |
| Unirradiated | A | 48.8 | 40.2 | 50.0 |
| | B | 46.6 | 39.2 | 50.0 |
| | C | 79.7 | 74.2 | 99.2 |
| | T0 | 0.1 | 0.8 | 0.0 |
| Capsule U | A | 42.8 | 37.3 | 50.0 |
| | B | 40.6 | 36.3 | 50.0 |
| | C | 88.3 | 96.8 | 100.7 |
| | T0 | 15.2 | 19.3 | 3.3 |
| Capsule V | A | 44.3 | 39.2 | 50.0 |
| | B | 42.1 | 38.2 | 50.0 |
| | C | 93.1 | 109.4 | 77.1 |
| | T0 | 16.9 | 19.7 | 2.6 |
| Capsule X | A | 34.8 | 31.6 | 50.0 |
| | B | 32.6 | 30.6 | 50.0 |
| | C | 77.7 | 84.0 | 81.1 |
| | T0 | 56.4 | 70.4 | 45.1 |

**Table C-16. Unirradiated Surveillance Charpy V-Notch Impact Data
for HNP Heat-Affected-Zone Material**

| Specimen | Test Temp (°F) | Impact Energy (ft-lb) | Lateral Expansion (mils) | Shear Fracture (%) |
|-----------------|-------------------------------|--------------------------------------|---|-----------------------------------|
| --- | -160 | 7.0 | 2.0 | 5 |
| --- | -160 | 13.0 | 9.0 | 25 |
| --- | -120 | 12.0 | 4.0 | 10 |
| --- | -120 | 16.0 | 5.0 | 10 |
| --- | -90 | 9.0 | 2.0 | 15 |
| --- | -90 | 11.0 | 5.0 | 13 |
| --- | -60 | 23.0 | 16.0 | 37 |
| --- | -60 | 24.0 | 16.0 | 35 |
| --- | -60 | 30.0 | 18.0 | 30 |
| --- | -30 | 30.0 | 21.0 | 40 |
| --- | -30 | 34.0 | 26.0 | 40 |
| --- | -30 | 39.0 | 30.0 | 40 |
| --- | 0 | 36.0 | 26.0 | 45 |
| --- | 0 | 48.0 | 33.0 | 55 |
| --- | 0 | 52.0 | 38.0 | 55 |
| --- | 40 | 63.0 | 46.0 | 80 |
| --- | 40 | 76.0 | 56.0 | 75 |
| --- | 75 | 83.0 | 65.0 | 100 |
| --- | 75 | 84.0 | 70.0 | 100 |
| --- | 75 | 94.0 | 67.0 | 100 |
| --- | 140 | 75.0 | 58.0 | 100 |
| --- | 140 | 78.0 | 57.0 | 100 |
| --- | 220 | 79.0 | 63.0 | 100 |
| --- | 220 | 87.0 | 63.0 | 100 |
| --- | 300 | 97.0 | 69.0 | 100 |

Table C-17. HNP Capsule U Surveillance Charpy Impact Data for Heat-Affected-Zone Material, Irradiated to 5.52×10^{18} n/cm² (E>1.0 MeV)

| Specimen | Test Temp (°F) | Impact Energy (ft-lb) | Lateral Expansion (in) | Lateral Expansion (mils) | Shear Fracture (%) |
|-----------------|-----------------------|------------------------------|-------------------------------|---------------------------------|---------------------------|
| QH10 | -80 | 10.0 | 0.006 | 6.0 | 10 |
| QH7 | -40 | 19.0 | 0.014 | 14.0 | 35 |
| QH12 | -40 | 18.5 | 0.013 | 13.0 | 30 |
| QH5 | 0 | 31.5 | 0.024 | 24.0 | 50 |
| QH14 | 0 | 27.5 | 0.024 | 24.0 | 40 |
| QH11 | 40 | 41.0 | 0.034 | 34.0 | 65 |
| QH3 | 70 | 54.0 | 0.044 | 44.0 | 50 |
| QH13 | 70 | 65.0 | 0.050 | 50.0 | 100 |
| QH15 | 110 | 63.0 | 0.048 | 48.0 | 100 |
| QH2 | 175 | 72.5 | 0.055 | 55.0 | 100 |
| QH4 | 225 | 78.0 | 0.058 | 58.0 | 100 |
| QH6 | 275 | 75.0 | 0.061 | 61.0 | 100 |
| QH8 | 375 | 78.0 | 0.060 | 60.0 | 100 |
| QH1 | 450 | 84.0 | 0.064 | 64.0 | 100 |
| QH9 | 550 | 90.5 | 0.070 | 70.0 | 100 |

Table C-18. HNP Capsule V Surveillance Charpy Impact Data for Heat-Affected-Zone Material, Irradiated to 1.32×10^{19} n/cm² (E>1.0 MeV)

| Specimen | Test Temp (°F) | Impact Energy (ft-lb) | Lateral Expansion (in) | Lateral Expansion (mils) | Shear Fracture (%) |
|-----------------|-----------------------|------------------------------|-------------------------------|---------------------------------|---------------------------|
| QH29 | -40 | 11.0 | 0.008 | 8.0 | 20 |
| QH22 | 0 | 26.0 | 0.022 | 22.0 | 40 |
| QH27 | 40 | 50.0 | 0.039 | 39.0 | 45 |
| QH26 | 70 | 58.0 | 0.042 | 42.0 | 80 |
| QH19 | 110 | 74.0 | 0.056 | 56.0 | 100 |
| QH20 | 110 | 65.0 | 0.050 | 50.0 | 70 |
| QH17 | 140 | 70.0 | 0.055 | 55.0 | 100 |
| QH23 | 170 | 78.0 | 0.065 | 65.0 | 100 |
| QH16 | 225 | 66.0 | 0.047 | 47.0 | 100 |
| QH18 | 275 | 85.0 | 0.064 | 64.0 | 100 |
| QH28 | 275 | 68.0 | 0.053 | 53.0 | 80 |
| QH24 | 325 | 87.0 | 0.061 | 61.0 | 100 |
| QH30 | 375 | 80.0 | 0.062 | 62.0 | 100 |
| QH21 | 475 | 83.0 | 0.061 | 61.0 | 100 |
| QH25 | 550 | 100.0 | 0.070 | 70.0 | 100 |

Table C-19. HNP Capsule X Surveillance Charpy Impact Data for Heat-Affected-Zone Material, Irradiated to 3.25×10^{19} n/cm² (E>1.0 MeV)

| Specimen | Test Temp (°F) | Impact Energy (ft-lb) | Lateral Expansion (in) | Lateral Expansion (mils) | Shear Fracture (%) |
|-----------------|-----------------------|------------------------------|-------------------------------|---------------------------------|---------------------------|
| QH57 | -76 | 2.5 | 0.003 | 3.0 | 0 |
| QH59 | -36 | 16.5 | 0.008 | 8.0 | 10 |
| QH55 | 4 | 22.5 | 0.014 | 14.0 | 40 |
| QH56 | 24 | 30.5 | 0.019 | 19.0 | 50 |
| QH51 | 44 | 40.0 | 0.028 | 28.0 | 60 |
| QH48 | 74 | 46.5 | 0.032 | 32.0 | 60 |
| QH50 | 104 | 59.5 | 0.045 | 45.0 | 100 |
| QH58 | 104 | 41.5 | 0.032 | 32.0 | 50 |
| QH52 | 129 | 53.5 | 0.043 | 43.0 | 85 |
| QH60 | 129 | 76.5 | 0.056 | 56.0 | 100 |
| QH54 | 154 | 56.0 | 0.043 | 43.0 | 95 |
| QH49 | 204 | 67.5 | 0.049 | 49.0 | 100 |
| QH47 | 254 | 61.5 | 0.046 | 46.0 | 100 |
| QH46 | 304 | 62.5 | 0.054 | 54.0 | 100 |
| QH53 | 404 | 67.0 | 0.055 | 55.0 | 100 |

Table C-20. Hyperbolic Tangent Curve Fit Coefficients for HNP Heat-Affected-Zone Material

| | Hyperbolic Tangent Curve Fit Coefficients | | | |
|--------------|---|-----------------|---------------|------------------------|
| | Coefficient | Absorbed Energy | Lateral Expan | Percent Shear Fracture |
| Unirradiated | A | 45.5 | 33.4 | 50.0 |
| | B | 43.3 | 32.4 | 50.0 |
| | C | 86.4 | 73.0 | 92.3 |
| | T0 | -11.7 | -9.3 | 0.0 |
| Capsule U | A | 41.7 | 31.6 | 50.0 |
| | B | 39.5 | 30.6 | 50.0 |
| | C | 107.9 | 102.9 | 97.4 |
| | T0 | 33.0 | 28.3 | 6.4 |
| Capsule V | A | 41.8 | 30.7 | 50.0 |
| | B | 39.6 | 29.7 | 50.0 |
| | C | 88.4 | 81.8 | 88.3 |
| | T0 | 35.7 | 28.6 | 27.0 |
| Capsule X | A | 33.5 | 26.3 | 50.0 |
| | B | 31.3 | 25.3 | 50.0 |
| | C | 85.7 | 87.5 | 92.6 |
| | T0 | 33.4 | 48.1 | 36.0 |

Figure C-1. Unirradiated Surveillance Charpy V-Notch Impact Data for HNP Base Metal Plate, Heat No. B4197-2, Longitudinal (LT) Orientation - Refitted Using Hyperbolic Tangent Curve-Fitting Method

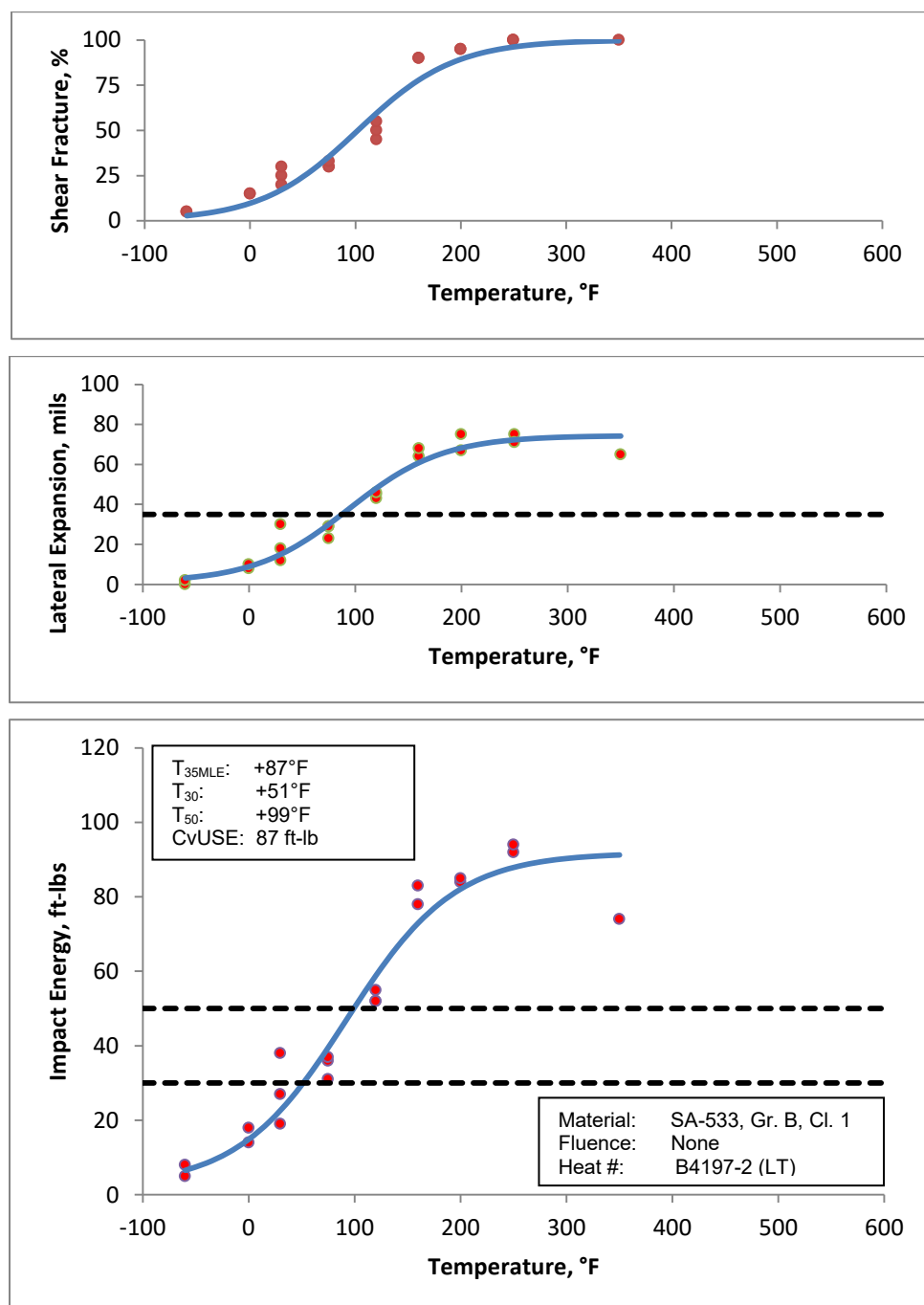


**Figure C-2. HNP Capsule U Surveillance Charpy V-Notch Impact
Data for Base Metal Plate, Heat No. B4197-2, Longitudinal (LT)
Orientation - Refitted Using Hyperbolic Tangent Curve-Fitting Method**

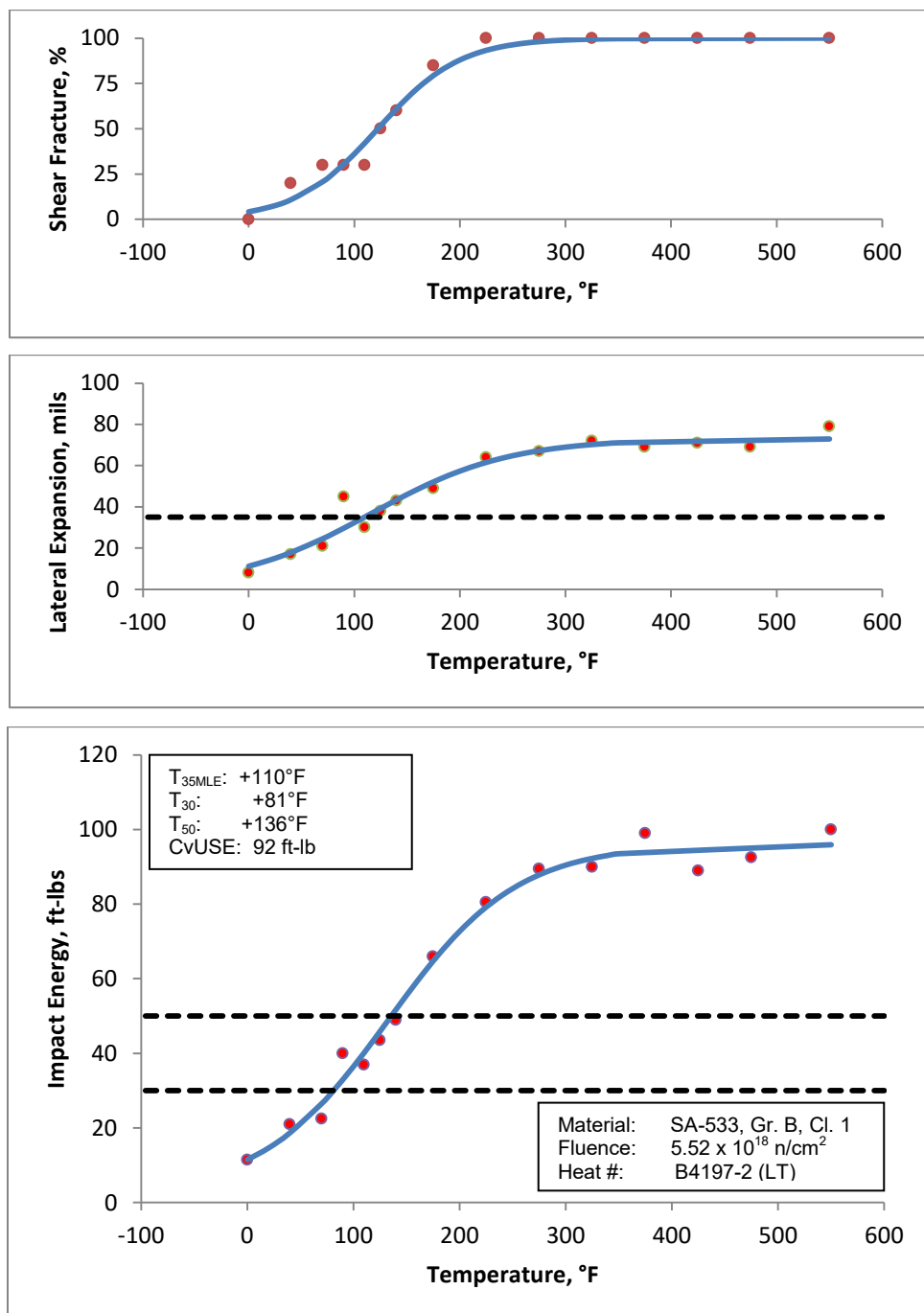


**Figure C-3. HNP Capsule V Surveillance Charpy V-Notch Impact
Data for Base Metal Plate, Heat No. B4197-2, Longitudinal (LT)
Orientation - Refitted Using Hyperbolic Tangent Curve-Fitting Method**

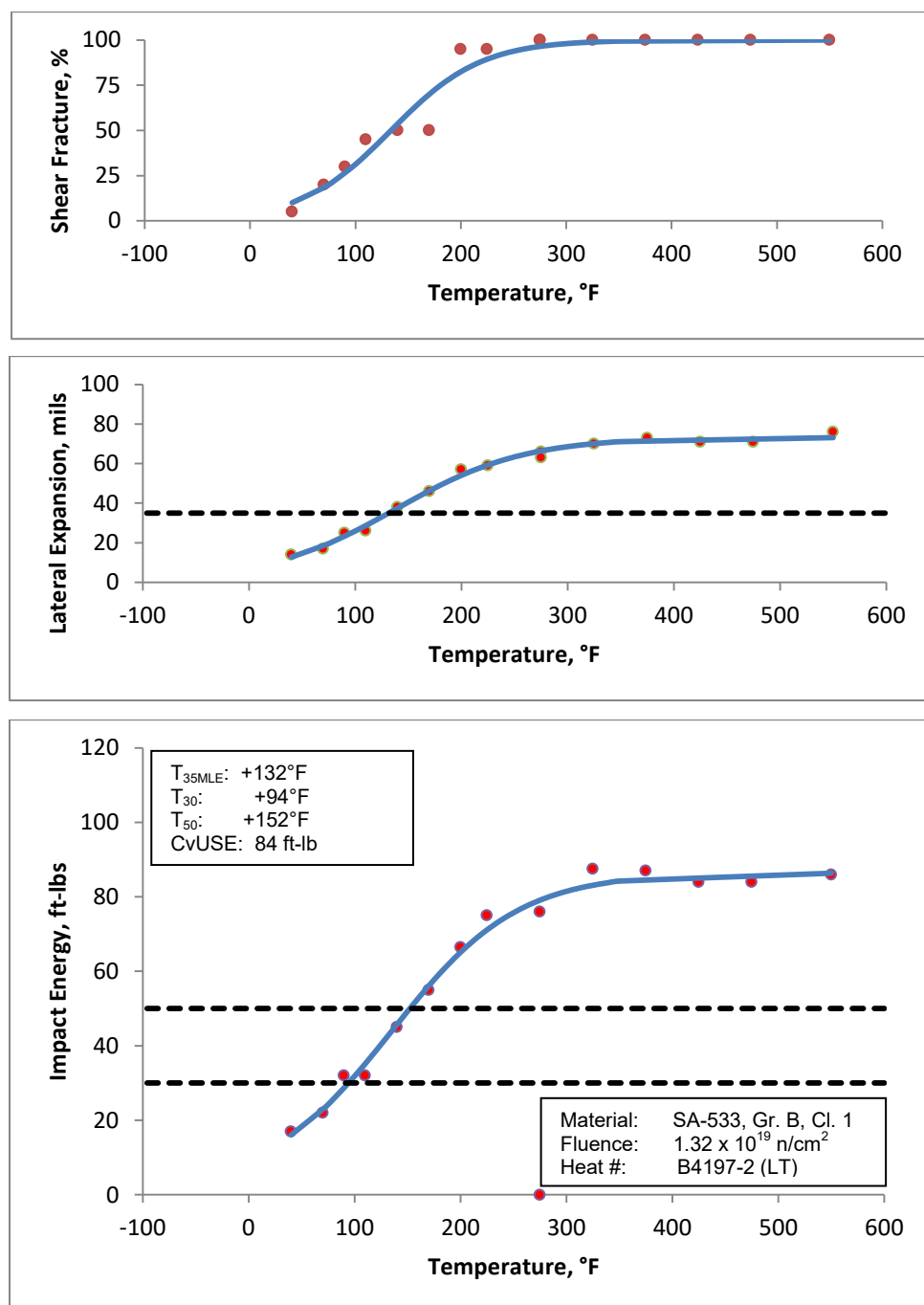


Figure C-4. HNP Capsule X Surveillance Charpy V-Notch Impact Data for Base Metal Plate, Heat No. B4197-2, Longitudinal (LT) Orientation - Refitted Using Hyperbolic Tangent Curve-Fitting Method

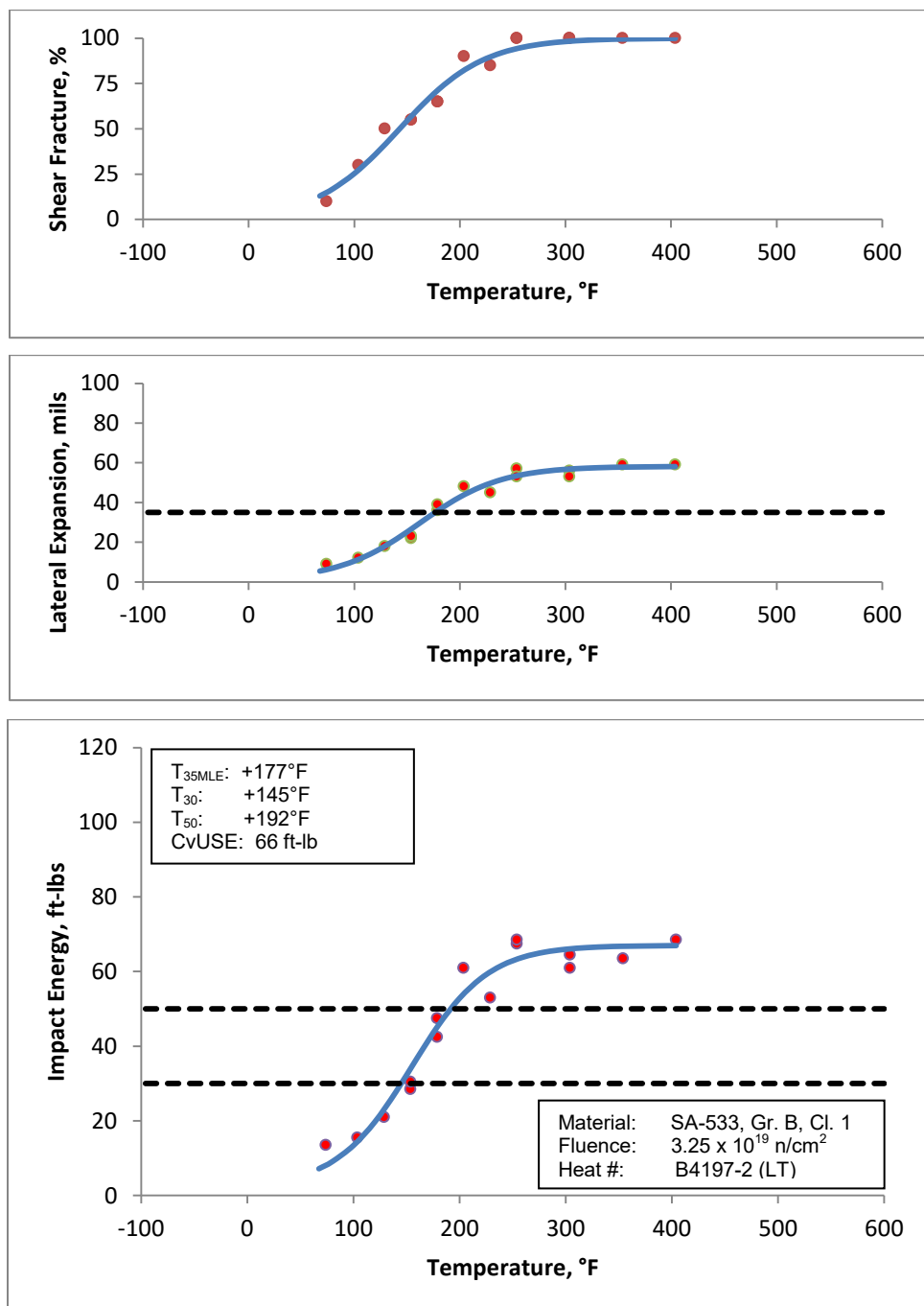


Figure C-5. Unirradiated Surveillance Charpy V-Notch Impact Data for HNP Base Metal Plate, Heat No. B4197-2, Transverse (TL) Orientation - Refitted Using Hyperbolic Tangent Curve-Fitting Method

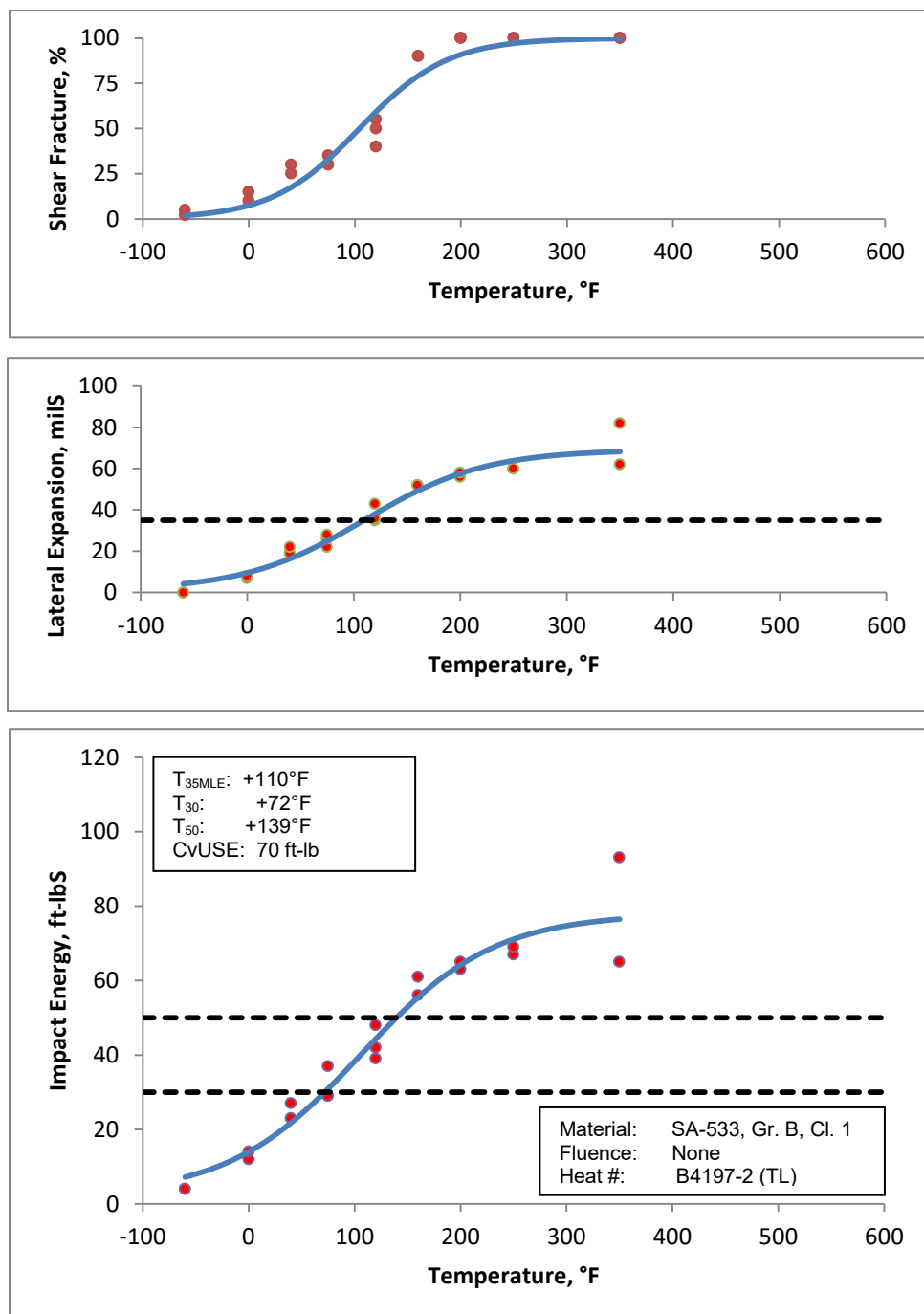
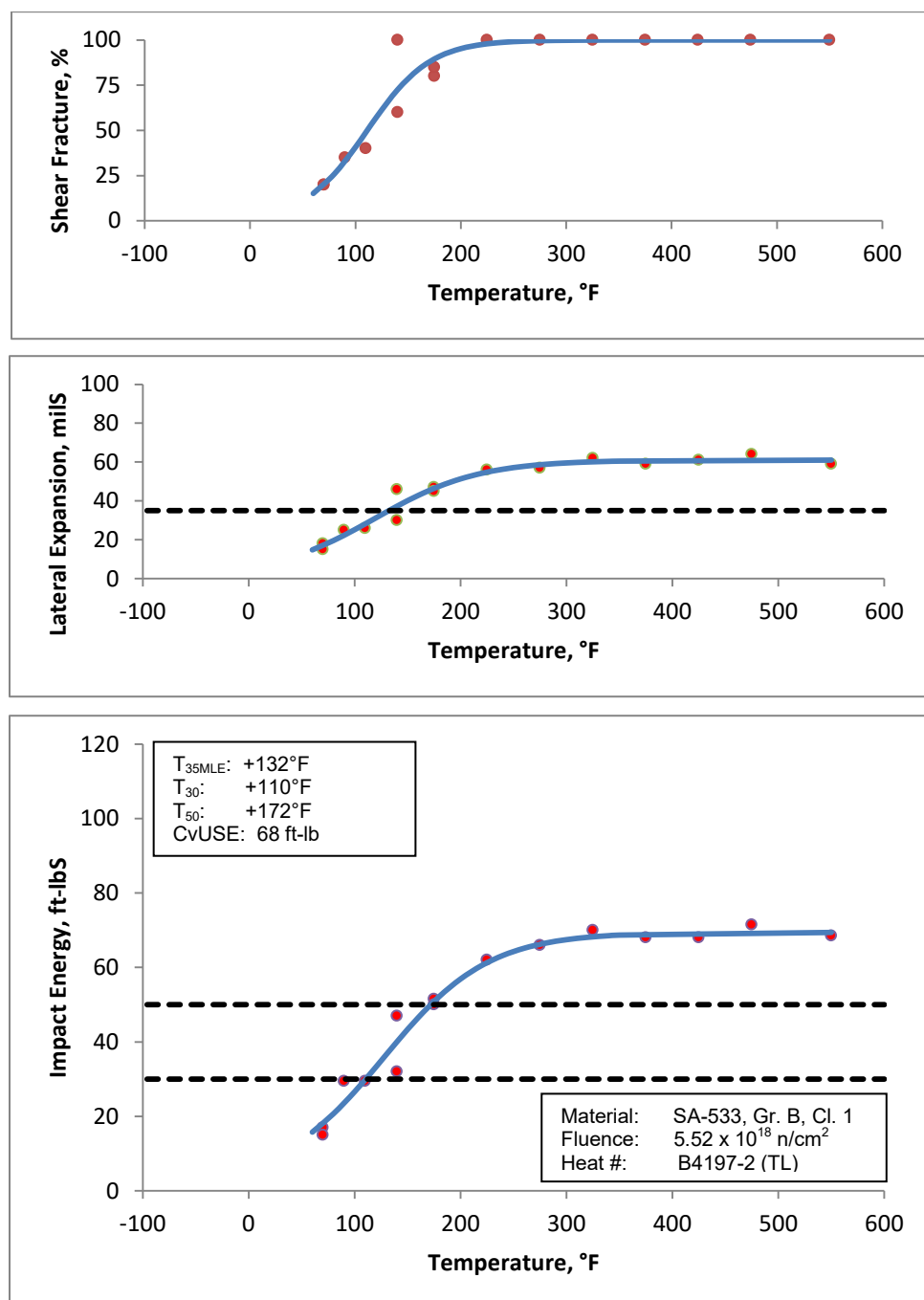


Figure C-6. HNP Capsule U Surveillance Charpy V-Notch Impact Data for Base Metal Plate, Heat No. B4197-2, Transverse (TL) Orientation - Refitted Using Hyperbolic Tangent Curve-Fitting Method



**Figure C-7. HNP Capsule V Surveillance Charpy V-Notch Impact
Data for Base Metal Plate, Heat No. B4197-2, Transverse (TL)
Orientation - Refitted Using Hyperbolic Tangent Curve-Fitting Method**

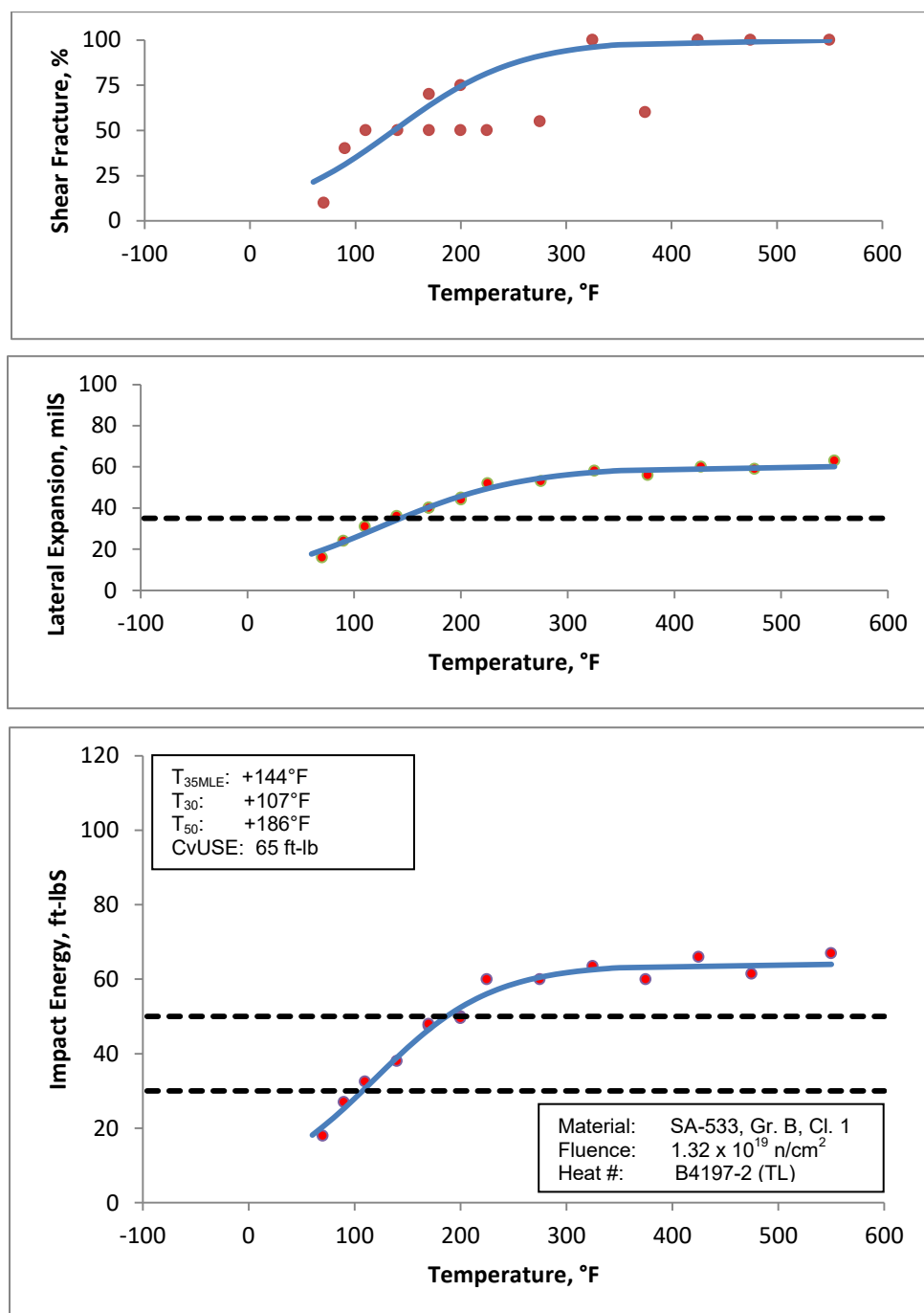


Figure C-8. HNP Capsule X Surveillance Charpy V-Notch Impact Data for Base Metal Plate, Heat No. B4197-2, Transverse (TL) Orientation - Refitted Using Hyperbolic Tangent Curve-Fitting Method

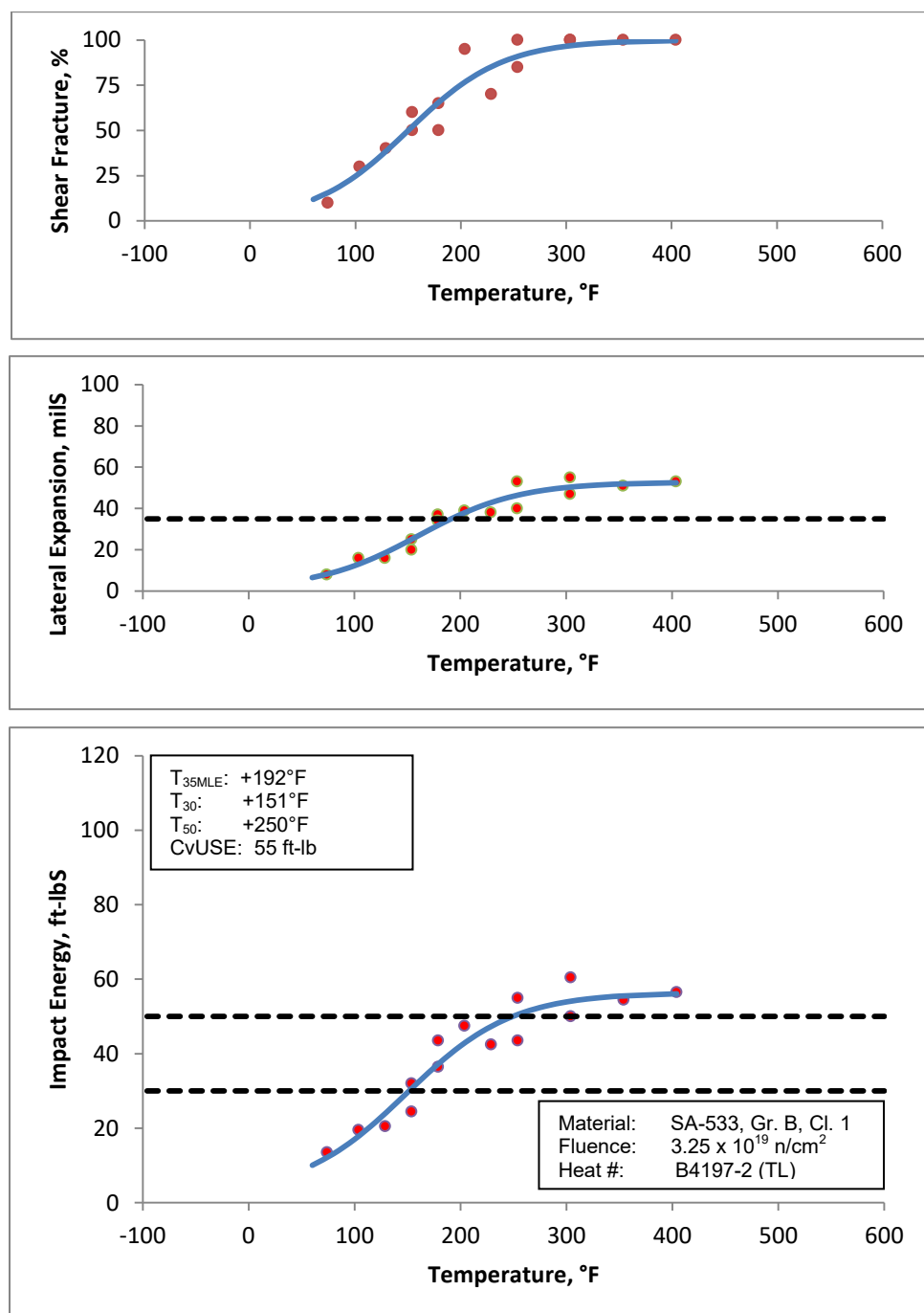
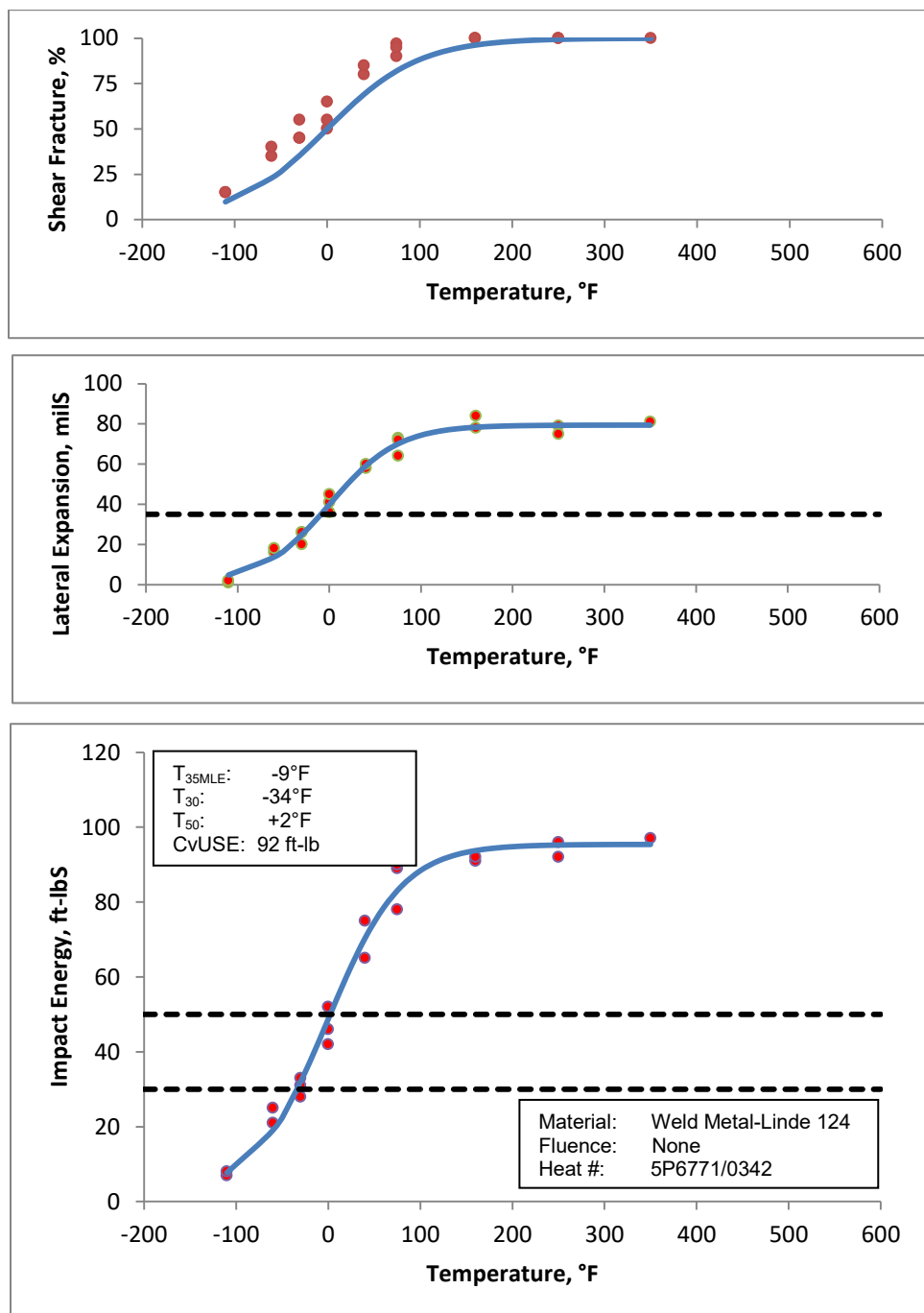


Figure C-9. Unirradiated Surveillance Charpy V-Notch Impact Data for HNP Weld Metal, Wire Heat 5P6771/Flux Lot 0342 - Refitted Using Hyperbolic Tangent Curve-Fitting Method



**Figure C-10. HNP Capsule U Surveillance Charpy V-Notch Impact
Data for Weld Metal, Wire Heat 5P6771/Flux Lot 0342 - Refitted Using
Hyperbolic Tangent Curve-Fitting Method**

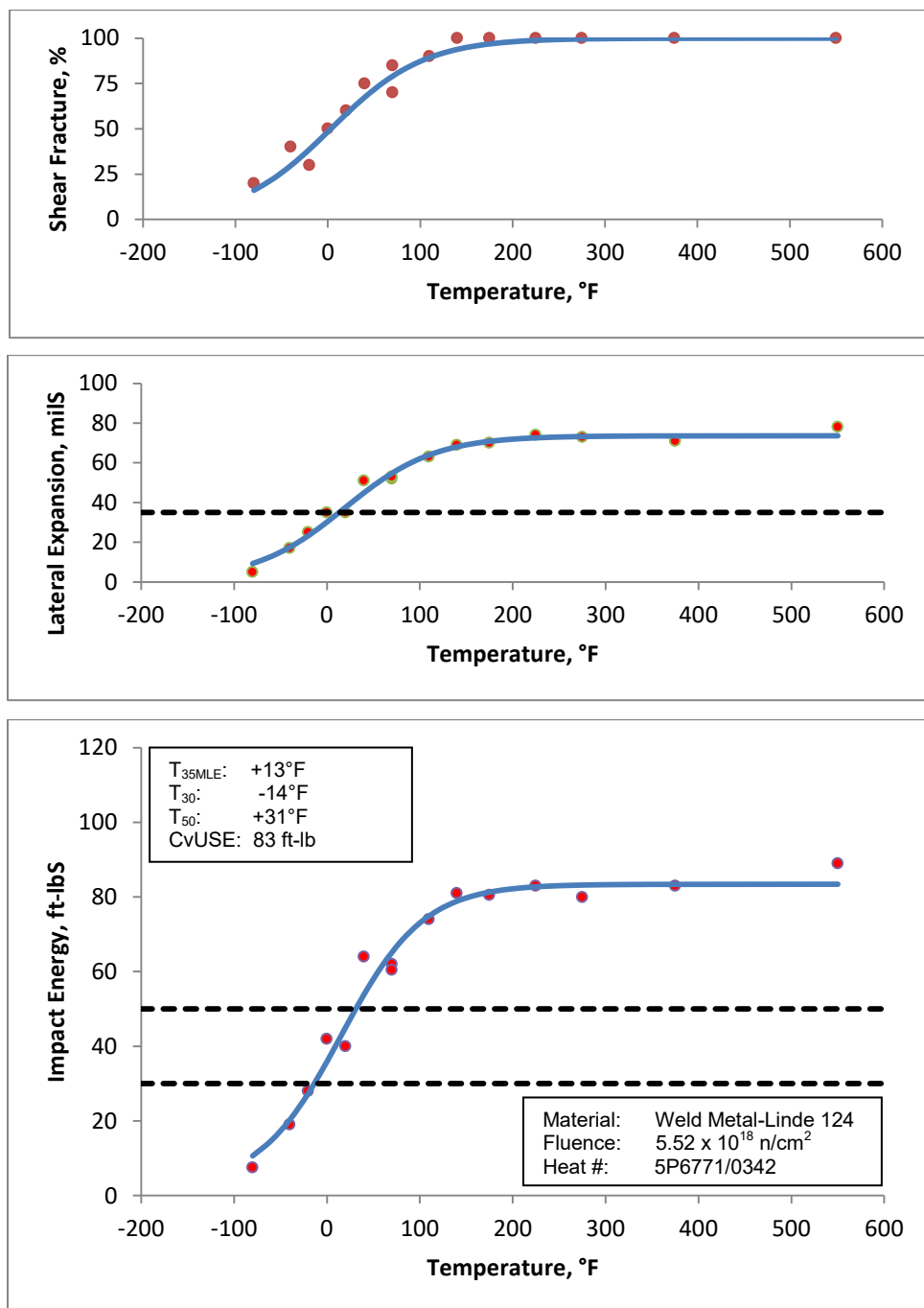


Figure C-11. HNP Capsule V Surveillance Charpy V-Notch Impact Data for Weld Metal, Wire Heat 5P6771/Flux Lot 0342 - Refitted Using Hyperbolic Tangent Curve-Fitting Method

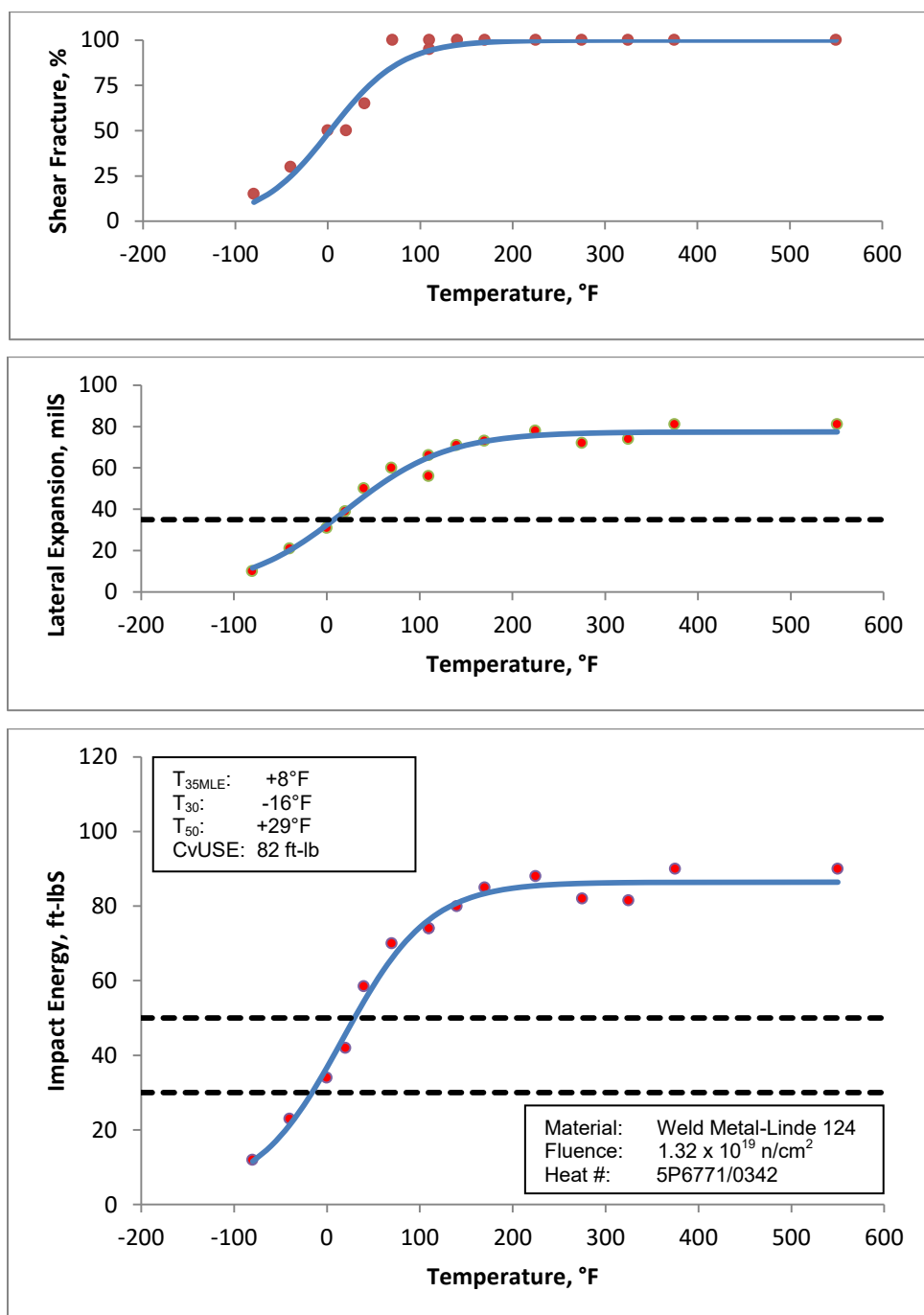


Figure C-12. HNP Capsule X Surveillance Charpy V-Notch Impact Data for Weld Metal, Wire Heat 5P6771/Flux Lot 0342 - Refitted Using Hyperbolic Tangent Curve-Fitting Method

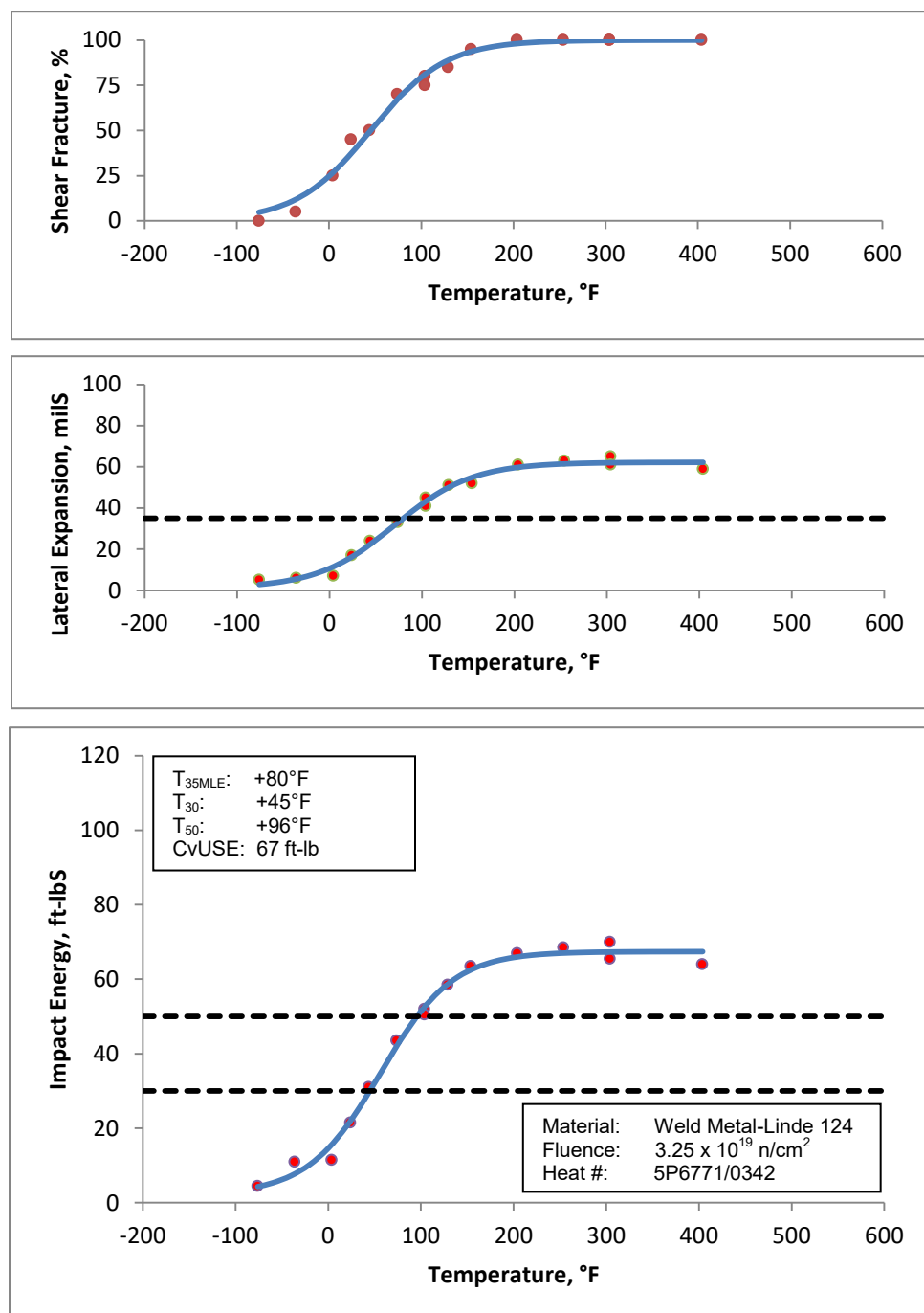


Figure C-13. Unirradiated Surveillance Charpy V-Notch Impact Data for HNP Heat-Affected-Zone Material - Refitted Using Hyperbolic Tangent Curve-Fitting Method

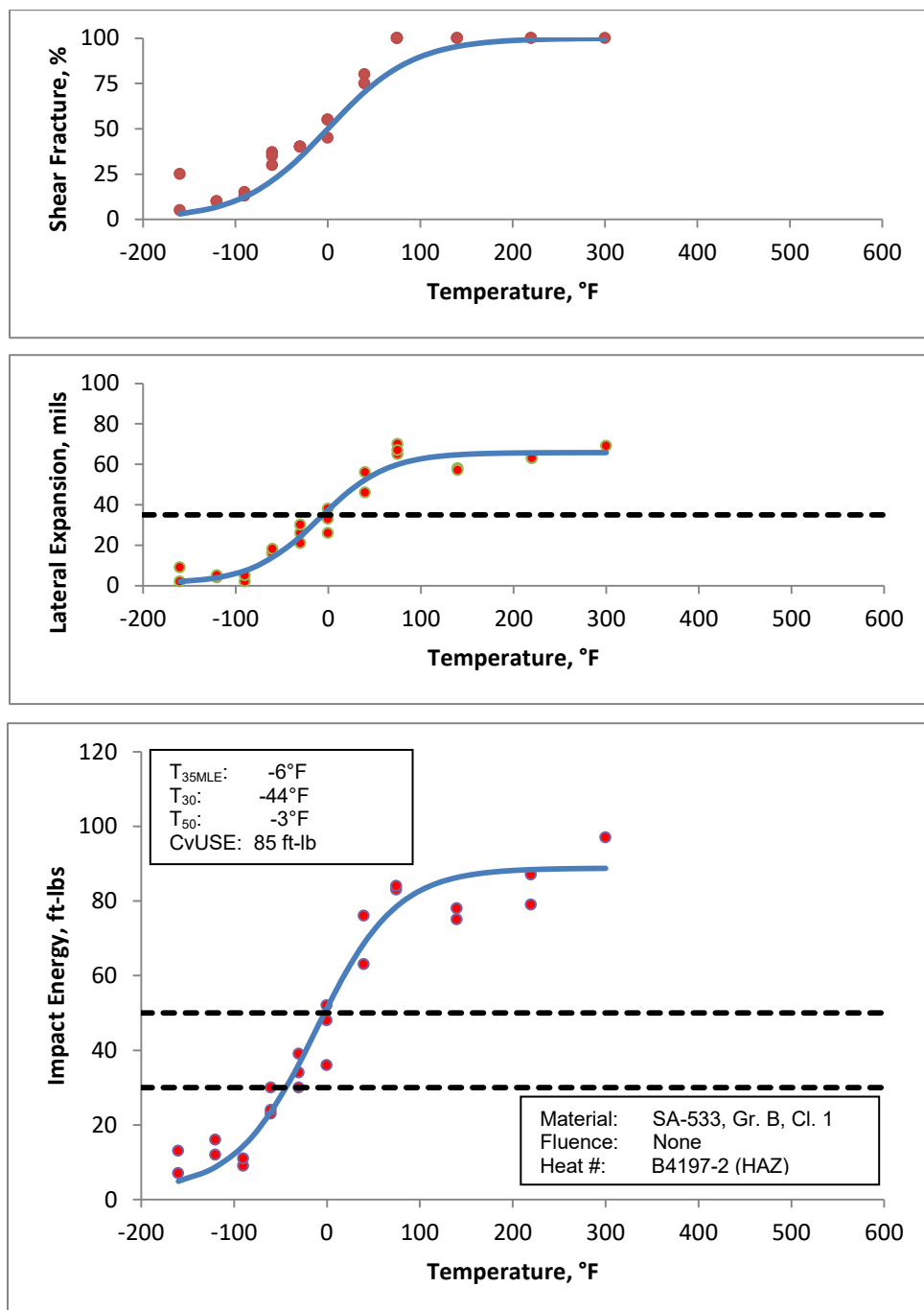


Figure C-14. HNP Capsule U Surveillance Charpy V-Notch Impact Data for Heat-Affected-Zone Material - Refitted Using Hyperbolic Tangent Curve-Fitting Method

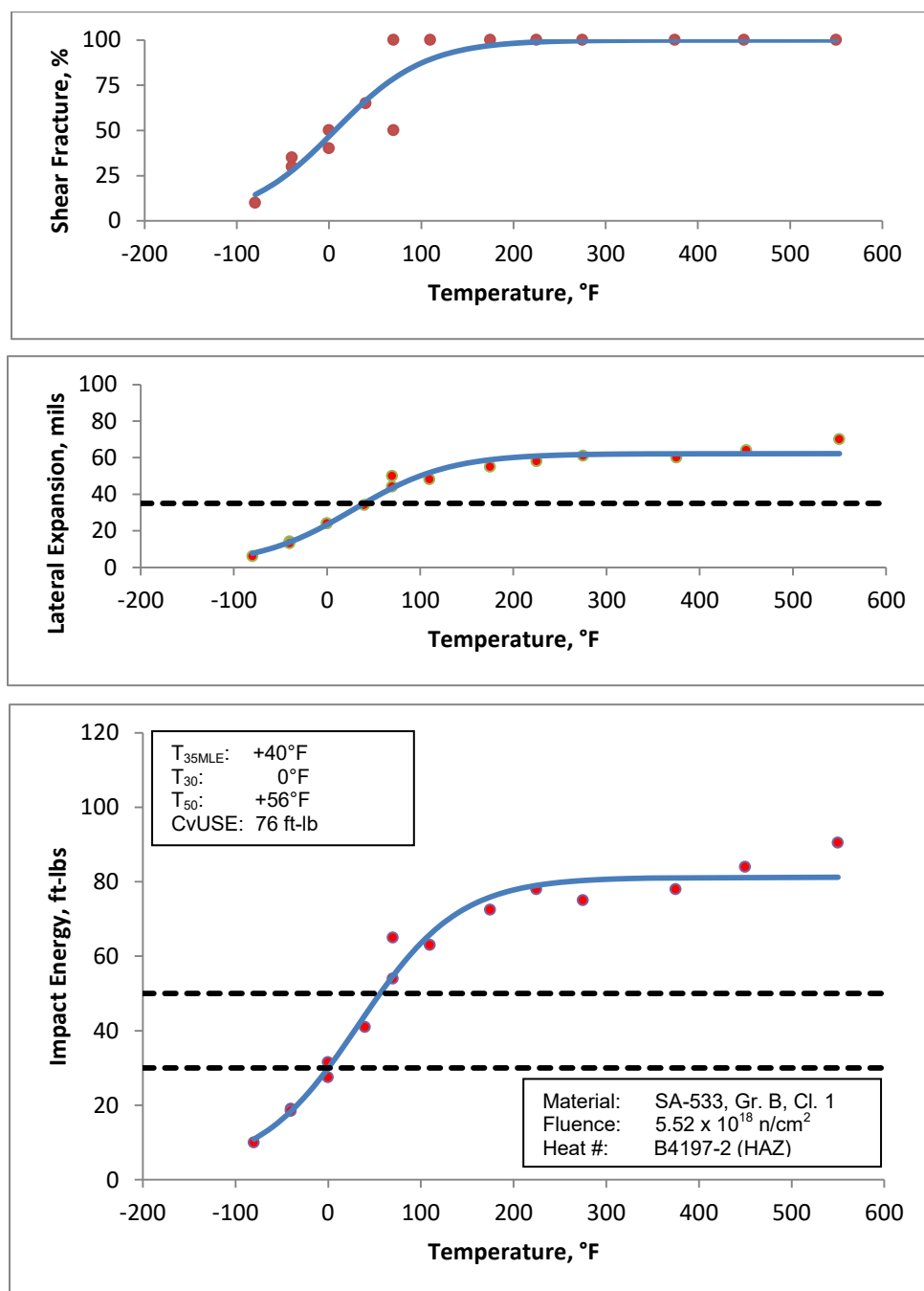


Figure C-15. HNP Capsule V Surveillance Charpy V-Notch Impact Data for Heat-Affected-Zone Material - Refitted Using Hyperbolic Tangent Curve-Fitting Method

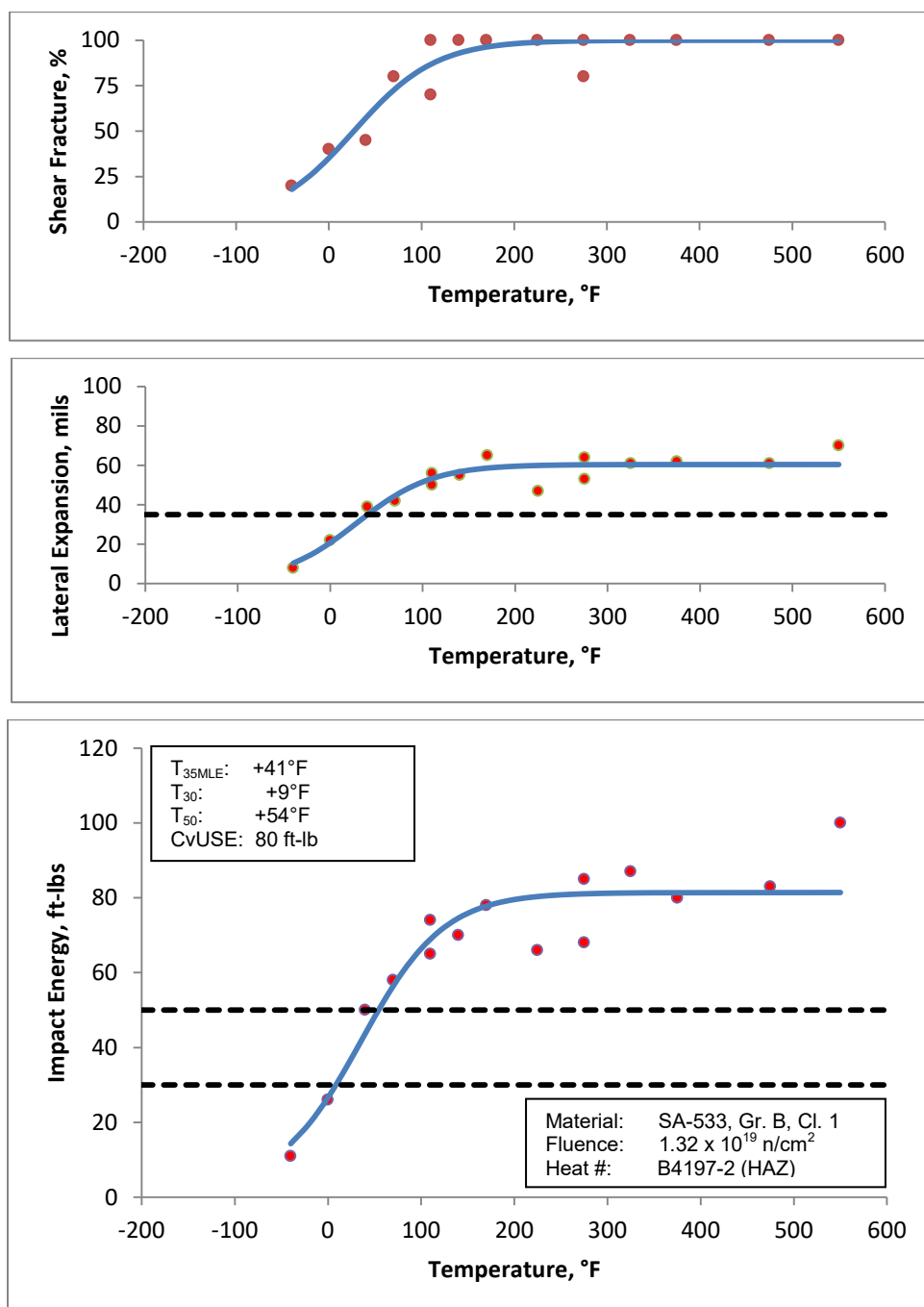
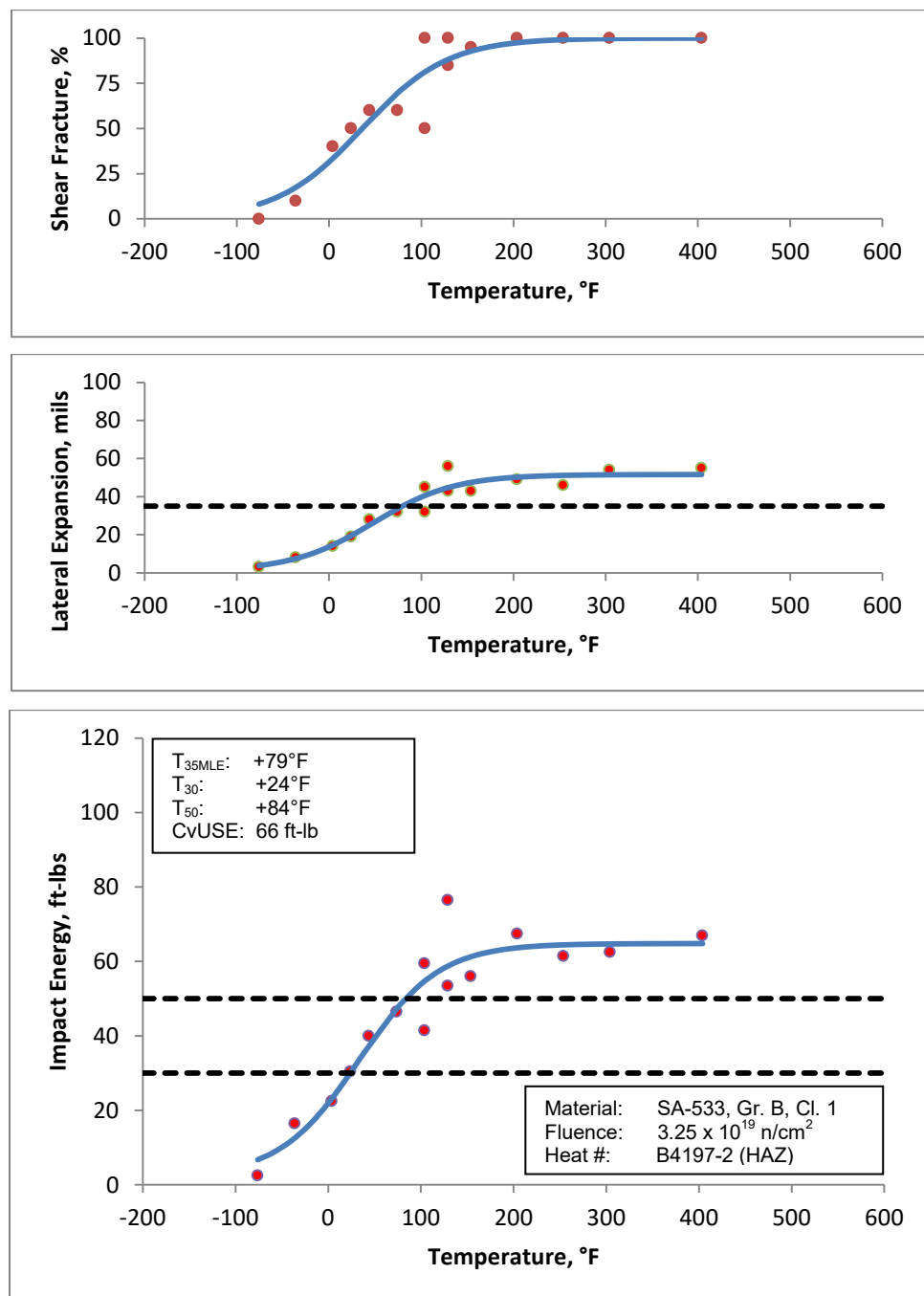


Figure C-16. HNP Capsule X Surveillance Charpy V-Notch Impact Data for Heat-Affected-Zone Material - Refitted Using Hyperbolic Tangent Curve-Fitting Method



**APPENDIX D CHARPY V-NOTCH SHIFT COMPARISON: HAND-DRAWN
CURVE FITTING VS. HYPERBOLIC TANGENT CURVE FITTING****Table D-1. Comparison of Curve Fit Transition Temperature Shifts
for HNP Surveillance Material, Base Metal Plate, Heat No. B4197-2,
Longitudinal (LT) Orientation**

| Capsule | Fluence, $\times 10^{19} \text{ n/cm}^2$ ($E > 1.0$ MeV) | 30 ft-lb Transition Temperature | | | |
|--------------|--|---------------------------------|-----------|------------------------------|-----------|
| | | Hand-Drawn Curve Fit | | Hyperbolic Tangent Curve Fit | |
| | | Avg, °F | Shift, °F | Avg, °F | Shift, °F |
| Unirradiated | --- | 60 | --- | 51 | --- |
| U | 0.552 | 85 | 25 | 81 | 30 |
| V | 1.32 | 101 | 41 | 94 | 43 |

| Capsule | Fluence, $\times 10^{19} \text{ n/cm}^2$ ($E > 1.0$ MeV) | 50 ft-lb Transition Temperature | | | |
|--------------|--|---------------------------------|-----------|------------------------------|-----------|
| | | Hand-Drawn Curve Fit | | Hyperbolic Tangent Curve Fit | |
| | | Avg, °F | Shift, °F | Avg, °F | Shift, °F |
| Unirradiated | --- | 110 | --- | 99 | --- |
| U | 0.552 | 141 | 31 | 136 | 37 |
| V | 1.32 | 153 | 43 | 152 | 53 |

| Capsule | Fluence, $\times 10^{19} \text{ n/cm}^2$ ($E > 1.0$ MeV) | 35 MLE Transition Temperature | | | |
|--------------|--|-------------------------------|-----------|------------------------------|-----------|
| | | Hand-Drawn Curve Fit | | Hyperbolic Tangent Curve Fit | |
| | | Avg, °F | Shift, °F | Avg, °F | Shift, °F |
| Unirradiated | --- | 90 | --- | 87 | --- |
| U | 0.552 | 123 | 33 | 110 | 23 |
| V | 1.32 | 132 | 42 | 132 | 45 |

**Table D-2. Comparison of Curve Fit Transition Temperature Shifts
for HNP Surveillance Material, Base Metal Plate, Heat No. B4197-2,
Transverse (TL) Orientation**

| Capsule | Fluence, $\times 10^{19} \text{ n/cm}^2$ ($E > 1.0$ MeV) | 30 ft-lb Transition Temperature | | | |
|--------------|--|---------------------------------|-----------|------------------------------|-----------|
| | | Hand-Drawn Curve Fit | | Hyperbolic Tangent Curve Fit | |
| | | Avg, °F | Shift, °F | Avg, °F | Shift, °F |
| Unirradiated | --- | 65 | --- | 72 | --- |
| U | 0.552 | 110 | 45 | 110 | 38 |
| V | 1.32 | 102 | 37 | 107 | 35 |

| Capsule | Fluence, $\times 10^{19} \text{ n/cm}^2$ ($E > 1.0$ MeV) | 50 ft-lb Transition Temperature | | | |
|--------------|--|---------------------------------|-----------|------------------------------|-----------|
| | | Hand-Drawn Curve Fit | | Hyperbolic Tangent Curve Fit | |
| | | Avg, °F | Shift, °F | Avg, °F | Shift, °F |
| Unirradiated | --- | 130 | --- | 139 | --- |
| U | 0.552 | 173 | 43 | 172 | 33 |
| V | 1.32 | 188 | 58 | 186 | 47 |

| Capsule | Fluence, $\times 10^{19} \text{ n/cm}^2$ ($E > 1.0$ MeV) | 35 MLE Transition Temperature | | | |
|--------------|--|-------------------------------|-----------|------------------------------|-----------|
| | | Hand-Drawn Curve Fit | | Hyperbolic Tangent Curve Fit | |
| | | Avg, °F | Shift, °F | Avg, °F | Shift, °F |
| Unirradiated | --- | 105 | --- | 110 | --- |
| U | 0.552 | 131 | 26 | 132 | 22 |
| V | 1.32 | 133 | 28 | 144 | 34 |

**Table D-3. Comparison of Curve Fit Transition Temperature Shifts
for HNP Surveillance Material, Weld Metal, Wire Heat 5P6771/Flux Lot
0342**

| Capsule | Fluence, $\times 10^{19} \text{ n/cm}^2$ ($E > 1.0$ MeV) | 30 ft-lb Transition Temperature | | | |
|--------------|--|---------------------------------|-----------|------------------------------|-----------|
| | | Hand-Drawn Curve Fit | | Hyperbolic Tangent Curve Fit | |
| | | Avg, °F | Shift, °F | Avg, °F | Shift, °F |
| Unirradiated | --- | -35 | --- | -34 | --- |
| U | 0.552 | -11 | 24 | -14 | 20 |
| V | 1.32 | -10 | 25 | -16 | 18 |

| Capsule | Fluence, $\times 10^{19} \text{ n/cm}^2$ ($E > 1.0$ MeV) | 50 ft-lb Transition Temperature | | | |
|--------------|--|---------------------------------|-----------|------------------------------|-----------|
| | | Hand-Drawn Curve Fit | | Hyperbolic Tangent Curve Fit | |
| | | Avg, °F | Shift, °F | Avg, °F | Shift, °F |
| Unirradiated | --- | 0 | --- | 2 | --- |
| U | 0.552 | 42 | 42 | 31 | 29 |
| V | 1.32 | 34 | 34 | 29 | 27 |

| Capsule | Fluence, $\times 10^{19} \text{ n/cm}^2$ ($E > 1.0$ MeV) | 35 MLE Transition Temperature | | | |
|--------------|--|-------------------------------|-----------|------------------------------|-----------|
| | | Hand-Drawn Curve Fit | | Hyperbolic Tangent Curve Fit | |
| | | Avg, °F | Shift, °F | Avg, °F | Shift, °F |
| Unirradiated | --- | -15 | --- | -9 | --- |
| U | 0.552 | 3 | 18 | 13 | 22 |
| V | 1.32 | 7 | 22 | 8 | 17 |

**Table D-4. Comparison of Curve Fit Transition Temperature Shifts
for HNP Surveillance Material, Heat-Affected-Zone Material**

| Capsule | Fluence, $\times 10^{19} \text{ n/cm}^2$ ($E > 1.0$ MeV) | 30 ft-lb Transition Temperature | | | |
|--------------|--|---------------------------------|-----------|------------------------------|-----------|
| | | Hand-Drawn Curve Fit | | Hyperbolic Tangent Curve Fit | |
| | | Avg, °F | Shift, °F | Avg, °F | Shift, °F |
| Unirradiated | --- | -45 | --- | -44 | --- |
| U | 0.552 | 0 | 45 | 0 | 44 |
| V | 1.32 | 10 | 55 | 9 | 53 |

| Capsule | Fluence, $\times 10^{19} \text{ n/cm}^2$ ($E > 1.0$ MeV) | 50 ft-lb Transition Temperature | | | |
|--------------|--|---------------------------------|-----------|------------------------------|-----------|
| | | Hand-Drawn Curve Fit | | Hyperbolic Tangent Curve Fit | |
| | | Avg, °F | Shift, °F | Avg, °F | Shift, °F |
| Unirradiated | --- | 0 | --- | -3 | --- |
| U | 0.552 | 57 | 57 | 56 | 59 |
| V | 1.32 | 47 | 47 | 54 | 57 |

| Capsule | Fluence, $\times 10^{19} \text{ n/cm}^2$ ($E > 1.0$ MeV) | 35 MLE Transition Temperature | | | |
|--------------|--|-------------------------------|-----------|------------------------------|-----------|
| | | Hand-Drawn Curve Fit | | Hyperbolic Tangent Curve Fit | |
| | | Avg, °F | Shift, °F | Avg, °F | Shift, °F |
| Unirradiated | --- | 0 | --- | -6 | --- |
| U | 0.552 | 39 | 39 | 40 | 46 |
| V | 1.32 | 40 | 40 | 41 | 47 |

APPENDIX E FLUENCE ANALYSIS METHODOLOGY

The primary tool used in the determination of the flux and fluence exposure to the welds, plates, and surveillance capsule specimens is the two-dimensional discrete ordinates transport code, DORT.^[E-1] The primary technique used to verify the accuracy and uncertainty in the flux and fluence is a benchmark to measured data. Capsule Z dosimetry was used in benchmark comparisons for the HNP cycles analyzed in this analysis.

The HNP surveillance capsule Z dosimetry is located in the capsule holder attached to the neutron pad at 20° (off of the major axis). The power distributions in the analyzed cycle's irradiations were symmetric both in θ and Z. That is, the axial power shape is roughly the same for any angle and, conversely, that the azimuthal power shape is the same for any height. This means that the flux at some point (R, θ , Z) can be considered to be a separable function of (R, θ) and (R, Z). Therefore, the analyzed cycle's irradiation can be modeled using the standard Framatome synthesis procedures.^[E-8]

Figure E-1 depicts the analytical procedure that is used to determine the fluence accumulated over the cycles analyzed. As shown in the figure, the analysis is divided into several tasks:

- generation of the neutron source,
- development of the DORT geometry models,
- calculation of the macroscopic material cross sections,
- synthesis of the results,
- estimation of the calculational bias,
- the calculational uncertainty, and
- the final fluence.

Each of these tasks is discussed in greater detail in the following sections.

Generation of Neutron Source

The time-average space- and energy-dependent neutron source for cycles analyzed was calculated using the SORREL code.^[E-2] The effects of burnup on the spatial distribution of the neutron source are accounted for by calculating the cycle average fission spectrum for each of the four significant fissile isotopes on an assembly-by-assembly basis, and by determining the cycle-average specific neutron emission rate. This data is then used with the normalized time-weighted, average pin-by-pin relative power density (RPD) distribution to determine the space and energy-dependent neutron source. The azimuthally averaged, time-averaged, axial power shape in the peripheral assemblies is used with the fissile nuclide-weighted, fission spectrum of the peripheral assemblies to determine the neutron source for the axial DORT run. These two neutron source distributions provide input to DORT as indicated in Figure E-1.

Development of the Geometrical Models

The system geometry models for DORT were developed using standard Framatome interval size and configuration guidelines. The R θ model extends radially from the center of the core to the concrete bioshield and azimuthally from the major axis to 45°. The axial model extends radially from the center of the core to approximately two feet into the concrete bio-shield and axially from approximately 1.5 feet

below the active core region to approximately the top of the nozzles above the active core region. In all cases, cold dimensions are used. The geometrical models either meet or exceeded all guidance criteria concerning interval size that are provided in Regulatory Guide 1.190.^[E-4] The geometry models serve as input to the DORT code as indicated in Figure E-1. These models will be used in all subsequent fluence analyses that may be performed by Framatome for Harris Nuclear Plant Unit 1.

Calculation of Macroscopic Material Cross Sections

In accordance with BAW-2241P-A,^[E-8] the BUGLE-96^[E-5] cross section library is used. The GIP code^[E-6] was used to calculate the macroscopic energy-dependent cross sections for all materials used in the analysis – radially from the core out through the cavity and into the concrete and axially from approximately 1.5 feet below the active core region to approximately the top of the nozzles above the active core region. The ENDF/B-VI dosimeter reaction cross sections are used to generate the response functions that are used to calculate the DORT-calculated “saturated” specific activities. The cross section sets generated by GIP provide input to the DORT code as indicated in Figure E-1.

DORT Analysis

The cross sections, geometry, and appropriate source were combined to create a set of DORT models (R θ and RZ) for the analyses for cycles 9-21. Each R θ DORT run utilized a P₃ Legendre expansion of scattering cross sections, seventy directions (S₁₀), and the appropriate boundary conditions. All outer boundaries employed vacuum boundary conditions. A theta-weighted flux extrapolation model was used, and all other requirements of Regulatory Guide 1.190^[E-4] that relate to the various DORT parameters were either met or exceeded for all DORT runs.

Synthesized Three-Dimensional Results

The DORT analyses produce two sets of two-dimensional flux distributions, one for channels of vertical cylinders and one for radial planes. The vertical cylinders, which are referred to as RZ planes, are defined as planes bounded axially by approximately 1.5 feet below the active core region and the top of the nozzles and radially by the center of the core out into the concrete cavity shield. The radial (horizontal) planes, referred to as the R θ planes, are defined as the planes bounded radially by the center of the core and a point located in the concrete cavity shield and azimuthally by the major axis and the adjacent 45° radius. The vessel flux varies significantly in all three cylindrical-coordinate directions (R, θ , Z). Since the three-dimensional flux is a separable function,^[E-8] the two-dimensional data sets are mathematically combined to estimate the flux at all three-dimensional points (R, θ , Z) of interest. The synthesis procedure outlined in Regulatory Guide 1.190^[E-4] forms the basis for the Framatome flux-synthesis process.

The extrapolation of neutron fluence is discussed in Section 6.1.

Calculated Activities and Measured Activities

The calculated activities for each dosimeter type “d” were determined using the following equation:

$$A_d = \sum_{g=1}^G \phi_g(\vec{r}_d) \cdot RF_g^d \cdot B_d \cdot NSF_d$$

where

| | | |
|---------------------|---|---|
| A_d | = | specific activity for dosimeter “d” in μCi of product isotope per gram of target isotope |
| $\phi_g(\vec{r}_d)$ | = | three dimensional flux for dosimeter “d” at position \vec{r}_d for energy group “g” |
| $RF_{d,g}$ | = | dosimeter response function for dosimeter “d” and energy group “g” |
| B_d | = | bias correction factors for dosimeter “d” |
| NSF_d | = | non-saturation correction factor (NSF) |

The type of bias correction factors (B_d) in the specific activity calculation above are listed in Table E-1.

Table E-1. Bias Correction Factors

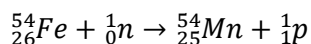
| Dosimeter Type | Bias |
|--------------------------------------|----------------------------|
| Activation (n, p), (n, α) | Short Half Life |
| Fission | Photofission Impurities |

The two fission related bias factors are photofission and ^{235}U impurity which both enhance the ^{137}Cs fission product from the $^{238}\text{U}(\text{n},\text{f})$ fission process. A photofission factor is applied to correct for the fact that some of the ^{137}Cs atoms present in the dosimeter were produced by (γ , f) reactions. The impurity correction for the ^{235}U that is in the ^{238}U dosimeters is accounted for in the defined response function. Dosimeter activities are calculated on a cycle by cycle basis and the activity is renormalized based power history for subsequent cycles. Thus, a short half-life factor is not applied.

C/M Ratios

The following explanation defines the terms “measurement” (M) and “calculation” (C) as used in this analysis.

- **Measurement:** The meaning of the term “measurement” as used by Framatome is the measurement of the physical quantity of the dosimeter (specific activity) that responded to the fluence. The term is not associated with a “measured fluence,” which is not measured, but “unfolded” by means of a calculational procedure. For example, an iron dosimeter measurements refers to specific activity of ^{54}Mn ($\mu\text{Ci/g}$), which is the product isotope from the ^{54}Fe dosimeter reaction over irradiation time:



- Calculation: The calculational methodology produces two primary results: the calculated dosimeter activities and the neutron flux at all points of interest. The meaning of the term “calculation” as used by Framatome is the calculated dosimeter activity. The calculated activities are determined in such a way that they are directly comparable to the measurement values. That is, saturated values are determined by the DORT calculation. When the effects of time are included with a “non-saturation factor” (NSF), the values are directly comparable to the measured values. ENDF/B-VI based dosimeter reaction cross sections ^[E-5] and response functions were used in determining the calculated values for each individual dosimeter. It should be stressed that the calculated values in the Framatome approach ^[E-8] are independent of the measurement values.

Uncertainty

The fluence rates, time-averaged flux values, and thereby the fluence values throughout the HNP reactor and vessel, were calculated with the DORT ^[E-1] discrete ordinates computer code using three dimensional synthesis methods. The basic theory for synthesis is described in Section 3.0 of BAW-2241P. ^[E-8] The DORT three-dimensional synthesis results were the bases for the fluence predictions using the Framatome “Semi-Analytical” (calculational) methodology.

The uncertainties in the HNP flux values were evaluated to ensure that the greater than 1.0 MeV values are accurate (with no discernible bias) and have a mean standard deviation that is consistent with the Framatome benchmark database of uncertainties. Consistency between the fluence uncertainties in the updated calculations for the cycles in this analysis, and those in the Framatome benchmark database, ensure that the vessel fluence predictions are consistent with the 10 CFR 50.61 ^[E-9] Pressurized Thermal Shock (PTS) screening criteria, and the Regulatory Guide 1.99 ^[E-3] radiation embrittlement evaluations.

The verification of the fluence uncertainty for HNP includes:

- estimating the uncertainties in the Capsule Z dosimetry measurements,
- estimating the uncertainties in the Capsule Z benchmark comparison of calculations to measurements,
- evaluating design and operational changes,
- estimating the uncertainties in the cycles 9 through 21 reactor vessel fluence, and
- determining if the specific measurement and benchmark uncertainties for Capsule Z are consistent with the Framatome database of generic uncertainties in the measurements and calculations.

The embrittlement evaluations in Regulatory Guide 1.99 ^[E-3] and those in 10 CFR 50.61 ^[E-9] for the PTS screening criteria apply a margin term to the reference temperatures. The margin term includes the product of a confidence factor of 2.0 and the mean embrittlement standard deviation. The factor of 2.0 implies a very high level of confidence in the fluence uncertainty as well as the uncertainty in the other variables contributing to the embrittlement. The eleven dosimeter measurements from HNP Capsule Z

analyses directly support this high level of confidence. Moreover, the evaluation of the HNP Capsule Z dosimeter measurement uncertainties found that they are consistent with the Framatome database. Therefore, the measurement-to-calculational uncertainties in the updated fluence predictions for HNP are supported by 728 additional dosimeter measurements and 39 benchmark comparisons of calculations to measurements as shown in Appendix A of the topical.^[E-8] The calculational uncertainties are also supported by the fluence sensitivity evaluation of the uncertainties in the physical and operational parameters, which are included in the vessel fluence uncertainty.^[E-8]

The Framatome generic uncertainty in the capsule dosimetry measurements has been determined to be unbiased and has an estimated standard deviation of 7.0 percent for the qualified set of dosimeters. Part of the evaluation for the HNP Capsule Z dosimetry measurement uncertainties was to determine if any biases were evident and to estimate the standard deviation. The dosimetry measurements were found to be appropriately calibrated to standards traceable to the National Institute of Standards and Technology (NIST). Moreover, the measurement methodology has been certified by NIST to be unbiased as a result of comparative tests in a reference field.^[E-8] Thus, no bias was found in the dosimetry measurements. The mean measurement uncertainty associated with Capsule Z is shown below:

| Cycle | $\sigma_{\bar{M}}$ (%) |
|-----------|------------------------|
| Capsule Z | 6.05 |

This measurement standard deviation for the random uncertainties was determined from Equation 7.6 in the topical.^[E-8] The value indicates that there is consistency with the Framatome database. Consequently, when the Framatome database is updated, the HNP dosimetry measurement uncertainties may be combined with the other 728 dosimeters. Since the Capsule Z measurements are consistent with the Framatome database, it is estimated that the HNP dosimeter measurement uncertainty may be represented by the Framatome database standard deviation of 7.0 percent. Based on the Framatome database, there appears to be a 95 percent level of confidence that 95 percent of the HNP1 Capsule Z dosimetry measurements, for fluence reactions above 1.0 MeV, are within ± 14.2 percent of the true values.

The Framatome generic uncertainty for benchmark comparisons of capsule dosimetry calculations relative to the measurements indicates that any benchmark bias in the greater than 1.0 MeV results is too small to be uniquely identified. The estimated standard deviation between the calculations and measurements is 9.9 percent. This implies that the root mean square deviation between the Framatome calculations of the HNP Capsule Z dosimetry and the measurements should be approximately 9.9 percent in general and bounded by ± 20.0 percent for a 95 percent confidence interval with thirty-nine independent benchmarks.

The weighted mean values of the ratio of calculated dosimeter activities to measurements ($\overline{C/M}$) for HNP Capsule Z have been statistically evaluated using Equation 7.15 from the topical.^[E-8]

The standard deviation in the benchmark comparisons is:

| Cycle | $\sigma_{\overline{C/M}}$ (%) |
|-----------|-------------------------------|
| Capsule Z | 18.05 |

This standard deviation indicates that the benchmark comparisons are consistent with the Framatome database. Consequently, when the Framatome database is updated, the HNP Capsule Z benchmark

uncertainties may be included with the other 39 benchmark uncertainties in the topical.^[E-8] The consistency between the HNP Capsule Z benchmark uncertainties and those in the Framatome database indicates that the HNP fluence calculations for cycles 9 through 21 have no discernible bias in the greater than 1.0 MeV values. In addition, the consistency indicates that the fluence values can be represented by the Framatome reference set which includes a standard deviation of 7.0 percent at dosimetry locations.

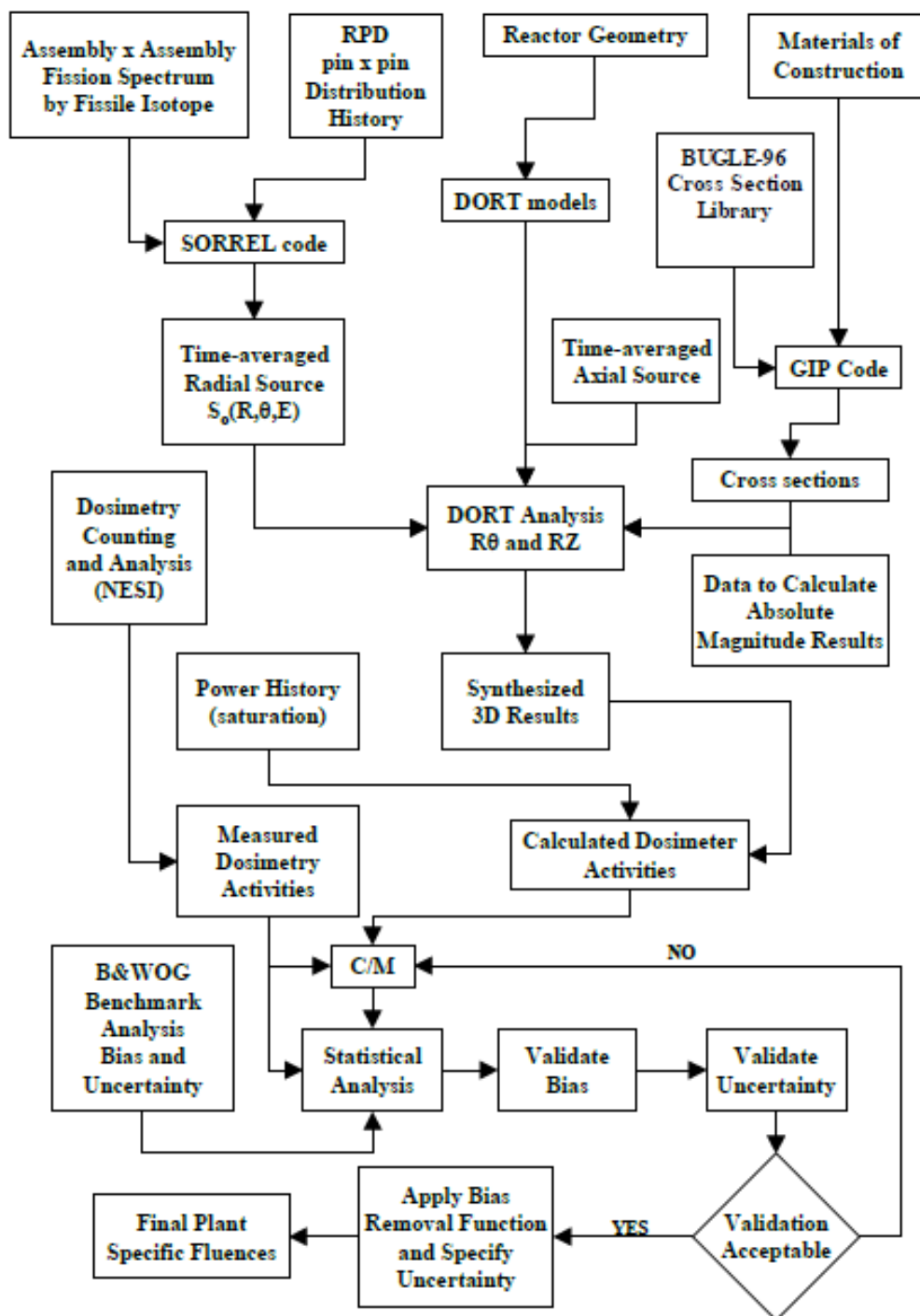
The reference set of uncertainties are shown in Table E-2.^[E-8]

Table E-2. Reference Calculational Fluence Uncertainties

| Type of Calculation | Uncertainty (%) |
|-----------------------------------|--|
| | Standard Deviation (σ) ^(a) |
| Capsule | 7.0 |
| Reactor Vessel (maximum location) | << 20.0 |
| Reactor Vessel (extrapolation) | << 20.0 |

^(a) U. S. NRC Regulatory Guide 1.190^[E-4] suggests a standard deviation that is equal or less than 20% ($\sigma \leq 20\%$) is appropriate for the industry database in Regulatory Guide 1.99^[E-3] and 10 CFR 50.61.^[E-9] The HNP reactor vessel fluence uncertainty for cycles 9 through 21 is less.

Figure E-1. Fluence Analysis Methodology



References

- E-1. Ed. M.A. Rutherford, N. M. Hassan, et al., "*DORT, Two Dimensional Discrete Ordinates Transport Code*," BWNT-TM-107, Framatome Technologies, Inc., Lynchburg, Virginia, May 1995.
- E-2. L. A. Hassler and N. M. Hassan, "*SORREL, DOT Input Generation Code User's Manual*," NPGD-TM-427, Revision 8, Framatome Technologies, Inc., Lynchburg, Virginia, July 1992.
- E-3. U.S. Nuclear Regulatory Commission, "*Radiation Embrittlement of Reactor Vessel Materials*," Regulatory Guide 1.99, Revision 2, May 1998.
- E-4. U. S. Nuclear Regulatory Commission, "*Calculational and Dosimetry Methods for Determining Pressure Vessel Neutron Fluence*," Regulatory Guide 1.190, March 2001.
- E-5. Oak Ridge National Laboratory, "*BUGLE-96: Coupled 47 Neutron, 20 Gamma-ray Group Cross Section Library Derived from ENDF/B-VI for LWR Shielding and Pressure Vessel Dosimetry Applications*," DLC-185, Radiation Safety Information Computational Center, Oak Ridge, Tennessee, March 1996.
- E-6. L.A. Hassler and N. M. Hassan, "*GIP Users Manual for B&W Version, Group Organized Cross Section Input Program*," NPGD-TM-456, Revision 11, Framatome Technologies, Inc., Lynchburg, Virginia, August 1994.
- E-7. Not used.
- E-8. J. R. Worsham III, "*Fluence and Uncertainty Methodologies*," BAW-2241P, Revision 1, Framatome Technologies, Inc., Lynchburg, Virginia, April 1999.
- E-9. Code of Federal Regulations, Title 10, "*Domestic Licensing of Production and Utilization Facilities*," Part 50.61, "*Fracture Toughness Requirements for Protection Against Pressurized Thermal Shock*," Effective Date: August 28, 1996.

APPENDIX F CAPSULE SURVEILLANCE DATA CREDIBILITY ASSESSMENT

Upon the removal of a surveillance capsule, an assessment, which follows the methodology presented in NRC Generic Letter 92-01 and RPV Integrity Assessment,^[F-1] must be performed to determine credibility of the plant-specific data. The results from the plant-specific surveillance program must be integrated into reactor vessel integrity calculations if the plant-specific surveillance data has been deemed credible as judged by the following criteria:

1. The materials in the surveillance capsules must be those which are controlling material with regard to radiation embrittlement.
2. Scatter in the plots of Charpy energy versus temperature for the irradiated and unirradiated conditions must be small enough to permit the determination of the 30 ft-lb temperature unambiguously.
3. Where there are two or more sets of surveillance data from one reactor, the scatter of ΔRT_{NDT} values must be less than 28°F for welds and 17°F for base metals. Even if the range in the capsule fluences is large (two or more orders of magnitude), the scatter may not exceed twice those values.
4. The irradiation temperature of the Charpy specimens in the capsule must equal the vessel wall temperature at the cladding/base metal interface within $\pm 25^\circ\text{F}$.
5. The surveillance data for the correlation monitor material in the capsule, if present, must fall within the scatter band of the data base for the material.

The surveillance data deemed credible according to the criteria specified above must be used to determine a material-specific value of CF for use in the following equation:

$$\Delta RT_{NDT} = CF * ff$$

A material specific value of CF is determined from the following equation:

$$CF = \frac{\sum[\Delta RT_{NDT} * ff]}{\sum ff^2}$$

Where:

- ΔRT_{NDT} is measured value of ΔRT_{NDT} from the surveillance data
- ff is fluence factor for each surveillance data point

For cases in which the results from a credible-plant-specific surveillance program are used, the value of σ_Δ to be used is 14°F for welds, and 8.5°F for base metals; however the value of σ_Δ may not exceed one-half ΔRT_{NDT} .

F.1 Surveillance Data Credibility**Criterion 1**

HNP-1 surveillance data available include the following materials:

Base Metal Heat No. B4197-2

Weld Wire Heat No. 5P6771/Flux Lot No. 0342

All these heats of material lie within the beltline region of the HNP-1 reactor vessel as defined by 10 CFR 50, Appendix G.^[F-2] Therefore, these materials could be controlling with regard to radiation embrittlement.

Criterion 2

The available Charpy V-notch data for the surveillance data permit the determination of the 30 ft-lb temperatures and the upper-shelf energies; these data are presented in their respective RVSP reports.

Criterion 3

The scatter of the measured ΔRT_{NDT} values for the available surveillance data are presented in Table F-1. The scatter of the measured ΔRT_{NDT} values for the surveillance base material is greater than 17°F and the scatter of the measured ΔRT_{NDT} values for the surveillance weld material is greater than 28°F.

Table F-1. Credibility Assessment for HNP-1 Surveillance Materials

| Material | Capsule | Fluence ($\times 10^{19}$) n/cm ² | Fluence Factor | Measured ΔRT_{NDT} (°F) | Predicted ΔRT_{NDT} from Best Fit Line (°F) ^a | (Measured – Predicted) ΔRT_{NDT} (°F) | Measured - Predicted (Base Metal < $\pm 17^\circ\text{F}$ Weld Metal < $\pm 28^\circ\text{F}$) (Y/N) |
|-----------------------------|---------|--|-------------------|------------------------------------|--|---|---|
| Plate B4197-2 (LT) | U | 0.552 | 0.834 | 30 | 52.5 | -22.5 | N |
| Plate B4197-2 (TL) | U | 0.552 | 0.834 | 38 | 52.5 | -14.5 | Y |
| Plate B4197-2 (LT) | V | 1.32 | 1.077 | 43 | 67.8 | -24.8 | N |
| Plate B4197-2 (TL) | V | 1.32 | 1.077 | 35 | 67.8 | -32.8 | N |
| Plate B4197-2 (LT) | X | 3.25 | 1.310 | 94 | 82.4 | 11.6 | Y |
| Plate B4197-2 (TL) | X | 3.25 | 1.310 | 79 | 82.4 | -3.4 | Y |
| Plate B4197-2 (LT) | Z | 9.45 | 1.507 | 120.8 | 94.8 | 26.0 | N |
| Plate B4197-2 (TL) | Z | 9.45 | 1.507 | 123.2 | 94.8 | 28.4 | N |
| Weld Metal (5P6771/0342) | U | 0.552 | 0.834 | 20 | 48.1 | -28.1 | N |
| | V | 1.32 | 1.077 | 18 | 62.2 | -44.2 | N |
| | X | 3.25 | 1.310 | 79 | 75.6 | 3.4 | Y |
| | Z | 9.45 | 1.507 | 131.1 | 86.9 | 44.2 | N |

NOTE

- a. $\text{Predicted } \Delta RT_{NDT} = (\text{Slope}_{\text{best fit}}) * (\text{Fluence Factor})$
Where $\text{Slope}_{\text{best fit}} = \Sigma(\Delta RT_{NDT} * ff) / \Sigma(ff^2)$
(for the base metal, $\text{Slope}_{\text{best fit}} = 62.9^\circ\text{F}$)
(for the weld metal, $\text{Slope}_{\text{best fit}} = 57.7^\circ\text{F}$)

Criterion 4

The HNP-1 capsules are positioned inside the reactor vessel between the neutron shielding pads and the vessel wall. Therefore, the irradiation temperature of the HNP-1 capsule specimens is considered to be within 25°F of the reactor vessel inside surface cold-leg temperature.

Criterion 5

The HNP-1 plant-specific RVSP program does not include a correlation monitor plate material. Therefore, this criterion is not applicable with respect to HNP-1 surveillance data analysis.

Based on the above evaluation of the five criteria for assessing credibility that is from Regulatory Guide 1.99, Revision 2^[F-3] and 10 CFR 50.61^[F-4], the HNP-1 surveillance base metal and weld metal are considered not credible.

F.2 Table CF Conservatism Assessment

In accordance with the methodology presented in NRC Generic Letter 92-01 and RPV Integrity Assessment,^[F-1] because the surveillance data for base metal B4197-2 and weld wire heat 5P6771 are non-credible, the CF value is calculated from the generic tables in Regulatory Guide 1.99, Revision 2/10 CFR 50.61 unless the CF determined from the surveillance data is significantly greater than that from the generic tables, indicating the Table CF is non-conservative. To determine if the generic Table CF is non-conservative, the following steps are performed:

1. Determine the CF from the generic tables based on the surveillance specimen chemical composition; use this CF to determine the predicted ΔRT_{NDT} for each capsule:

$$\text{Predicted } \Delta RT_{NDT} = CF_{Table, Surv. Avg. Chem.} * ff_{capsule}$$

2. Determine the difference between the predicted ΔRT_{NDT} and the measured (temperature/ratio adjusted, if required) ΔRT_{NDT} .

If the predicted ΔRT_{NDT} value is 2 standard deviations (i.e., 34°F for base metals and 56°F for weld metals) or greater than the (temperature/ratio adjusted) measured ΔRT_{NDT} , the Table CF is considered non-conservative. When the Table CF is determined to be non-conservative, the CF determined from the non-credible surveillance data is used in the assessment of reactor vessel integrity.

The above process produced results listed in Table F-2 and the generic Table CFs for base metal B4197-2 and weld wire heat 5P6771 are non-conservative.

Table F-2. Regulatory Guide 1.99, Revision 2/10 CFR 50.61, Table Chemistry Factor Conservatism Assessment for HNP-1 Base Metal B4197-2 & Weld Metal 5P6771 Surveillance Data

| Material | Capsule | Table CF (Surv. Avg.) | Capsule Fluence Factor (ff) | Adjusted ΔRT_{NDT} ($^{\circ}F$) | Predicted ΔRT_{NDT} ($^{\circ}F$) ^b | (Adjusted - Predicted) ΔRT_{NDT} ($^{\circ}F$) |
|------------------|---------|-----------------------|-----------------------------|--|--|--|
| B4197-2 LT | U | 58.0 | 0.834 | 30 ^a | 48.4 | -18.4 |
| B4197-2 TL | U | 58.0 | 0.834 | 38 ^a | 48.4 | -10.4 |
| B4197-2 LT | V | 58.0 | 1.077 | 43 ^a | 62.5 | -19.5 |
| B4197-2 TL | V | 58.0 | 1.077 | 35 ^a | 62.5 | -27.5 |
| B4197-2 LT | X | 58.0 | 1.310 | 94 ^a | 76.0 | 18.0 |
| B4197-2 TL | X | 58.0 | 1.310 | 79 ^a | 76.0 | 3.0 |
| B4197-2 LT | Z | 58.0 | 1.507 | 120.8 ^a | 87.4 | 33.4 |
| B4197-2 TL | Z | 58.0 | 1.507 | 123.2 ^a | 87.4 | 35.8 |
| Weld 5P6771/0342 | U | 32.6 | 0.834 | 20 ^a | 27.2 | -7.2 |
| Weld 5P6771/0342 | V | 32.6 | 1.077 | 18 ^a | 35.1 | -17.1 |
| Weld 5P6771/0342 | X | 32.6 | 1.310 | 79 ^a | 42.7 | 36.3 |
| Weld 5P6771/0342 | Z | 32.6 | 1.507 | 131.1 ^a | 49.1 | 82.0 |

NOTES

- There is no variance in temperature or CF; therefore the Adjusted ΔRT_{NDT} is the Measured ΔRT_{NDT} .
- Predicted $\Delta RT_{NDT} = (\text{Table Chem. Factor, Surv. Cap. Avg.}) * (\text{Capsule Fluence Factor})$

F.3 Calculation of Chemistry Factor for Base Metal Heat No. B4197-2

- No temperature adjustments are required since the capsule irradiation temperature equals the vessel irradiation temperature (i.e., the capsules were irradiated in the plant being assessed).
- No chemical composition adjustments are required.
- Determine the best-fit line relating the measured ΔRT_{NDT} to the capsule fluence factor (Table F-3). The slope of this best-fit line is the surveillance data chemistry factor ($CF_{\text{Surv. Data}}$) which is calculated to be 62.9 $^{\circ}F$.

Table F-3. Calculation of Base Metal Heat No. B4197-2 Chemistry Factor Using HNP-1 Surveillance Data

| Material | Capsule | Fluence ($\times 10^{19}$) n/cm ² | Fluence Factor (ff) | Measured ΔRT_{NDT} (°F) | Measured $\Delta RT_{NDT} * ff$ | ff ² |
|---|---------|--|---------------------------|---------------------------------------|------------------------------------|-----------------|
| B4197-2 LT | U | 0.552 | 0.834 | 30 | 25.0 | 0.695 |
| B4197-2 TL | U | 0.552 | 0.834 | 38 | 31.7 | 0.695 |
| B4197-2 LT | V | 1.32 | 1.077 | 43 | 46.3 | 1.160 |
| B4197-2 TL | V | 1.32 | 1.077 | 35 | 37.7 | 1.160 |
| B4197-2 LT | X | 3.25 | 1.310 | 94 | 123.1 | 1.715 |
| B4197-2 TL | X | 3.25 | 1.310 | 79 | 103.5 | 1.715 |
| B4197-2 LT | Z | 9.45 | 1.507 | 120.8 | 182.0 | 2.270 |
| B4197-2 TL | Z | 9.45 | 1.507 | 123.2 | 185.6 | 2.270 |
| CF = $\Sigma(\Delta RT_{NDT} * ff) / \Sigma(ff^2) = 62.9$ | | | | | | |

F.4 Calculation of the Chemistry Factor for Weld Wire Heat 5P6771

Using the available HNP-1 surveillance data, the chemistry factor for the weld wire (wire heat No. 5P6771/flux lot 0342) is calculated as follows:

1. No temperature adjustments are required since the capsule irradiation temperature equals the vessel irradiation temperature (i.e., the capsules were irradiated in the plant being assessed).
2. Adjust the measured ΔRT_{NDT} values for chemical composition differences between the surveillance weld chemistry and the reactor vessel beltline weld metal chemistry as follows:

$$\text{Ratio Adjusted } \Delta RT_{NDT} = \left[\frac{CF_{Table, Vessel Chem.}}{CF_{Table, Surv. Chem.}} \right] * \text{Measured } \Delta RT_{NDT}$$

The available copper and nickel chemistry data for weld metal heat 5P6771 are listed below.

| Data Source (Weld Heat 5P6771) | Copper (wt%) | Nickel (wt%) |
|---|--------------|--------------|
| CB&I Fabrication Record Test CN-161 [Single Wire] | 0.03 | 0.88 |
| CB&I Fabrication Record Test CN-161 [Tandem Wire] | 0.04 | 0.95 |
| WCAP-10502 [HNP-1 Surveillance Report – Unirradiated] | 0.023 | 0.87 |
| BAW-2083 [HNP-1 Surveillance Report – Irradiated] | 0.026 | 0.94 |
| BAW-2083 [HNP-1 Surveillance Report – Irradiated] | 0.019 | 1.07 |
| BAW-2083 [HNP-1 Surveillance Report – Irradiated] | 0.029 | 0.95 |

[illegible]

F.5 Conclusion

The evaluation of the available HNP-1 surveillance data yields the following results:

- Surveillance data for base metal B4197-2 and weld wire heat 5P6771 are considered not credible.
- The generic Table CFs for base metal B4197-2 and weld wire heat 5P6771 are non-conservative.
- The best-fit line slope for base metal B4197-2 is the surveillance data chemistry factor, which is calculated to be 62.9°F.
- The best-fit line slope for weld wire heat 5P6771 is the surveillance data chemistry factor, which is calculated to be 72.6°F.

F.6 References

- F-1. NRC Generic Letter 92-01 and RPV Integrity Assessment, NRC Accession No. ML110070570
- F-2. Code of Federal Regulation, Title 10, Part 50, *"Domestic Licensing of Production and Utilization Facilities," Appendix G, Fracture Toughness Requirements*, [60 FR 65474, Dec. 19, 1995; 73 FR 5723, Jan. 31, 2008; 78 FR 34248, Jun. 7, 2013; 78 FR 75450, Dec. 12, 2013].
- F-3. U.S. Nuclear Regulatory Commission, *"Radiation Embrittlement of Reactor Vessel Materials," Regulatory Guide 1.99, Revision 2*, May 1988.
- F-4. U.S. NRC Code of Federal Regulations, Title 10, Part 50.61, "Fracture Toughness Requirements for Protection Against Pressurized Thermal Shock Events," January 4, 2010 [60 FR 65468, Dec. 19, 1995, as amended at 61 FR 39300, July 29, 1996; 72 FR 49500, Aug. 28, 2007; 73 FR 5722, Jan. 31, 2008; 75 FR 23, Jan. 4, 2010].